U.PORTO
FACULDADE DE CIÊNCIAS
UNIVERSIDADE DO PORTO

Characterization of natural products in cone snails from the Cabo Verde archipelago

Sónia Raquel Gomes Ribeiro

Dissertação de Mestrado apresentada à
Faculdade de Ciências da Universidade do Porto em
Biologia Celular e Molecular

2021

MSc

2.º CICLO

FCUP
2021

U.PORTO

Characterization of natural products in cone snails from the Cabo Verde archipelago

Sónia Raquel Gomes Ribeiro

FC

U.PORTO
FACULDADE DE CIÊNCIAS
UNIVERSIDADE DO PORTO

MSc

Characterization of natural products in cone snails from the Cabo Verde archipelago

Sónia Raquel Gomes Ribeiro
Mestrado em Biologia Celular e Molecular
Departamento de Biologia
2021

Orientador
Jorge Neves, PhD, Centro Interdisciplinar de Investigação Marinha e Ambiental (CIIMAR)

Coorientador
Ralph Urbatzka, PhD, Centro Interdisciplinar de Investigação Marinha e Ambiental (CIIMAR)

U.PORTO

FACULDADE DE CIÊNCIAS
UNIVERSIDADE DO PORTO

Todas as correções determinadas pelo júri, e só essas, foram efetuadas.

O Presidente do Júri,

Porto, _____/_____/_____

“I have not failed. I've just found 10,000 ways that won't work.”

Thomas A. Edison

Acknowledgements

First and foremost, I want to express my gratitude to my supervisor, Dr. Jorge Neves, for all of the lessons you taught me, for all of the time you dedicated to me, and for admitting me into this project that is so dear to you. Thank you, Dr. Ralph Urbatzka, for your patience and time spent with me, and for allowing me to be a member of such an incredible team as Team Ralph. Thank you both so much for helping me to develop as a scientist, who is taking the first steps in science, and, most importantly, as a person.

I would also like to express my gratitude to Professor Vitor Vasconcelos for allowing me to join a group as qualified as BBE and work on my dissertation there, as well as for introducing me to wonderful colleagues who are always prepared to help, whom I also thank.

To Dr. Pedro Domingues from University of Aveiro that was kind enough to perform the proteomic analyses and spend time analyzing and interpreting the results.

Thank you to Team Ralph for all of your support and encouragement over the course of the year, which was anything but easy, and you were essential to this study success.

To all of my friends, especially Cris and Ju, for always being there for me, for understanding and listening to my existential crises. For always encouraging me and motivating me to keep going. For having your own staff to deal with but still make time to put up with me and go along with my craziness.

To my family for their love and support throughout this journey. To my parents for their unwavering support and efforts throughout the years to ensure that I can continue to study and pursue my ambition. For allowing me to develop as a person and encouraging me to develop professionally. To my brother, thank you for all of your encouragement, laughing, and silly jokes that encouraged me to keep going down this path with a sense of optimism. Also, thanks to the vast network of connections who contributed to the completion of this thesis, particularly Midjiga.

To the BYT program for providing me with the opportunity to be a part of such an innovative program that provides its participants so many valuable tools.

To the Interdisciplinary Centre of Marine and Environmental Research (CIIMAR) and Faculty of Sciences from the University of Porto (FCUP).

This work was funded by the structured program of R&D&I ATLANTIDA - Platform for the monitoring of the North Atlantic Ocean and tools for the sustainable exploitation of the marine resources (reference NORTE-01-0145-FEDER-000040), supported by the North Portugal Regional Operational Programme (NORTE2020), through the European Regional Development Fund (ERDF).

Cofinanciado por:

NORTE2020 PROGRAMA OPERACIONAL REGIONAL DO NORTE

PORTUGAL 2020

UNIÃO EUROPEIA
Fundo Europeu de Desenvolvimento Regional

Work dissemination

- ## Poster Communication

Ribeiro, S., Urbatzka, R., Vasconcelos, V., Neves, J. (2021). Characterization of natural products in cone snails from the Cabo Verde archipelago. IJUP 14.º Encontro de Jovens Investigadores da Universidade do Porto, 5th-7th May, Porto, Portugal.

Ribeiro, S., Urbatzka, R., Vasconcelos, V., Neves, J. (2021). Characterization of natural products in cone snails from the Cabo Verde archipelago. BLUE THINK CONFERENCE 2021, 23rd and 24th September, Matosinhos, Portugal.

- ## BYTplus Report

Ribeiro, S., Urbatzka, R., Vasconcelos, V., Neves, J. (2021). Characterization of natural products in cone snails from the Cabo Verde archipelago. The BYT BLUE YOUNG TALENT Journal, 2.

- ## Oral Communication – BYT program closing session

Ribeiro, S., Urbatzka, R., Vasconcelos, V., Neves, J. (2021). Characterization of natural products in cone snails from the Cabo Verde archipelago. The BYT BLUE YOUNG TALENT, 23rd Jully, Matosinhos, Portugal.

- ## Manuscript in Preparation

Ribeiro, S., Urbatzka, R., Vasconcelos, V., Neves, J. (2021). Cone Snails: Venom as a weapon that can fight against obesity?

Abstract

Conus, often known as cone snails, is one of the largest venomous marine animal genera known. These tropical sea gastropods are members of the Conidae family and the Conoidea superfamily (=Toxoglossa). They can be found in a variety of areas around the world, although they are more common in tropical and subtropical waters such as the Indo-Pacific, Western Pacific, and Macaronesian regions, such as Cabo Verde. These marine invertebrates are divided into three groups: (1) molluscivorous if they prey on other mollusks; (2) vermivorous, when they prey on worms like polychaete; (3) piscivores, when they prey on fishes. Cone snails developed a variety of defence and predation methods as a result of their limited vision, including powerful venoms (chemical defences) comprising conopeptides (conotoxins). The venoms of vermivorous cone snails native to the Cabo Verde archipelago (*Conus venulatus* and *Conus ateralbus*) and a non-endemic vermivorous species (*Conus genuanus*) were studied in this investigation. RP-HPLC was used to assess the variety and venom profile of conotoxins, and fractions were examined for distinct bioactivities. A zebrafish nile red fat metabolism (obesity), glucose uptake (diabetes), lipid content reduction in fatty acid-overloaded liver cells (steatosis) and pro- and anti-inflammatory assays were performed. According to Maldi-TOF profiles, *Conus ateralbus* may produce more compounds with lower molecular weight (mostly between 600 and 2000 Da) than *Conus venulatus*, which produced fewer compounds with a wider distribution of molecular weight. Anti-obesity studies revealed that *Conus ateralbus* fractions could result in a significant lipid reduction (40%) by fraction *C.ateralbus* R2.6. *Conus genuanus* fraction C3.1 also resulted in a significant lipid reduction (50%). *Conus venulatus*, on the other hand, showed no statistically significant differences from controls. Anti-diabetes assay showed no ability for *Conus* fractions to increase glucose uptake in zebrafish embryos, and anti-steatosis assays yielded no statistically significant differences from controls. Anti-inflammatory assays revealed that some fractions may have the ability to interfere with inflammatory processes, specifically with NO production pathways, whereas pro-inflammatory assays revealed that fractions had no ability to promote inflammatory processes. The bioactive fraction *C.ateralbus* R2.6 was analysed using LC-ESI-HR-MS/MS, and the molecular masses obtained were compared to conotoxins masses previously described in the literature. We were able to uncover ten conotoxins sequences that matched sequences found in our sample using this strategy.

In conclusion, the current study revealed that *Conus ateralbus* and *Conus genuanus* may produce conotoxins capable of modulating lipid metabolism. The research is now focusing on the identification of peptides in the bioactive fraction *C.ateralbus* R2.6. In the

future, fraction C3.1 will be investigated to discover the peptides present, as well as other fractions with anti-inflammatory activity.

Keywords: *Conus ateralbus*, *Conus venulatus*, *Conus genuanus*, obesity, diabetes, inflammation, steatosis, zebrafish.

Resumo

Conus, frequentemente conhecido como caracóis marinhos, é um dos maiores géneros de animais marinhos venenosos conhecidos. Estes gastrópodes marinhos tropicais são membros da família Conidae e da superfamília Conoidea (=Toxoglossa). Podem ser encontrados numa variedade de áreas em todo o mundo, embora sejam mais comuns em águas tropicais e subtropicais, tais como as regiões Indo-Pacífico, Pacífico Ocidental, e Macaronésicas, como Cabo Verde. Estes invertebrados marinhos estão divididos em três grupos: (1) moluscívoros, quando se alimentam de outros moluscos; (2) vermívoros, quando se alimentam de poliquetas; (3) piscívoros, quando se alimentam de peixes. Os caracóis marinhos desenvolveram uma variedade de métodos de defesa e predação como resultado da sua visão limitada, incluindo poderosos venenos (defesas químicas) que incluem conopeptideos (conotoxinas). Nesta investigação foram estudados os venenos de caracóis marinhos vermívoros nativos do arquipélago de Cabo Verde (*Conus venulatus* e *Conus ateralbus*) e uma espécie vermívora não endémica (*Conus genuanus*). A diversidade de conotoxinas e o perfil venómico foi avaliado por RP-HPLC e as frações recolhidas testadas em diversos ensaios de bioatividade. Foram realizados ensaios anti-obesidade (Zebrafish nile red fat metabolismo), anti-diabetes (glucose uptake), também se avaliou a possibilidade de redução do conteúdo lipídico em células hepáticas crescidas em exposição a ácidos gordos (anti-esteatose) e potencial pro e anti-inflamatório das frações. Os perfis RP-HPLC sugerem que o *Conus ateralbus* tem mais conotoxinas/péptidos no seu veneno do que *Conus venulatus*. De acordo com perfis Maldi-TOF, *Conus ateralbus* pode produzir mais compostos com menor peso molecular (principalmente entre 600 e 2000 Da) do que *Conus venulatus*, que produziu menos compostos com uma distribuição mais ampla do peso molecular. Estudos anti-obesidade revelaram que as frações de *Conus ateralbus* poderiam resultar numa redução lipídica significativa (40%) pela fração *C.ateralbus* R2.6. A fração C3.1 de *Conus genuanus* também resultou numa redução lipídica significativa (50%). *Conus venulatus*, por outro lado, não mostrou diferenças estatisticamente significativas em relação aos controlos. Os ensaios anti-diabetes revelaram que as frações de *Conus* não aumentaram o transporte de glucose para o interior das células em embriões de peixe-zebra e os ensaios de anti-esteatose não revelaram diferenças estatisticamente significativas em relação aos controlos. Os ensaios anti-inflamatórios revelaram que algumas frações podem ter a capacidade de interferir com processos inflamatórios, especificamente com as vias de produção de NO, enquanto os ensaios pró-inflamatórios revelaram que as frações não têm capacidade de promover processos inflamatórios. A fração bioativa *C.ateralbus* R2.6 foi analisada

utilizando LC-ESI-HR-MS/MS, e as massas moleculares obtidas foram comparadas com as massas de conotoxinas anteriormente descritas na literatura. Conseguimos descobrir dez sequências de conotoxinas que corresponderam às sequências encontradas na nossa amostra.

Em conclusão, o estudo revelou que *Conus ateralbus* e *Conus genuanus* podem produzir conotoxinas capazes de modular o metabolismo lipídico. A investigação centra-se agora na identificação de peptídeos na fração bioativa *C.ateralbus* R2.6. No futuro, a fração C3.1 será investigada para descobrir os peptídeos presentes, bem como outras frações com atividade anti-inflamatória.

Palavras-chave: *Conus ateralbus*, *Conus venulatus*, *Conus genuanus*, obesidade, diabetes, inflamação, esteatose, peixe-zebra.

Table of Contents

Work dissemination ..... ***VI***

Abstract ..... ***VII***

Resumo ..... ***IX***

Table of Contents ..... ***XI***

List of Figures ..... ***XIII***

List of Tables ..... ***XVI***

List of Abbreviations ..... ***XVII***

Appendixes index ..... ***XIX***

1. INTRODUCTION ***1***

1.1. Cone snails (*Conus*) 1

1.2. *Conus* biology 2

1.3. *Conus* in Cabo Verde archipelago 3

1.4. Venom Peptides 3

1.5. Metabolic diseases 6

1.5.1. Obesity 6

1.5.2. Diabetes 8

1.5.3. Non-alcoholic fatty liver disease 10

1.5.4. Inflammation 10

1.6. *In vivo* and *in vitro* models 12

1.6.1. Zebrafish 12

1.6.2. HepG2 cells 13

1.6.3. Raw 264.7 cells 14

1.7. Objectives 15

2. METHODS ***16***

2.1. Materials and reagents 16

2.2. Specimen collection and Venom preparation 16

2.3. Venom extraction 17

2.4. HPLC conopeptide fractionation 17

2.5. Zebrafish Nile Red Fat Metabolism Assay 18

2.6. Glucose Uptake Assay 18

2.7. Anti-steatosis Assay 19

2.8. Inflammatory Assay 20

2.9. Proteomics Analyses 21
2.10. MALDI-TOF Analyses 22
2.11. Statistical Analysis 22
3. RESULTS 23
3.1. HPLC profiling of *Conus ateralbus* and *Conus venulatus* 23
3.1.1. Gradient solvent optimization 23
3.2. Compounds mass range distribution 26
3.3. Bioactivity Assays 27
3.3.1. Lipid reducing activity in Zebrafish Larvae 27
3.3.1.1. *C.ateralbus* R2.6 proteomic analyses 30
3.3.2. Glucose Uptake in Zebrafish Larvae 33
3.3.3. Anti-Steatosis Activity in HepG2 Cells 37
3.3.4. Inflammatory assays 41
4. Discussion 47
4.1. Venoms chromatographic characterization 48
4.2. Screening for fractions with anti-obesity activity 49
4.3. Screening for fractions with anti-diabetic activity 51
4.4. Screening for fractions with anti-steatosis activity 52
4.5. Screening for fractions with inflammatory activity 54
4.6. Zebrafish as model organism on screening for conotoxins bioactivity 55
5. Conclusions 56
6. Future perspectives 57
References 58
Appendixes 68
- Appendixes I- Chromatographic profile of *Conus ateralbus* using gradiente 1 ... 68
- Appendixes II - Chromatographic profile of *Conus ateralbus* using a flow rate of 3 mL/min 69
- Appendixes III – Fractions masses 70
- Appendixes IV - Work dissemination 71

List of Figures

Figure 1 *Conus venom apparatus. Venoms are synthetized on epithelial cells and stored until needed. Conus use their proboscis to detect prey and when receiving the right stimuli venom duct content is expelled into the proboscis and then injected intravenously into the prey. Adapted from Oliveira (2002)……....2*

Figure 2 *Venom apparatus dissection. It is possible to observe the venom bulb (A), the venom duct (B). The venom was squeezed from the venom duct……16*

Figure 3 *Diagram of the 48-well plate used in Zebrafish Nile Red Fat Metabolism Assay. Yellow wells represent solvent controls (DMSO 0.1%). Red wells represent positive control (REV 50 µM). White wells represent fractions tested at a concentration of 10 µg/mL……..18*

Figure 4 *Diagram of the 96-well plate used in Glucose Uptake Assay. Yellow wells represent solvent controls (DMSO 0.1%). Green wells represent positive control (EMODIN 10 µM). White wells represent fractions tested at a concentration of 10 µg/mL……....19*

Figure 5 *Diagram of the 96-well plate used in Anti-steatosis Assay. Yellow wells represent negative control (DMSO 0.5%). Orange wells represent negative control (MeOH 0.5%). Red wells represent solvent control (DMSO 0.5% and SO 62 µM). Blue and green wells represent fractions tested at a concentration of 10 µg/mL. Fractions were tested in triplicate……....20*

Figure 6 *Diagram of the 96-well plate used in Inflammatory Assays. Orange wells represent negative controls (DMSO 0.5%). Red wells represent solvent control (LPS and DMSO). Green and blue wells served for internal quality evaluation of the assay. White wells represent fractions tested at a concentration of 10 µg/mL, co-exposed to LPS in the anti-inflammatory assays, and without LPS in the pro-inflammatory assay……...21*

Figure 7 *Chromatographic profile of Conus ateralbus using gradient 2. More polar compounds eluted around 13 min of running with good resolution. Nonpolar compounds eluted with almost 36% of solvent B. RP-HPLC revealed a profile with good peak resolution, compounds well separated and a low baseline. The most active fraction is marked by asterisks *……23*

Figure 8 *Chromatographic profile of Conus venulatus using gradient 2. More polar compounds eluted at 13 min of running. Nonpolar compounds eluted with approximately 36% of solvent B. RP-HPLC revealed a profile with good peak resolution, compounds well separated and a low baseline……..24*

Figure 9 *Molecular mass range distribution of venom compounds detected by Matrix-assisted laser desorption ionization couple to time-of-flight mass spectrometer (Maldi-TOF) analysis……....26*

Figure 10 *Representative images of zebrafish Nile red fat metabolism assay of fraction C.ateralbus R2.6 and Conus genuanus C.3.1. Top images show fluorescence with red contrast, and bottom images represent phase contrast of zebrafish larvae. Dimethyl sulfoxide (DMSO) was used as a solvent control, at a concentration of 0.1%, and resveratrol (Rev) was used as a positive control, at a concentration of 50 µM……...27*

Figure 11 *Quantification of the lipid-reducing effects of different fractions from three Conus species at a final concentration of 10 µg/mL using the zebrafish Nile red fat metabolism assay. Solvent control had 0.1% DMSO and the positive control 50 µM REV. Values are expressed as mean fluorescence intensity (MFI) percentage relative to the DMSO group. Data have been derived from 5-7 individuals per treatment group and are shown as box-and-whisker plots (5-95 percentiles). Statistical differences from solvent control (DMSO)*

*were analysed by Kruskal-Wallis with Dunn´s posthoc (C.ateralbus R1, C.venulatus R1, C.venulatus R2 and C.genuanus) and Brown-Forsythe and Welch ANOVA tests and Holm-Sidak's multiple comparisons test (C.ateralbus R2). Differences are indicated by asterisks, * p < 0.05; ** p < 0.01; *** p < 0.001; **** p < 0.0001……...29*

Figure 12 *Chromatographic profile of C.ateralbus R2.6 fraction. More abundante peaks in C.ateralbus R2.6 fraction eluted after 48 minutes of run……...30*

Figure 13 *Representative images of glucose uptake in zebrafish larvae. Top images show fluorescence with green contrast, and bottom images represent phase contrast of zebrafish larvae. Dimethyl sulfoxide (DMSO) was used as a solvent control, at a concentration of 0.1%, and EMODIN was used as a positive control, at a concentration of 10 µM……..33*

Figure 14 *Quantification of glucose uptake in yolk sac by embryos expose to fractions from three Conus species at a final concentration of 10 µg/mL. Solvent control had 0.1% DMSO and the positive control 10 µM EMODIN. Values are expressed as mean fluorescence intensity (MFI) percentage relative to the DMSO group. Data have been derived from 5-6 individuals per treatment group and are shown as box-and-whisker plots (5-95 percentiles). Statistical differences from solvent control (DMSO) were analysed by Kruskal-Wallis with Dunn´s posthoc (C.ateralbus R1) and by Brown-Forsythe and Welch ANOVA tests and Holm-Sidak's multiple comparisons test (C.ateralbus R2, C.venulatus R1, C.venulatus R2, C.genuanus) and are indicated by asterisks, * p < 0.1; ** p < 0.01; *** p < 0.001; **** p < 0.0001……..34*

Figure 15 *Quantification of glucose uptake in eyes of embryos expose to fractions from three Conus species at a final concentration of 10 µg/mL. Solvent control had 0.1% DMSO and the positive control 10 µM EMODIN. Values are expressed as mean fluorescence intensity (MFI) percentage relative to the DMSO group. Data have been derived from 5-6 individuals per treatment group and are shown as box-and-whisker plots (5-95 percentiles). Statistical differences from solvent control (DMSO) were analysed by Ordinary one-way ANOVA (C.ateralbus R1, C.ateralbus R2, C.venulatus R2), by Kruskal-Wallis with Dunn´s posthoc (C.venulatus R1) and by Brown-Forsythe and Welch ANOVA tests and Holm-Sidak's multiple comparisons test (C.genuanus) and are indicated by asterisks, * p < 0.1; ** p < 0.01; *** p < 0.001; **** p < 0.0001……...36*

Figure 16 *Representative images of anti-steatosis activity in HepG2 cells. Methanol (MeOH) at a final concentration of 0.5%, and Dimethyl sulfoxide (DMSO) at 0.5% were used as negative controls. Sodium oleate (SO) was used to induce the formation of lipid droplets, which can be observed as intense lipid accumulation in cells, at a final concentration of 62 µM. Hoechst 33342 (HO) was used as staining for DNA (blue) and Nile red (NR) was used as a lipid staining (orange)……..37*

Figure 17 *Bioactivity screening using the anti-steatosis assay in HepG2 cells. Values are expressed as mean fluorescence intensity (MFI) percentage relative to solvent control (DMSO 0.5%, SO 62 µM). Two negative controls (MeOH 0.5%, DMSO 0.5%) were included. HepG2 cells were exposed for 6 h to 62 µM sodium oleate (SO 62 µM) and 10 µg mL^{-1} Conus fractions. The data are shown as box-and-whisker plots (5-95 percentiles). Statistical differences from solvent control were analysed by Brown-Forsythe and Welch ANOVA tests and Holm-Sidak's multiple comparisons test and are indicated by asterisks, * p < 0.1, ** p < 0.01, *** p < 0.001, **** p < 0.0001……..38*

Figure 18 *Cell viability after 6h of exposure to Conus fractions at a concentration of 10 µg mL^{-1}. Cells on solvent control were exposed to DMSO 0.5% and SO 62 µM. Two negative controls (MeOH 0.5%, DMSO 0.5%) were included. The data are shown as column bar graph. Statistical differences from DMSO control were analysed by Brown-Forsythe and Welch ANOVA tests and Holm-Sidak's multiple comparisons test (C.ateralbus R1,*

*C.ateralbus R2) and by Ordinary one-way ANOVA test (C.venulatus R1, C.venulatus R2, C.genuanus) and are indicated by asterisks, * p < 0.1; ** p < 0.01; *** p < 0.001; **** p < 0.0001……40*

Figure 19 *Bioactivity screening using pro-inflammatory assay in RAW 264.7 macrophages. Cells on positive control were exposed to DMSO 0.5% and LPS 1µg/mL. A solvent control (DMSO 0.5%) and two quality controls (LPS and Blanc) were included. Values are expressed as percentage of NO production relative to solvent group (DMSO). Raw 264.7 were exposed for 24 h to Conus fractions at a final concentration of 10 µg mL^{-1}. The data are shown as box-and-whisker plots (5-95 percentiles). Statistical differences from solvent control were analysed by Kruskal-Wallis with Dunn´s posthoc and are indicated by asterisks, * p < 0.1, ** p < 0.01, *** p < 0.001, **** p < 0.0001……42*

Figure 20 *Cell viability after 24h of exposure to Conus fractions at a concentration of 10 µg mL^{-1}. Cells on positive control were exposed to DMSO 0.5% and LPS 1µg/mL. A solvent control (DMSO 0.5%) and two quality controls (LPS and Blanc) were included. The data are shown as column bar graph. Statistical differences from solvent control (DMSO) were analysed by Kruskal-Wallis with Dunn´s posthoc and are indicated by asterisks, * p < 0.1, ** p < 0.01, *** p < 0.001, **** p < 0.0001……43*

Figure 21 *Bioactivity screening using anti-inflammatory assay in RAW 264.7 macrophages. Cells on solvent control were exposed to DMSO 0.5% and LPS 1µg/mL. A negative control (DMSO 0.5%) and two quality controls (LPS and Blanc) were included. Values are expressed as percentage of NO production relative to solvent group (DMSO and LPS) from cell exposed to Conus fractions. Raw 264.7 were exposed for 24 h to Conus fractions at a final concentration of 10 µg mL^{-1}. The data are shown as box-and-whisker plots (5-95 percentiles). Statistical differences from solvent control were analysed by Kruskal-Wallis with Dunn´s posthoc and are indicated by asterisks, * p < 0.1, ** p < 0.01, *** p < 0.001, **** p < 0.0001……45*

Figure 22 *Cell viability after 24h of exposure to Conus fractions at a concentration of 10 µg mL^{-1}. Cells on solvent control were exposed to DMSO 0.5% and LPS 1µg/mL. A solvent negative control (DMSO 0.5%) and two quality controls (LPS and Blanc) were included. The data are shown as column bar graph. Statistical differences from solvent negative control (DMSO) were analysed by Brown-Forsythe and Welch ANOVA tests and Holm-Sidak's multiple comparisons test and are indicated by asterisks, * p < 0.1, ** p < 0.01, *** p < 0.001, **** p < 0.0001……46*

List of Tables

Table 1 *Classification used to group conopeptides into categories. Classification used for poor disulfide conopeptides is shown in superior part of the table and classification for rich disulfide conopeptides is shown in the inferior part of the table. Poor disulfide conopeptides are classified into families with known and unknown pharmacological targets. Rich disulfide conopeptides are classified accordingly to sequence homology in superfamilies, cysteine framework and pharmacological targets. 5*

Table 2 *Investigated conopeptides for the development of new drugs and therapeutics against and treatable disorder, mechanism of action and clinical stage of tests.....6*

Table 3 *Anti-obesity drugs approved by FDA in 2018. Adapted from Srivastava & Apovian, (2018). 8*

Table 4 *New glucose lowering medications approved by FDA in the last decade. Adapted from Sterrett et al. (2016). 9*

Table 5 *Effect of several known nutraceuticals on pro-inflammatory mechanisms. Adapted from Huang et al. (2004). 12*

Table 6 *Solvent gradients and mobile phase composition used in RP-HPLC method. 17*

Table 7 *Peptides detected by LC-ESI-HR-MS/MS, relative abundance peptides masses and putative sequences by mass-matching using BLAST search on UniProtKB database. ...31*

Table 8 *Conotoxins identification by BLAST search on UniProtKB database. Signal peptide, propeptide and mature peptide are shown in orange, green and blue, respectively. Peptides identified by LC-ESI-HR-MS/MS are underlined. 32*

List of Abbreviations

2-NBDG 2-(N-(7-Nitrobenz-2-oxa-1,3-diazol-4-yl)Amino)-2-Deoxyglucose

AA Arachidonic acid

ACN Acetonitrile

BBE Blue Biotechnology and Ecotoxicology

C18 Eighteen carbon chain bonded to silica particles

CART Cocaine- and amphetamine-regulated transcript peptide

CIIMAR Interdisciplinary Centre of Marine and Environmental

CO_2 Carbon dioxide

COX Cyclo-oxygenase

COX Cyclooxygenase enzymes

CRF Corticotropin releasing factor

dH_2O Distilled water

DMEM Dulbecco's modified Eagle's medium

DMSO Dimethyl sulfoxide

DPF Days post fertilization

DRG Dorsal root ganglion

EMODIN (6-methyl-1,3,8-trihydroxyanthraquinone)

FA Formic acid

FDA Food and Drug Administration

H_2O Water molecule

H_3PO_4 Phosphoric acid

HBSS Hanks' Balanced Salt Solution

HO-33342 Hoechst 33342

HPF Hours post fertilization

HPLC High-pressure liquid chromatography

IFN-γ Inferon gamma

IL-10 Interleukin 10

IL-4 Interleukin 4

iNOS Inducible nitric oxide synthase

LC-ESI-HR-MS/MS Liquid Chromatography Electrospray Ionization Tandem Mass Spectrometric

LOX Lipoxygenase

LPS Lipopolysaccharides

Maldi-TOF Matrix-assisted laser desorption ionization couple to time-of-flight mass spectrometer

MeOH Methanol

MFI Mean fluorescence intensity

MS-222 Tricaine mesylate

MTT (3-(4,5-Dimethylthiazol-2-yl)-2

NAFLD Non-alcoholic fatty liver disease

NASH Non-alcoholic steatohepatitis

NFκB Factor nuclear kappa B

NO Nitric oxide

NOS Nitric Oxide synthase

NPY Neuropeptide Y

NSAID Non-steroidal anti-inflammatory drugs

PLA_2 Phospholipase A2

PTU Propylthiouracil

REV Resveratrol

RP-HPLC Reversed Phase High Performance Liquid Chromatography

RP-HPLC Reverse-phase high performance liquid chromatography

rpm Revolutions per minute

SAID Steroidal anti-inflammatory drugs

SD Standard deviation

SO Sodium oleate

SRB Sulforhodamine B

TCA Trichloroacetic acid

TFA Trifluoroacetic acid

TNF-α Tumor necrosis factor alpha

Tris-HCl Tris hydrochloride

TTX-S Tetrodotoxin sensitive

WAT White adipose tissue

WHO World Health Organization

Appendixes index

Appendixes I- Chromatographic profile of *Conus ateralbus* using gradiente 1 68

Figure A Chromatographic profile of *Conus ateralbus* using gradiente 1. More polar compounds eluted around 7 min of running with good resolution. Nonpolar compounds eluted with almost 36% of solvent B. Compounds eluted in this phase show poor separation, suggesting a mixture of detected compounds……68

Appendixes II - Chromatographic profile of *Conus ateralbus* using a flow rate of 3 mL/min……..69

Figure A Chromatographic profile of *Conus ateralbus* using a flow rate of 3 mL/min. It was observed a higher intensity in the recorded peaks, but it was also obvious a premature elution of compounds, indicating that compounds did not have enough time to bind to the column and were dragged at the beginning of race……69

Appendixes III – Fractions masses……70

Table A Fractions weight after dried. Fractions were dissolved in DMSO 40% to a concentration of 4 mg/mL……70

Appendixes IV - Work dissemination 71

Figure A Poster communication for IJUP 14.º Encontro de Jovens Investigadores da Universidade do Porto 2021……71

Figure B Poster communication for BLUE THINK CONFERENCE 2021……72

1. INTRODUCTION

1.1. Cone snails (*Conus*)

Conoidea (= Toxoglossa) is a superfamily of marine snails present in marine habitats all the way from the tropics to the poles, from shallow to deep water, and from hard to soft substrates (Puillandre *et al.*, 2008). This superfamily comprises a wide range of recent and fossil genera and described species (Puillandre *et al.*, 2008; Olivera *et al.*, 2013). Conoidea was originated in the Cretaceous and during the Cenozoic occurred the major adaptive radiations leading to the lineages found today (Olivera *et al.*, 2013). According to the literature (Olivera *et al.*, 2013; Puillandre *et al.*, 2017), this marine snails superfamily can be divided into three families based on shell shape: (1) Conidea, also known as cone snails, characterized by their conical shells, low spire and narrow slit-like aperture; (2) Terebridae, also called Auger snails, with a tall multi-whorled spire, short siphonal canal and low aperture; and (3) Turridae, characterized by intermediate shell proportions and form the least characterized and most heterogeneous family, leading to a polyphyletic group.

The Conidae family is perhaps the most important family of Toxoglossa due to its immense diversity. With approximately 800 species reported, this exclusively marine family exhibits a remarkable variety of shell colors, and can be found in tropical waters of all oceans, although they are particularly present in the Indo-Pacific and Western Pacific regions (Díaz *et al.*, 2005; Flores-Garza *et al.*, 2014; Olivera *et al.*, 2014; Prashanth *et al.*, 2016). Cone snails inhabit different types of sea bottom, which includes rocky areas, coral reefs, seagrass, shallow waters, and can be present in intertidal zones to 1000 m of depth (Díaz *et al.*, 2005; Neves *et al.*, 2013; Flores-Garza *et al.*, 2014). The shells of cone snails are particularly variable, especially when the parameter evaluated is the size of adult specimens, which can fluctuate from less than 1 cm in the small species to almost 22 cm in the largest species, as well as when evaluated the colour pattern. Typically, the shell is broad at the top of the last whorl and tapers gradually to a narrow base. The spire is a step-like or looks like a broad, short cone. Cone snails also show a long and narrow aperture, and a thin and sharp outer lip (Díaz *et al.*, 2005). Until recent reports, all living cone snails were assigned into a single genus (*Conus*), but the expansion of molecular database for these marine gastropods allowed the definition of genus *Conus* and introduced other accepted genera of cone snails (Olivera *et al.*, 2014). *Conus* species form one of the largest single genera of living marine invertebrates, which makes them an important contributor for oceanic biodiversity.

1.2. *Conus* biology

Cone snails are carnivores' animals that hunt typically at night and are very active around sunset and sunrise. As slow-moving molluscs and with poor sight, although cone snails have two eyestalks, they depend on their proboscis to detect prey and a very specialized venom apparatus (Figure 1) to envenomate and capture them (Olivera, 2002; Livett *et al.*, 2012; James *et al.*, 2014). Cone snail's proboscis is a muscular and hydrostatically appendage with small structures (sensory papillae) on its tip that allows chemo and mechanosensory detection of prey (Terlau & Olivera, 2004; James *et al.*, 2014). Sensory papillae are thought to be crucial on determine the type of prey and its exact location, allowing a correct and efficient envenomation and capture of prey (James *et al.*, 2014). Proboscis is usually retracted into the rostrum, but when prey is chemically sensed it extends and starts the searching behaviour (Marshall *et al.*, 2002). A radular tooth is near the proboscis tip when searching begins. This hollow radular tooth is individually moved into the proboscis, and scrape or bites during feeding process, working as an harpoon and hypodermic needle that will inject venom into the prey (Marshall *et al.*, 2002; Olivera, 2002; Neves, 2016). Generally, all cone snails produce venom and use it as an attack and defence strategy. Venoms are synthesized and delivered with the help of venom apparatus. Venom biologically active components are synthesized on epithelial cells of venom duct and stored until needed. When receiving the right stimuli, the venom duct content is expelled into the proboscis by a muscular bulb. Venom is then injected intravenously into the prey (Neves, 2016).

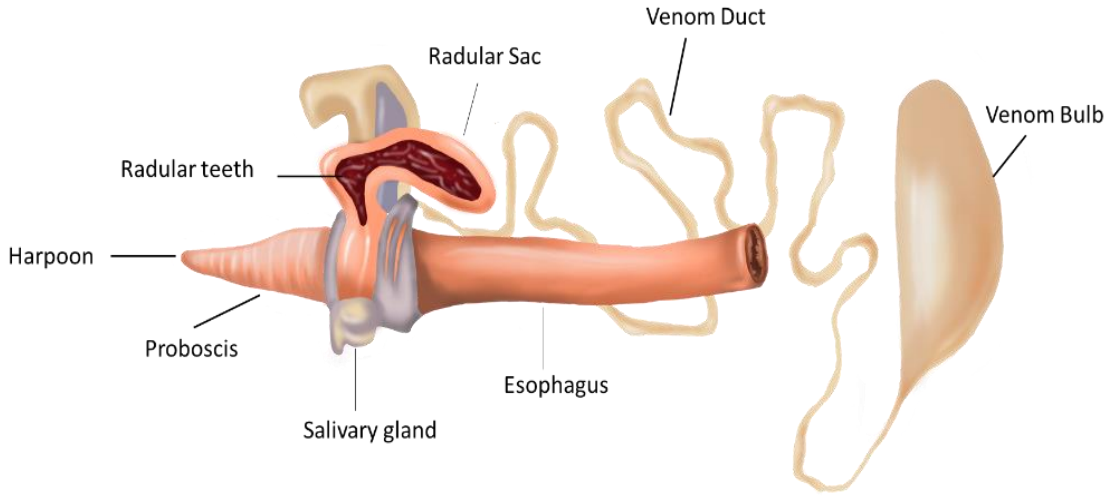

Figure 1 *Conus venom apparatus. Venoms are synthetized on epithelial cells and stored until needed. Conus use their proboscis to detect prey and when receiving the right stimuli venom duct content is expelled into the proboscis and then injected intravenously into the prey. Adapted from Oliveira (2002).*

Cone snails in general have a wide spectrum of prey, however typically *Conus* species only envenomate a single species of prey (Olivera, 2002). *Conus* can be classified into three groups depending on their feeding habits: (1) vermivorous cone snails feed on worms from Annelida phylum, and in some cases hemichordates and echiurid, and represent about 75% of *Conus* species; (2) molluscivorous species prey on other gastropods like snails; (3) piscivorous cone snails are fish-hunting species that can rapidly immobilize fish and represent 10% of *Conus* diversity. Given their ability to lethally injure humans this is the best studied group (Terlau & Olivera, 2004; Neves, 2016).

1.3. *Conus* in Cabo Verde archipelago

Conus species have a wide distribution and can occupy a region as big as the Indo-Pacific region, or be restricted to an archipelago, a single island or even a single bay (da Cunha Oliveira, 2008). Cabo Verde archipelago, located in the Central Atlantic, belongs to the Region of Macaronesia and is a hotspot for cone snails species. These islands comprise about 10% of *Conus* diversity (Cunha *et al.*, 2008). In this archipelago we can find 57 endemic *Conus* species and only 3 non-endemic (*Conus ermineus*, *C. genuanus*, and *C. tabidus*) (Cunha, 2008). As reported by Cunha (2008), *Conus* from Cabo Verde exibit two main morphological groups accordingly to shell size. With a bigger shell, *Conus venulatus* and *Conus pseudinivifier* inhabit Boavista, Maio and Santiago islands. *Conus venulatus* also occurs in Sal. *Conus ateralbus* can only be found in Sal, and *Conus trochulus* only occurs in Boavista. Small shelled species are usually restricted to an island or single bay (Cunha *et al.*, 2005; da Cunha Oliveira, 2008; Cunha *et al.*, 2008). Oscillations in sea-level lead to modifications on coastline and distance between islands, ecological and geographically isolating individuals and introducing changes in marine species biology. Transition from planktotrophic to lecitotrophic larval feeding mode is a clear exemple of these modifications. High endemism observed in Cabo Verde cone snail species is thought to be related with allopatric speciation due to species isolation and limited dispersal capacity of larvae of small shelled *Conus* (Cunha *et al.*, 2008; Kauferstein *et al.*, 2011).

1.4. Venom Peptides

All known *Conus* species can synthetise venoms strong enough to rapidly immobilize and capture prey. Depending on feeding habits, species location, interspecific relationships and other factors, each *Conus* species is under different environmental pressures. Therefore, synthetised venoms are very diferent, having its own complement of peptides (Vianna Braga *et al.*, 2005). Each *Conus* venom contains 100 to 200 different

toxins, which are known as conopeptides or conotoxins. Conotoxins are usually classified as small peptides with 12 to 35 amino acids and 1 to 4 disulfide bridges (Kaas *et al.*, 2010). Most research work done until now has focused on conopeptides disulfide-rich peptides, but it is also common the existence of disulfide-poor peptides, conopeptides with one or none disulfide bridges (Halai & Craik, 2009; Kaas *et al.*, 2010; Neves, 2016; George & Aisheck, 2020). Conopeptides with no disulfide bonds are classified in contulakins, conantokins, conorfamides, conolysins, conophans and conomarphins, depending on their targets. One disulfide bond peptides can be classified as contryphans and conopressins. Conotoxins usually are disulfide-rich peptides. Conopeptides classification system is based on sequence clustering of precursor protein processed in endoplasmic reticulum (gene superfamily), on pattern of cysteines found in the sequence (cysteine framework) and peptides specific targets (pharmacological target) (Kaas *et al.*, 2010; George & Aisheck, 2020). Table 1 shows the classification system used to group conopeptides into categories.

With 100,000 conopeptides synthetized by *Conus* and high specificity to target membrane proteins, like ion-channels, receptors and transporters, these small peptides have been largely studied in order to determine their pharmacological potential (George & Aisheck, 2020). Conopeptides have shown high specificity for certain classes of receptors, without interacting with others, leading to a precise outcome on metabolic pathways and less significant side effects (Mir *et al.*, 2016).

Antiepileptic, cardioprotective, neuroprotective and antinociceptive are among the activities observed when conopeptides are administered, revealing a possibility to use them against psychiatric and neuromuscular disorders and even cancer (Livett *et al.*, 2004; Mir *et al.*, 2016). Table 2 shows conopeptides under investigation for the development of new therapeutics and drugs, based on Mir *et al.* (2016) and Livett *et al.* (2004) reports.

Table 1 *Classification used to group conopeptides into categories. Classification used for poor disulfide conopeptides is shown in superior part of the table and classification for rich disulfide conopeptides is shown in the inferior part of the table. Poor disulfide conopeptides are classified into families with known and unknown pharmacological targets. Rich disulfide conopeptides are classified accordingly to sequence homology in superfamilies, cysteine framework and pharmacological targets.*

Poor disulfide conopeptides			
No disulfide bonds		**One disulfide bond**	
Family	**Pharmacological target**	**Family**	**Pharmacological target**
Contulakins	Neurotensin receptor	Contryphans	-
Conantokins	N-methyl-D-aspartic acid receptor		
Conorfamides	RFamide receptor		
Conolysins	Cellular membranes	Conopressins	Vasopressin homologs
Conophans	**-**		
Conomarphins	**-**		
Rich disulfide conopeptides/ conotoxins			
Gene superfamily	**Cysteine framework**	**Family**	**Pharmacological target**
A	I/II IV	α, ρ, αA, κA	nAChR; Adrenergic receptor nAChR; K^+ channel
I	XI; XII	κ	K^+ channel
J	XIV	κ	Kv 1.6 channel; nAChR
L	XIV	α	nAChR
M	II, III, IV, XVI, VI/VII	μ, ψ, κM	Na^+channel, nAChR, K^+ channel
O	VI/VII, XII, XV	δ, μO, κ, ω, γ	Na^+channel; K^+ channel, Ca^{2+} channel
P	IX	-	-
S	VIII	α, σ	nAChR, 5-HT_3 receptor
T	V, X	ε, χ	NE transporter
V	XV	-	-
Y	XX	-	-

α- alpha; ρ- rho; κ- kappa; μ- micro; ψ- psi; δ- delta; ω- omega; γ- gamma; σ- sigma; ε- epsilon; χ- chi; - unknown; NE- norepinephrine; nAChR- nicotinic acetylcholine receptor.

Table 2 *Investigated conopeptides for the development of new drugs and therapeutics, treatable disorder, mechanism of action and clinical stage of tests.*

Commercial name	Conopeptide	Disorder	Action mechanism	Clinical stage
Prialt, Zicotide	ω-MVIIA	Intractable pain	N-type calcium channels blocker	Phase IV (FDA approved)
CGX-1160	Contulakin-G	Neuropathic pain	Neurotensin receptor agonist	Phase Ib (sciatica patients)
ACV-1	α-Vc1.1	Neuropathic pain	Nicotinic acetylcholine receptors antagonist	Phase II
Xen2174	χ-MrIA	Neuropathic pain	Norepinephrine transporter inhibitor	Phase IIa (cancer patients)
CGX-1002	μO-MrVIB	Neuropathic pain	Sodium channels blocker	Pre-clinical
AM-336	ω-CVID	Neuropathic pain	N-type calcium channels blocker	Phase IIa (cancer patients)
CGX-1007	Contulakin-G	Intractable epilepsy	NMDA receptor antagonist	Phase I
CGX-1051	κ-PVIIA	Acute myocardial infarct, cardioprotection	K-channel blocker	Pre-clinical
PEG-SIIIA	μ-SIIIA	Inflammatory pain	Sodium channels blocker	Pre-clinical

1.5. Metabolic diseases

1.5.1. Obesity

Obesity is defined by the World Health Organization (WHO) as an abnormal and excessive body fat accumulation that can lead to severe consequences on individuals health (Anjos, 2006; Chooi *et al.*, 2019). The prevalence of this metabolic disorder has been increasing worldwide and, in 2005, about one third of world population was overweight or obese, and it is estimated, that by 2030, 57.8% of world population will be overweight or obese (Kelly *et al.*, 2008; Chooi *et al.*, 2019). Obesity is a condition that can occur both in adults, with special prevalence in women, as well as in children of all

ages, and is independent from geographic localisation, ethnicity, or socioeconomic level (Chooi *et al.*, 2019). The emergence of fast-food chains, sedentary lifestyle and overconsumption of energy-dense and nutrient-poor food are pointed as the main causes for this global issue by Chooi *et al.* (2019).

Obesity is caused by a long period of excessive energy consumption and low energy expenditure, where excess energy is transformed in triglyceride and stored in adipose tissue (Chooi *et al.*, 2019). According to Urbatzka *et al.* (2018), fat accumulation occurs mainly in adipocytes, that increase in size (adipocyte hypertrophy) or number (adipocyte hyperplasia), increasing body fat and causing weight gain. Althought adipocytes major function is calorie storage, they also play a crucial role as endrocrine cells, with mature adipocytes secreting cytokines that interfeers with food intake, inflamation, glucose and energy homeostasis, lipid metabolism and angiogeneses, affecting the whole-body metabolism (Church *et al.*, 2012; Urbatzka *et al.*, 2018). Chooi *et al.* (2019) said that obese individuals have higher risk to develop several other conditions associated with obesity, such as diabetes mellitus, cardiovascular diseases, cancer, musculoskeletal disorders, as well as mental health problems. There are several approaches to fight obesity including different diets, exercise, psychological therapies but these usually do not lead to a sustainable weight loss and results are disapointing at long-term. In particular, lifestyle changes, education for incorporating better nutrition and more physical exercise are important measures for the prevention of obesity. In severe cases of obesity, bariatic surgery is still the most effective way to guarantee weight loss and increase survival chances (Rodgers *et al.*, 2012). In 2018, six medications (Table 3) were approved by Food and Drug Administration (FDA) in USA for the treatment of obesity. These drugs included compounds that can regulate food intake, increase satiety, slowing gastric emptying, decrease intestinal lipid absorptions and decrease appetite (Srivastava & Apovian, 2018; Urbatzka *et al.*, 2018). Among these medications, Orlistat represents an interesting compound. Orlistat is a saturated derivative of lipstatin, a known inhibitor of pancreatic lipase and essential in intestinal fat digestion. Lipstatin was first isolated from the bacterium *Streptomyces toxytricini*, showing that anti-obesity compounds can be naturally produced by organisms (Barbier & Schneider, 1987; Weibel *et al.*, 1987).

Table 3 *Anti-obesity drugs approved by FDA in 2018. Adapted from Srivastava & Apovian, (2018).*

Medication	Mechanism of action	Year
Phentermine	TAAR1 agonists	1959
Orlistat	Lipase inhibition	1999
Phentermine/topiramate	Appetite suppressant/stimulant of the amphetamine and phenethylamine class; Anticonvulsant	2012
Lorcaserin	5-HT_{2C} receptor agonist	2012
Naltrexone/bupropion sustained-release	Opioid receptor antagonist; Norepinephrine-dopamine reuptake inhibitor and nicotinic acetylcholine receptor antagonist	2014
Liraglutide 3.0 mg	GLP-1 receptor agonist	2014

1.5.2. Diabetes

According to the World Health Organization (WHO), diabetes is defined as a chronic disease that occurs when the pancreas does not generate enough insulin, or the body cannot efficiently use the insulin it produces. In 2014, diabetes affected 8.5% of adults with 18 years or older and, in 2019, diabetes was the direct cause of 1.5 million deaths. This disease is among the main causes of diabetic macro and microvascular complications, major damage to the blood vessels, kidneys, eyes, nerves, and heart, resulting in disability of affected individuals, lower productivity, premature mortality, reduced life quality, and a substantial increase with health care costs (Tamayo *et al.*, 2014; American Diabetes Association, 2018). Diabetes condition can already be considered a global epidemic issue, one that is expected to continue to grow as the population ages, as obesity rates increases in adults, and as the minority groups that are at higher risk to develop diabetes also increases (Deshpande *et al.*, 2008). Tamayo *et al.* (2014) said that obesity, lack of physical activity, smoking, environmental pollutants, and socioeconomic deprivation are modifiable risk factors that can contribute for the increase of diabetic condition, and it is expected to exist more 10 million people living with diabetes in Europe by 2035.

Diabetes is a metabolic condition characterized by elevated blood glucose levels, also known as hyperglycaemia, that can lead to extensive damages to the body systems, especially nerves and blood vessels (Deshpande *et al.*, 2008). Clinically, there are 4 types of diabetes (Deshpande *et al.*, 2008):

I. Type 1, represents 5-10% of all diabetics and is usually caused by autoimmune, genetic or environmental factors;

II. Type 2, accounts 90-95% of all diagnosed cases of diabetes and is caused by an increasing resistance to insulin, and eventually pancreas cannot produce enough insulin to overcome the resistance;
III. Gestational diabetes, affects some women during pregnancy and requires a strict glycemic control and management of women in order to prevent birth complications, and problems in the developing chill. These women have 20-50% more risk for develop type 2 diabetes later in life;
IV. Diabetes caused by genetic defects, drugs, or chemicals.

Type 2 diabetes was, until recently, an adult disease, but with increasing childhood obesity rates, it is now common the diagnose among children and young adults. This is becoming a serious health problem that ends with more people dealing with diabetes most part of their lives, and with more risk of suffer from heart attacks, strokes, infections, foot ulcers, limb amputation, blindness, kidney failure, and other problems. In the last decade, several glucose lowering medications were approved by FDA, providing type 2 patients a way to manage their condition (Table 4). However, as diabetes is frequently accompanied with various co-morbidities and pharmaceuticals have a variety of side effects, including cardiovascular difficulties, acute renal failure, and pancreatitis, diabetes treatment requires a careful selection of medications for each patient (Sterrett *et al.*, 2016).

Table 4 *New glucose lowering medications approved by FDA in the last decade. Adapted from Sterrett et al. (2016).*

Class	Approved agents
GLP-1 Agonists	Exenatide, Exenatide extended release, Liraglutide, Dulaglutide and Albiglutide
SGLT-2 Inhibitors	Canagliflozin, Dapagliflozin and Empagliflozin
DPP-4 Inhibitors	Sitagliptin, Saxagliptin, Alogliptin and Linagliptin
Colesevelam	Colesevelam (Welchol)
Bromocriptine	Bromocriptine-QR

1.5.3. Non-alcoholic fatty liver disease

Non-alcoholic fatty liver disease (NAFLD) is a metabolic syndrome defined by an excessive accumulation of fat in the liver of patients that do not have an alcohol problem, a viral infection or other specific etiology of liver disease (Musso *et al.*, 2011; Buzzetti *et al.*, 2016). This condition affects 30-40% of adult world population and is most frequent in industrialized countries, being associated with the Western diet pattern (Buzzetti *et al.*, 2016; Teng *et al.*, 2020; Shih *et al.*, 2021). Most patients with NAFLD are asymptomatic and have other pathologies associated, such as obesity, hypertension, insulin resistance, inflammation, or type 2 diabetes, making it necessary to treat this condition in association with other metabolic diseases (Buzzetti *et al.*, 2016; Shih *et al.*, 2021). According to the literature, NAFLD comprises several conditions, from a simple fat accumulation in the liver (steatosis) to a histological phenotype non-alcoholic steatohepatitis (NASH) that can progress to advance steatosis plus necroinflammation, originating different stages of fibrosis and ultimately cirrhosis (Musso *et al.*, 2011; Buzzetti *et al.*, 2016). About 2.4 to 12.8% of NAFLD-associated cirrhosis patients develop a NAFLD-associated hepatocellular carcinoma (Teng *et al.*, 2020).

The complexity of this disease due to diverse etiologies, long period of development and genetic and physiological variations makes it difficult to understand the mechanisms underlaying its deterioration (Zhao *et al.*, 2021). Among the pathways described as important for NAFLD occurrence is the absorption, biosynthesis and excretion of cholesterol, absorption, lipogenesis and oxidation of triglycerides and fatty acid metabolism, which can represent targets for NAFLD therapeutics (Zhao *et al.*, 2021). Although no drug has been approved for the treatment of NAFLD condition, several compounds like polyphenols, lipids, proteins, and vitamins showed the ability to ameliorate NAFLD conditions. Marine proteins like from *Spirulina* biomass already showed beneficial effects for treating non-alcoholic fatty liver disease as a dietary supplement, and a small peptides (Metabolitin - MTL) also showed potential to be used as a therapeutic strategy (Teng *et al.*, 2020).

1.5.4. Inflammation

Inflammation is an important process involved in animal cells defence against injuries and pathogens, and can be acute or chronical (Abdulkhaleq *et al.*, 2018). Neurodegenerative disorders, cardiovascular diseases and cancer are some of the causes of chronic inflammation (Abdulkhaleq *et al.*, 2018). On the other hand, acute inflammation avert the host from pathogens and accelerate the healing process (Piwowarski *et al.*, 2015). Inflammation process is instigated by cellular and vascular

events that lead to changes on physical location of white blood cells, plasma, and fluids at the site of inflammation (Abdulkhaleq *et al.*, 2018). Macrophage's activation is an important step during initiation and dissemination of inflammatory response. These white blood cells produce inflammatory mediators like cytokines, tumor necrosis factor-alpha (TNF-α), nitric oxide (NO) and prostaglandins, involved in diseases like asthma, pulmonary fibrosis, rheumatoid arthritis and atherosclerosis (Kim *et al.*, 2006; Reddy & Reddanna, 2009; Lee, 2011). The oxidation of l-arginine by NO synthase (NOS) produces a reactive radical molecule (nitric oxide – NO) essential to host immune responses, but also to regulate physiological functions like neurotransmission, neurotoxicity and vasodilation, however, when in excess, it promotes the development of inflammatory diseases and autoimmune disorders (Cherng *et al.*, 2007; Yoon *et al.*, 2009). Therefore, inhibition of NO production is considered a main target for anti-inflammatory drugs development (Kim *et al.*, 2006; Cherng *et al.*, 2007; Yoon *et al.*, 2009).

Non-steroidal inflammatory drugs (NSAIDs) are the most used compounds to fight inflammation. These affect mostly the prostaglandins production by interfering with cyclo-oxygenase (COX) system (Vane & Botting, 1998; Howes, 2017). COX-1, a COX isozyme, has constitutive expression and produce prostaglandins that protect stomach and kidney against damage. On the other hand, COX-2 is stimulated by cytokines during inflammation and produce prostaglandins involved in pain and swelling (Vane & Botting, 1998). Drugs development focus mostly on selective COX-2 inhibitors, sidestepping COX-1 which is thought to be the main cause of adverse reaction especially in the gastro-intestinal tract (Rainsford, 2007). COX-2 inhibitors also showed some concerning side effects like higher risk of myocardial infarctions, hypertension, or higher blood pressure (Rainsford, 2007). Nutraceuticals may present a complement for anti-inflammatory drugs that allow dose reduction and amelioration of side effects (Al-okbi, 2014). Several nutraceuticals have already shown the ability to inhibit molecular targets implicated in the inflammatory process, sharing common molecular targets with NSAIDs and steroidal drugs (SAIDs) (Table 5) (Huang *et al.*, 2004).

Table 5 *Effect of several known nutraceuticals on pro-inflammatory mechanisms. Adapted from Huang et al. (2004).*

Nutraceuticals	Effects on pro-inflammatory mechanisms
Vitamin E	Inhibits oxidative stress Inhibits leukocyte adhesion to endothelium
Vitamin C	Suppress TNFα-induced NFκB activation Blocks inflammatory cytokine expression
Curcumin	Inhibits activity of PLA_2, COX_2, LOX, iNOS and myeloperoxidase
Resveratrol	Inhibits activity of iNOS, AA release, production of pro-inflammatory cytokines, and expression of COX_2
Green tea	Inhibits activation and translocation of NFκB, and expression of COX_2
Black tea	Inhibit carcinogen-induced expression of COX_2, iNOS, glutathione-S-transferase, and NFκB activation
Genistein	Inhibits production of pro-inflammatory cytokines, COX_2 expression, NFκB activation
Omega-3 fatty acid	Decreases PGE_2 and LTB_4 levels

1.6. *In vivo* and *in vitro* models

1.6.1. Zebrafish

Drugs investigation requires several biochemical and cellular assays to better understand its mechanisms of action before testing in animal model organisms and clinical trials (Zon & Peterson, 2005). Model organisms can be defined as well studied species that allow the investigation of a wide range of biological processes and collected data may have some applicability to other organisms (Leonelli & Ankeny, 2013). Rodents, dogs, and pigs were until recently the model organisms used in the preclinical analysis for human diseases given its complexity and similarity to humans. Laboratory maintenance and pressure to decrease animal usage in research promoted the discovery of other organisms that can be an useful and cost-effective alternative to mammalian models (Zon & Peterson, 2005). Zebrafish (*Danio rerio*) is a cyprinoid teleost and a small freshwater fish first found in rivers in India and are now common in pet stores and aquariums all over the world (Banga, 1998). Easy to maintain in aquariums, with short generation time and a large offspring, these animals became a central key in modern biological investigation (Banga, 1998). With all key organs involved in

metabolism control in humans, from the appetite circuits in the hypothalamus to the pancreas and insulin-sensitive tissue [liver, muscle and white adipose tissue (WAT)], zebrafish is a good model to study metabolic diseases such as diabetes and obesity (Seth *et al.*, 2013). Zebrafish, on the other hand, lack brown adipocyte tissue and are ectodermal creatures, whose metabolic rate is controlled by temperature, whereas humans are endothermal. Furthermore, genome duplications that result in the existence of multiple copies of various genes, such as the duplication of the genes encoding leptin-a and leptin-b, may contribute to metabolic pathway redundancy and reduce the utility of zebrafish in genetic studies (Nguyen *et al.*, 2013). Although as in humans, these striped animals store excess nutrients in lipid droplets in white adipocytes and use the liver as an adipose store. Regulation of energy balance is also conserved between humans and zebrafish, and response of leptin receptor, melanocortin system and neuropeptide NPY leads to an increase in food intake, as well as administration of cocaine and amphetamine regulated transcript peptide (CART) and corticotropin releasing factor (CRF) decrease food consumption (Seth *et al.*, 2013). Like in humans, zebrafish also possesses a pancreas with exocrine and endocrine compartments connected by a ductal system to the digestive tract. Pancreatic islets are constituted by β-cells (insulin-producers), α-cells (glucagon-producers), δ-cells (somatostatin producers) and ε-cells (ghrelin producers), and primary islets can be identified at 24 hours post-fertilization (hpf) (Seth *et al.*, 2013). Optical transparency of zebrafish embryos allows the study of functional and morphological changes in yearly stages of development (Zon & Peterson, 2005), especially when using staining compounds like Nile red (lipid staining) and 2-NBDG (fluorescent glucose analog). In this way, zebrafish reveals to be a model organism suitable for the study of metabolic diseases like obesity and diabetes, as well as for the screening of bioactive compounds (Zang *et al.*, 2018).

1.6.2. HepG2 cells

Drug induced hepatotoxicity is one of the reasons for candidate drugs rejection in the later stages of drug development. Therefore, *in vitro* assays are essential to determined drugs potential to induce liver injury before testing in animals and clinical trials (Gerets *et al.*, 2012). HepG2 cells have proven to be a convenient and quantifiable *in vitro* model, useful for a better understanding of pathogenesis and effects of therapies in NAFLD (Cui *et al.*, 2010). Human hepatoma cell lines, like HepG2, are commonly used to study drugs metabolism and hepatotoxicity due to their high availability, stable phenotype and easy handling (Gerets *et al.*, 2012). These cells are highly differentiated and exhibit a genotype of normal liver cells, being capable of synthetise and secrete plasma proteins, metabolize cholesterol and triglycerides, metabolize and transport lipoproteins, insulin

signalling, among other hepatic functions (Gerets *et al.*, 2012; Vinken & Rogiers, 2015). Assays involving Nile red binding to HepG2 cells have showed good results when tested with compounds known to stimulate hepatic steatosis and demonstrated to be an helpful *in vitro* model to screen for new potential medications (McMillian *et al.*, 2001). Although these cells show low metabolic capacity when compared with primary hepatocytes, and reduced expression of enzymes and transporters involved in drugs metabolism, they show similar sensitivity to steatosis-inducing compounds as primary hepatocytes (McMillian *et al.*, 2001; Gerets *et al.*, 2012; Vinken & Rogiers, 2015). Consequently, HepG2 cells prove to be a suitable model to study compounds able to affect intracellular lipid accumulation.

1.6.3. Raw 264.7 cells

Cell lines are used for *in vitro* and *in vivo* studies given their similar genotype and phenotype through consecutive passages, consistency availability, and experimental reproducibility (Merly & Smith, 2017; Taciak *et al.*, 2018). RAW 264.7, originated from Abelson leukemia virus transformed cell line derived from BALB/c mice cells, are used in investigation as a monocyte/macrophage model (Kong *et al.*, 2019). Macrophages are able to rapidly adapt to different environmental conditions and new stimuli, and can be classified accordingly to produced cytokines and expressed surface markers (Taciak *et al.*, 2018). M1 macrophages are activated by lipopolysaccharide (LPS) and inferon gamma (IFN-γ) and are pro-inflamatory cells (Taciak *et al.*, 2018). M2 macrophages are anti-inflamatory cells activated by interleukin 4 (IL-4) and interleukin 10 (IL-10) (Taciak *et al.*, 2018). These murine-derived cells are capable of pinocytosis and phagocytosis and when stimulated with lipopolysaccharide (LPS), nitric oxide (NO) production is augmented and phagocytosis increased (Taciak *et al.*, 2018; Kong *et al.*, 2019). These cells have being used as an indicative of the potential response of primary human cells and diverse studies have been performed in order to stablish anti-inflammatory proprieties of compounds using these cell line (Kim *et al.*, 2006; Reddy & Reddanna, 2009; Piwowarski *et al.*, 2015). In this way, RAW 264.7 cells prove to be an appropriate model to screen for compounds able to interfere with inflammatory pathways.

1.7. Objectives

This work aimed to study the bioactivity potential of cone snails endemic from Cabo Verde archipelago, which represent a major part on the diversity found in the genus *Conus*. To do so, two vermivorous species of cone snails were analysed, namely *Conus venulatus* and *Conus ateralbus*. These species are little studied from chemical and the pharmacological point of view, existing only one conotoxin described for *C. ateralbus*. These conotoxin was first reported in Neves *et al.* (2019), an δ-conotoxin-like AtVIA with high homology to conotoxins already described for species in the subgenus Tesseliconus, also worm-eating species and with proved bioactivity on vertebrate Na^+ channels.

To study species of *Conus* endemic from Cabo Verde, on the specific objectives were the following:

I. Analysis and characterization of the venom of different cone snails endemic from Cabo Verde archipelago;
II. Analysis of toxins diversity within the venoms including identification, and comparison of toxins' molecular masses;
III. Evaluation of the bioactivity of *Conus* species for metabolic diseases considering assays relevant for obesity, diabetes, steatosis and inflammation;
IV. Identify conotoxins / conopeptides in the venom of active samples, which may be interesting from a pharmacological point of view.

2. METHODS

2.1. Materials and reagents

C18 Vydac 218TP column was purchase from Hichrom (Berkshire, United Kingdom). Acetonitrille (ACN, gradient grade for HPLC) was purchase from Carlo Erba Reagents (Barcelona, Spain). Trifluoroacetic acid (TFA) was purchase from Sigma-Aldrich (Missouri, USA). Ethyl 3-aminobenzoate methanesulfonate 98% (MS-222) was purchase from ACROS Organics. Nile red was purchase from Sigma-Aldrich. 1-Phenyl-2-thiourea 97% (PTU) was purchase from ACROS Organics. Dimethyl sulfoxide (DMSO) was purchase from VWR. Sulforhodamine B (SRB) was purchase from Sigma-Aldrich. N-(1-Naphtyl)-ethylenediamine dihydrochloride was purchase from Sigma-Aldrich. All reagents used in HPLC were of analytical grade.

2.2. Specimen collection and Venom preparation

Specimens of *Conus ateralbus* were collected from the Sal island, and *Conus venulatus* were collected from Boavista island in Cabo Verde archipelago. Dissection step was performed as described by Neves *et al.* (2019). Each frozen specimen was dissected, exposing the *Conus* venom apparatus, which is formed by a venom bulb and venom duct (Figure 2). Individual venom ducts of specimens were dissected. The venom was obtained from the venom ducts by placing each duct on an ice-cold metal spatula, then squeeze by Eppendorf pipette tips. The content of the venom duct was diluted in ~

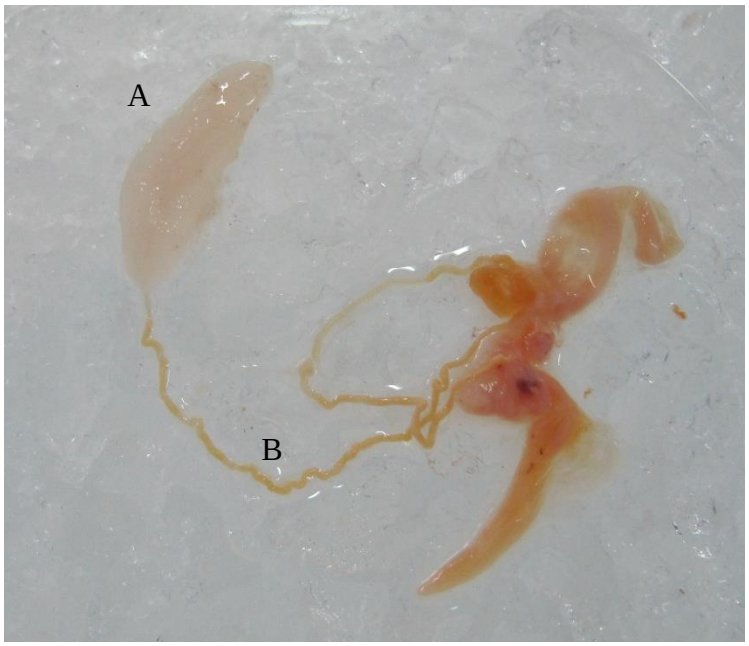

Figure 2 *Venom apparatus dissection. It is possible to observe the venom bulb (A) and the venom duct (B). The venom was squeezed from the venom duct.*

600 µL of 0.1 % formic acid freeze-dried and stored at -80ºC until use. The frozen venom was lyophilized (-54.4 ºC; 0.070 mBar) for 72 hours or more, until completely dehydrated. Venom was weighted and stored at -20ºC until use.

2.3. Venom extraction

Lyophilized venom (~ 40 mg) was resuspended in 3 mL of extraction solution (40% acetonitrile (ACN), 0.1% trifluoroacetic acid (TFA) in water). Each sample was mechanically disrupted in a tissue crusher (6 times; up and down), and centrifuged at 13000 rpm for 5 min (4 ºC). Supernatants were transferred to another Falcon tube and centrifuged at same conditions. Pellets and supernatants were store at -20 ºC, until further use.

2.4. HPLC conopeptide fractionation

Extracted venom was fractionated by reverse-phase high performance liquid chromatography (RP- HPLC) using an Alliance Waters e2695 separation module fitted with a detector and operated with the Empower 2.0 software. Fractionation was performed using a semipreparative C18 column (5 µm particle size, 10 /// 250 mm, Vydac 218TP). For a better chromatographic separation, several conditions were tested in *Conus ateralbus* samples, using an injection volume of 100 µL. The solvent gradient used during the tests are shown in Table 6. Flow rate of 1 ml/min and 3 ml/min was also tested under these conditions. Absorbance was monitored at 220nm and 280nm. Finally, a total of 51 fractions of the venom were collected using an injection volume of 800 µL, flow rate of 1mL/min and gradient 2. Fractions were dehydrated and stored at -20 ºC until further use.

Table 6 *Solvent gradients and mobile phase composition used in RP-HPLC method.*

	Solvent		
	Time (min)	**A (0.1% TFA: H_2O) %**	**B (90% ACN:0.1% TFA: H_2O) %**
Gradient 1	0	90	10
	10	80	20
	25	50	50
	50	0	100
Gradient 2	0	90	10
	5	90	10
	25	70	30
	50	50	50
	80	0	100
	95	0	100

2.5. Zebrafish Nile Red Fat Metabolism Assay

Collected fractions were screened for lipid reducing activity using zebrafish Nile red fat metabolism assay, as described in Urbatzka *et al.* (2018). Zebrafish embryos were raised from 1 DPF (days post-fertilization) in egg water (60 µg/mL marine sea salt dissolved in distilled H_2O) with 200 µM PTU (1-phenyl-2-thiourea) to inhibit pigmentation. From 3 to 5 DPF, zebrafish larvae were exposed to extracts at a final concentration of 10 µg/mL in egg water with daily renewal of water and extracts in a 48 well plate with a density of 5-7 larvae/well. A solvent control (0.1% dimethyl sulfoxide, DMSO) and positive control (REV, resveratrol, final concentration 50 µM) were included in the assay. Figure 3 shows a diagram of the 48-well plates used during this assay. Lipids were stained with Nile red overnight at the final concentration of 10 ng/mL. For imaging, the larvae were anaesthetized with tricaine (MS-222, 0.03%) for 5 min and analysed in a fluorescence microscope (Leica DM6000B, Wetzlar, Germany). Fluorescence intensity was quantified in individual zebrafish larvae by ImageJ.

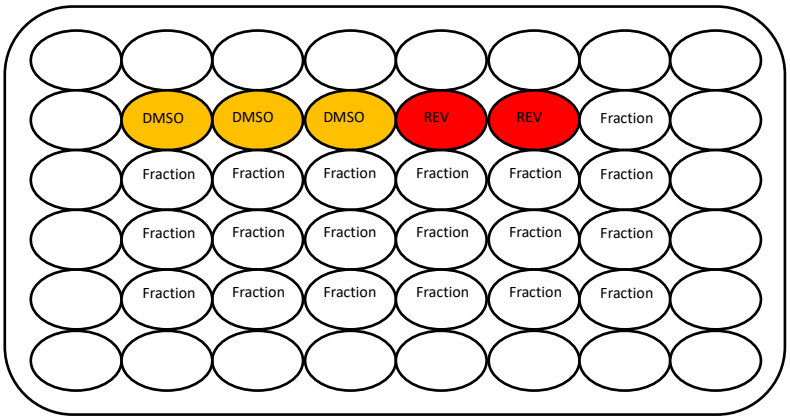

Figure 3 *Diagram of the 48-well plate used in Zebrafish Nile Red Fat Metabolism Assay. Yellow wells represent solvent controls (DMSO 0.1%). Red wells represent positive control (REV 50 µM). White wells represent fractions tested at a concentration of 10 µg/mL.*

2.6. Glucose Uptake Assay

Fractions were tested in a glucose uptake assay using 2-NBDG in zebrafish embryos, as described in Wang *et al.* (2020). Zebrafish embryos were raised from 1 DPF (days post-fertilization) in egg water (60 µg/mL marine sea salt dissolved in distilled H_2O) with 200 µM PTU (1-phenyl-2-thiourea) to inhibit pigmentation. 3 DPF zebrafish larvae were exposed to extracts at a final concentration of 10 µg/mL in egg water in a 96 well plate with a density of 5-6 larvae/well. A solvent control (0.1% DMSO) and a positive control (EMODIN, 6-methyl-1,3,8-trihydroxyanthraquinone, final concentration 10 µM) were included in the assay. Figure 4 shows a diagram of the 96-well plates used during this assay. One hour after exposure to the fractions, egg water and compounds were removed, and the larvae were incubated with egg water containing 2-NBDG (0.6 mM)

for 3h. After incubation period egg water and 2-NBDG were removed. The larvae were washed with egg water until yellow coloration completely removed, and anesthetized with tricaine (MS-222, 0.03%) for 5 min and analysed in a fluorescence microscope (Olympus, BX-41, Hamburg, Germany). Fluorescence intensity was quantified in individual zebrafish larvae by ImageJ.

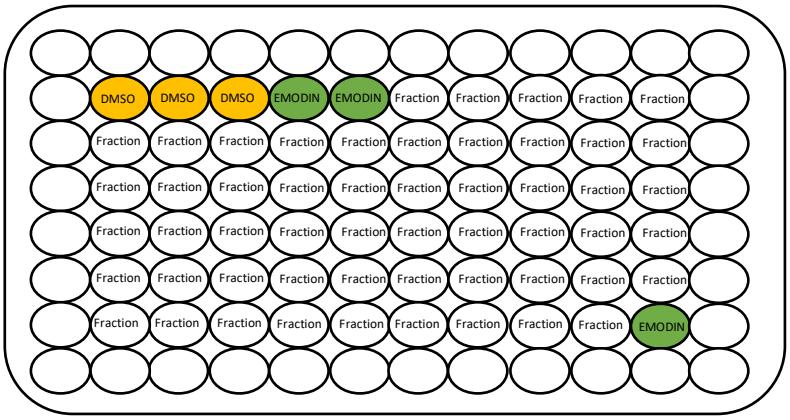

Figure 4 *Diagram of the 96-well plate used in Glucose Uptake Assay. Yellow wells represent solvent controls (DMSO 0.1%). Green wells represent positive control (EMODIN 10 µM). White wells represent fractions tested at a concentration of 10 µg/mL.*

2.7. Anti-steatosis Assay

HepG2 cells were obtained from American Type Culture Collection (ATCC) (Manassas, VA, USA) and cultured in Dulbecco Modified Eagle Medium (DMEM) (Gibco, Thermo Fisher Scientific, Waltham, MA, USA). Cells were grown in DMEM supplemented with 10% (v/v) fetal bovine serum, 1% penicillin/streptomycin (100 IU mL^{-1} and 10 mg mL^{-1}, respectively, and 0.1% amphotericin, and incubated in a humidified atmosphere with 5% CO_2, at 37 ºC. HepG2 cells were seeded in 96-well plates at $1.25x10^5$ cells/ml and adhered overnight. Lipid droplets were induced by medium change to DMEM supplemented with 62 µM sodium oleate. A solvent control (DMSO 0.5% and SO 62 µM) and two negative controls (MeOH 0.5%, DMSO 0.5%) were included in this assay. Fractions were added to wells at a final concentration of 10 µg/mL and incubated for 6 hours in a humidified incubator. Figure 5 shows a diagram of the 96-well plates used during this assay. Cell were stained with 75 ng/mL Nile red and 10 µg/mL Hoechst 33342 (HO-33342) in Hank's Buffered Salt Solution medium (HBSS), and incubated for 15 min in the dark, at 37 ºC. Cells were washed three times with HBSS and fluorescence was read in a BioTek™ Cytation™ 5 Cell Imaging Multi-Mode Reader with an imaging approach in the blue and red fluorescence channel with an 20x objective. Gen5+ software was used to detect cells, nucleus and cytoplasm. Nile red fluorescence (neutral lipids) was normalized to Hoechst 33342 fluorescence (nucleus stain) in order to correct the fluorescence for cell number variations. Following, cells were fixed with ice-cold 50%

(w/v) trichloroacetic acid (TCA) for 1 h at 4 ºC in the dark, and then washed four times with dH_2O. Plates were air-dried at room temperature, and stained with 0.4% (w/v) sulforhodamine B (SRB) in 1% of acetic acid, for 15 min. Unbound SRB was washed with acetic acid 1%, four times, and plates air-dried at room temperature. Bound dyes were solubilized with Tris hydrochloride (Tris-HCl) (10 mmol/L; pH=10.5), and absorbance was read in the microplate reader at 492 nm with reference at 554 nm for cell viability.

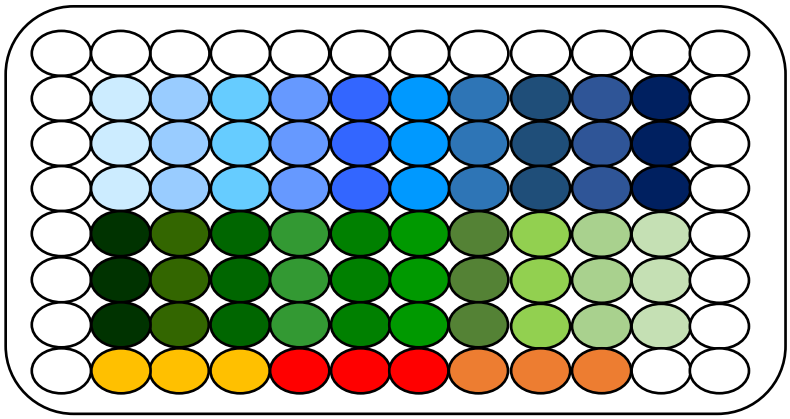

Figure 5 *Diagram of the 96-well plate used in Anti-steatosis Assay. Yellow wells represent negative control (DMSO 0.5%). Orange wells represent negative control (MeOH 0.5%). Red wells represent solvent control (DMSO 0.5% and SO 62 µM). Blue and green wells represent fractions tested at a concentration of 10 µg/mL. Fractions were tested in triplicate.*

2.8. Inflammatory Assay

RAW 264.7 macrophage cells were obtained from American Type Culture Collection (ATCC) (Manassas, VA, USA) and cultured in Dulbecco Modified Eagle Medium (DMEM) (Gibco, Thermo Fisher Scientific, Waltham, MA, USA). Cells were grown in DMEM supplemented with 10% (v/v) fetal bovine serum, 1% penicillin/streptomycin (100 IU mL^{-1} and 10 mg mL^{-1}, respectively, and 0.1% amphotericin, and incubated in a humidified atmosphere with 5% CO_2, at 37 ºC. RAW 264.7 cells were seeded in 96-well plates at $3.5x10^5$ cells/ml and adhered overnight. For the anti-inflammation activity, inflammation was induced by lipopolysaccharides (LPS) from *Escherichia coli* 0111:B4 (LPS, Sigma, USA) to a final concentration of 1µg/mL. In pro-inflammatory assay, medium was renewed and fractions were added to wells at a final concentration of 10 µg/mL and incubated for 24 hours in a humidified incubator. Figure 6 shows a diagram of the 96-well plates used during this assay. Liquid content of wells was transferred to new 96-well plates and 75 µL of Griess solution [sulfanilamide 1% (m/v); N-(1-Naphthyl)ethylenediamine dihydrochloride 0.1% (m/v) in H_3PO_4 2% (v/v)] was added. Plates were shacken in the dark for 15 min and NO absorbance was read in a Synergy HT multi-detection microplate reader (Biotek) at 562 nm. Seeded cells were exposed to

5 mg mL^{-1} MTT and incubated at 37 ◦C for 45 min. Medium was removed and 100 µL DMSO added to each well. Absorbance was read in a Synergy HT multi-detection microplate reader (Biotek) at 510 nm.

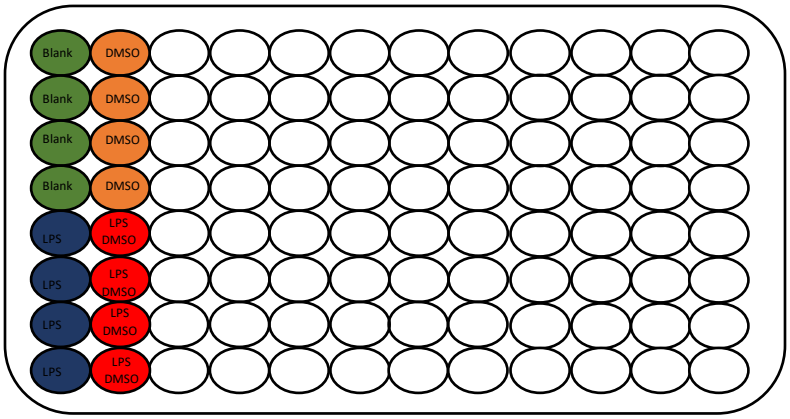

Figure 6 *Diagram of the 96-well plate used in Inflammatory Assays. Orange wells represent negative controls (DMSO 0.5%). Red wells represent solvent control (LPS and DMSO). Green and blue wells served for internal quality evaluation of the assay. White wells represent fractions tested at a concentration of 10 µg/mL, co-exposed to LPS in the anti-inflammatory assays, and without LPS in the pro-inflammatory assay*

2.9. Proteomics Analyses

A fraction with promising bioactivity was sent to the Chemistry Department from University of Aveiro (Prof. Pedro Domingues), in order to proceed with further identification and *de novo* sequencing of peptides, using LC-ESI-HR-MS/MS technique. For this procedure, clean-up of the LC fraction was performed using SPE solid-phase extraction (Pierce™ C18 Spin Columns, Pierce) according to the manufacturer´s protocol. The peptides recovered from the SPE column were resuspended in 1% formic acid (FA) and analysed with a QExactive Orbitrap (Thermo Fisher Scientific, Bremen, Germany) through the EASY-spray nano ESI source (Thermo Fisher Scientific) that was coupled to an Ultimate 3000 (Dionex, Sunnyvale, CA) high-pressure liquid chromatography (HPLC) system. The trap column (100 µm I.D. x 2 cm packed with Acclaim PepMap RSLC C18, 5 µm 100 Å) and the EASY-spray analytical (75 µm I.D. x 75 cm packed with Acclaim PepMap RSLC C18, 3 µm 100 Å) columns were from Thermo Fisher Scientific. Peptides were trapped at 30 µL/min in 96% solvent A (0.1% FA). Elution was achieved at a flow rate of 300 nL/min using a 92 min gradient used as follows: 0–3 min, 96% solvent A; 3–70 min, 4–25% solvent B; 70–90 min, 25–40% solvent B; 90–92 min, 90% solvent B; 92–100 min, 90% solvent B; 101-120 min, 96% solvent A. The mass spectrometer was operated at 1.8 kV in the data-dependent acquisition mode. A tandem MS (MS/MS) method was used with a survey scan from 400 to 1600 m/z (resolution

70,000; auto gain control (AGC) target 1E6). The 10 most intense peaks were subjected to higher-energy collisional dissociation to obtain MS/MS spectrum (resolution 17,500; AGC target 5E4, normalized collision energy 28%, max. injection time 100 ms and dynamic exclusion 35 s). Raw spectra generated were processed and analysed using Proteome Discoverer software version 2.2 (Thermo Fisher Scientific), with the MS Amanda (version 2.0, University of Applied Sciences Upper Austria, Research Institute of Molecular Pathology) and Sequest HT search engines. Uniprot (TrEMBL and Swiss-Prot) protein sequence database (version of July 2021) was used for all searches under "Gastropoda [6448]" annotation:(type:"tissue specificity" venom) AND reviewed:yes. The peptide mass tolerance was 10 ppm and fragment ion mass tolerance was 0.02 Da.

2.10. MALDI-TOF Analyses

Conus venulatus and *Conus ateralbus* venom samples were analysed using the MALDI-TOF technology in cooperation with the University of Utah to identify the mass range of peptides contained in the venoms. Procedures were performed as described in Neves *et al.*, 2013. Samples were concentrated and cleaned according to the manufacturer's instructions on a micro C18 ZipTiP column (Millipore, Bedford, MA, USA). The peptides were eluted directly onto the MALDI plate using the matrix α-cyano-4-hydroxycinnamic acid (α-CHCA) at 5 mg/mL prepared in ACN (50%), and formic acid (0.1%). Peptide mass spectrometry analyses were performed by MALDI-TOF/TOF (4700 Proteomics Analyzer, AB SCIEX, Foster City, CA, USA) in reflector positive mode (600–5000 Da).

2.11. Statistical Analysis

Statistical analysis was performed using GraphPad® Prism 7 program. The assumption for ANOVA was tested by a normality test, namely Shapiro-Wilk and Kolmogorov-Smirnov normality test (p value < 0.05). If normality was met, the difference between control group and all fractions was analysed by Ordinary one-way ANOVA with Dunnett's posthoc test (p value < 0.05). Equal variance was analysed by Barthlett's test, and if this assumption was not met, Brown-Forsythe and Welch ANOVA tests and Holm-Sidak's multiple comparisons test was applied. If data did not pass normality test, the difference between control group and all fractions was analysed by Kruskal-Wallis with Dunn's posthoc test (p value < 0.05). Data were represented as box-whisker plots with plot in 5-95 percentiles, and as column bar graphs with plot in mean with standard deviation (SD). Significant differences were indicated by asterisks (*).

3. RESULTS

3.1. RP-HPLC profiling of *Conus ateralbus* and *Conus venulatus*

3.1.1. Gradient solvent optimization

During the first couple of months the work was focused on *Conus* venom apparatus dissection to obtain the crude venom for subsequent analysis. After extraction of venom components, solvent gradient for RP-HPLC was optimized using *Conus ateralbus* venom, since this species is already studied and its chromatographic profile characterized (Neves *et al.*, 2019). Only gradient 1 and 2 are shown, since these were the ones that allowed a better separation of venom constituents during the initial tests. A flow rate of 1 mL/min and an injection volume of 100 µL was used for testing. Chromatographic profile of *Conus ateralbus* with gradient 1 is shown in Appendix I. With this gradient, initial peaks were detected after 7 min of run, which match to 17% of solvent B, revealing the polarity of several peptides found in the venoms. For instance, around

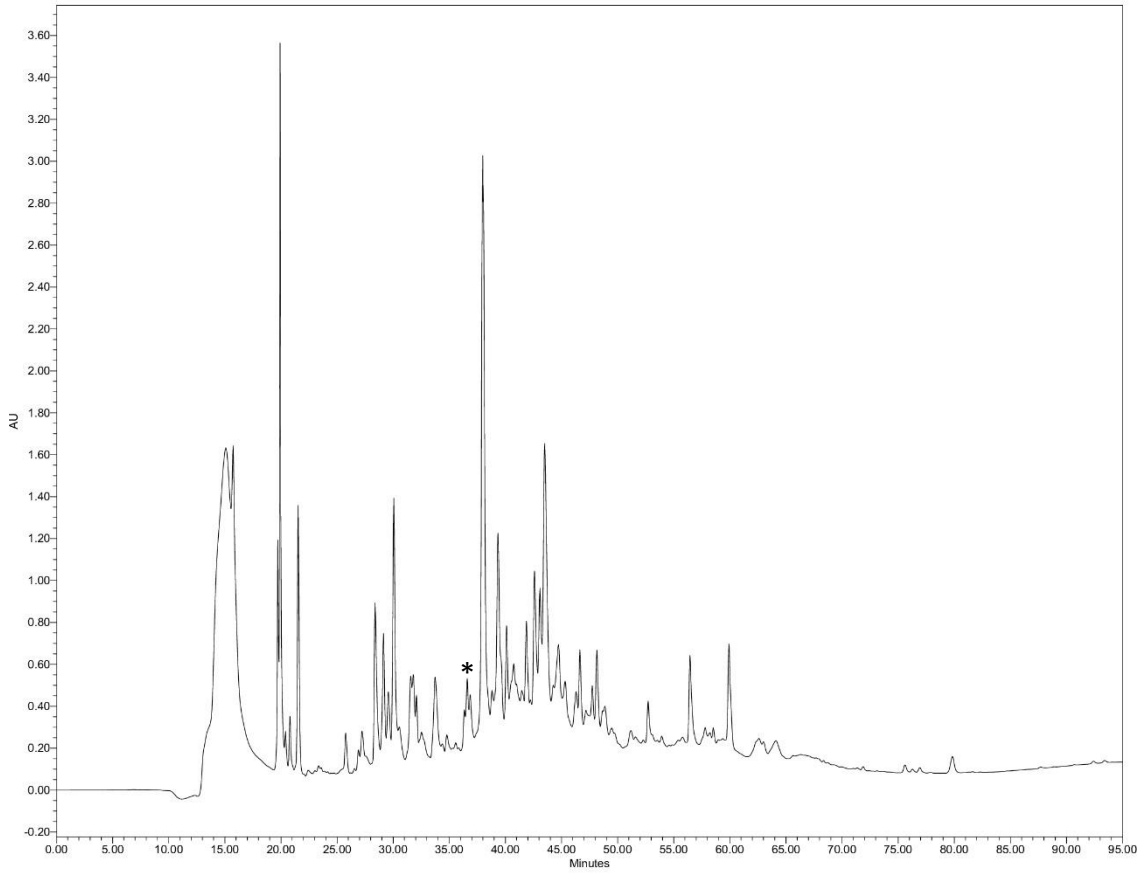

Figure 7 *Chromatographic profile of Conus ateralbus using gradient 2. More polar compounds eluted around 13 min of running with good resolution. Nonpolar compounds eluted with almost 36% of solvent B. RP-HPLC revealed a profile with good peak resolution, compounds well separated and a low baseline. The most active fraction is marked by asterisks *.*

28 min more peaks were observed, indicating the presence of nonpolar compounds. These compounds eluted at 36% of solvent B. Chromatogram analysis suggests that nonpolar peaks must represent a mixture of compounds since the peaks are not well separated and with little resolution, and the baseline is elevated. To separate these compounds, gradient 2 was created. Figure 7 shows the chromatogram obtained with this gradient. Initial peaks eluted with 18% of solvent B, with 13 min of the run, confirming the profile record with gradient 1. Using this gradient, the separation of the nonpolar compounds was achieved, approaching the registered baseline in control, and obtaining good resolution of the peaks. This gradient was also tested with *Conus venulatus* venom to determine chromatographic profile and to confirm if it would be suitable for this specie (Figure 8). Chromatogram analysis showed that *Conus venulatus* has less peaks/compounds than *Conus ateralbus*, although the elution times of the compounds are relatively similar. The most polar conopeptides were detected around 13 minutes of running, as in *Conus ateralbus*. In turn, the most apolar peaks eluted after 32 minutes, equivalent to about 36% solvent B. Gradient 2 showed good peak resolution and low baseline for both species and was chosen for fractionation of venoms. Compounds separation was established with an injection volume of 800 µL, at a concentration of 12

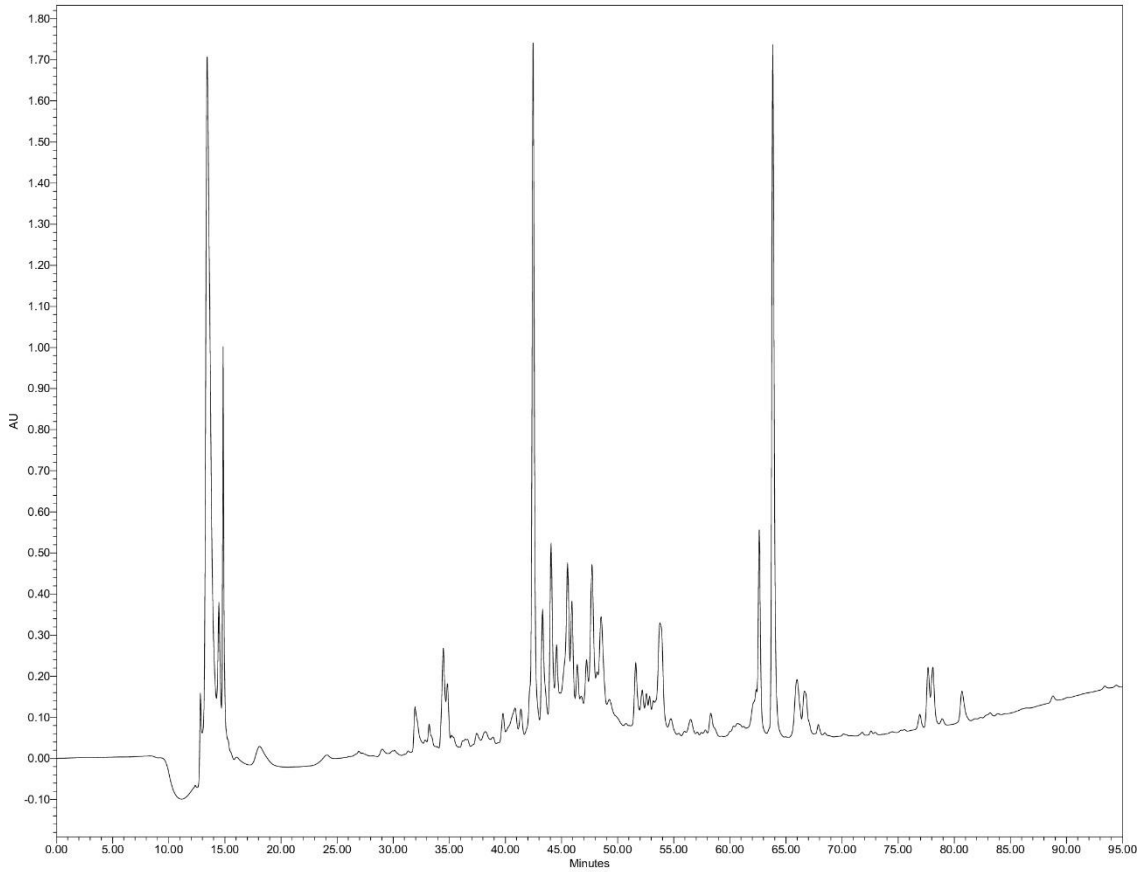

Figure 8 *Chromatographic profile of Conus venulatus using gradient 2. More polar compounds eluted at 13 min of running. Nonpolar compounds eluted with approximately 36% of solvent B. RP-HPLC revealed a profile with good peak resolution, compounds well separated and a low baseline.*

mg/mL. A flow rate of 3 mL/min was tested with this injection volume. The chromatogram obtained with these conditions can be consulted at Appendix II. An injection of 8x more sample volume led to higher intensity of detected peaks, consistent with the increase in the amount of injected compounds. It was also flagrant that all venom compounds eluted in an initial phase of running, which indicates that a flow rate of 3 mL/min conducted to a premature elution of compounds and consequently chromatographic profile reversion. Considering these results, separation and collection of fractions was done with a flow rate of 1 mL/min and an injection volume of 800 µL per sample. Two RP-HPLC runs were performed for fractionation and a total of 51 fractions were obtained. After dried, fractions were dissolved in DMSO 40% in water to a concentration of 4 mg/mL. Table A from Appendix III indicates fractions weight after dry.

3.2. Compounds mass range distribution

Venom samples from *Conus venulatus* and *Conus ateralbus* were analysed using Maldi-TOF to detect compound molecular masses within the venoms (Figure 9). The data showed here was previously gathered by Dr. Jorge Neves in collaboration with University of Utah. Compounds with molecular weights ranging from 600 to 5000 Da could be detected using this approach. There were 109 mass peaks in *Conus ateralbus* samples. Almost 66% of these masses had a molecular mass of 600 to 4000 Da, while 33% had a molecular mass of 4000 Da or higher. However, the majority of the peaks had a molecular mass of 1500 to 2000 Da (33%). *Conus venulatus*, on the other hand, has a different mass distribution than *Conus ateralbus*, and less mass peaks (81) in its venom. In this sample, molecules with molecular weights of 3000 Da or greater account for 63% of the venom composition, while smaller molecular masses account for just 36% of the venom. The most common molecular masses were greater than 5000 Da, accounting for around 30% of all masses discovered.

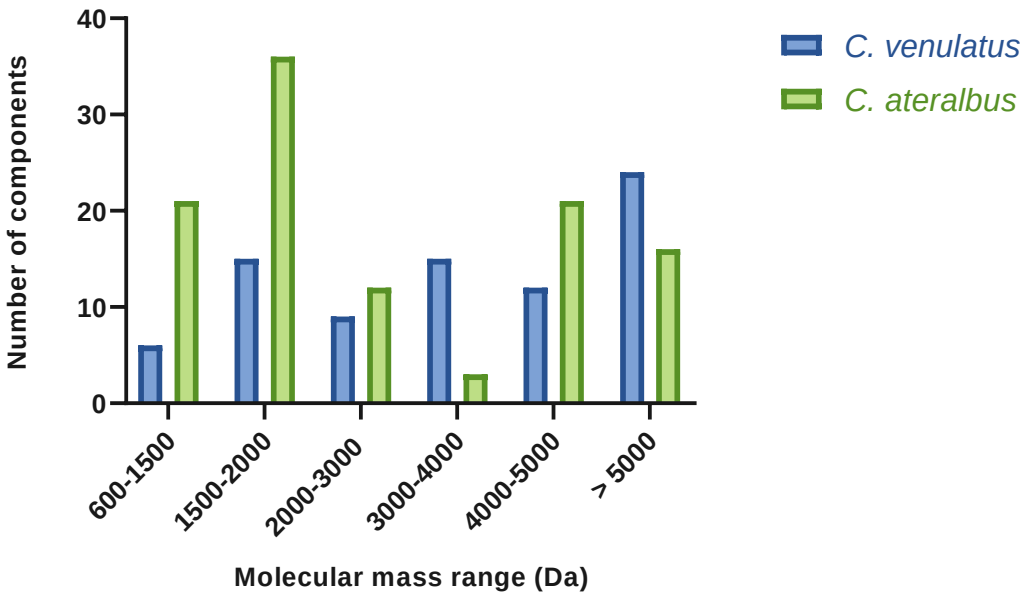

Figure 9 *Molecular mass range distribution of venom compounds detected by Matrix-assisted laser desorption ionization couple to time-of-flight mass spectrometer (Maldi-TOF) analysis.*

3.3. Bioactivity Assays

3.3.1. Lipid reducing activity in Zebrafish Larvae

Conus fractions obtained from RP-HPLC separation were tested in zebrafish and cellular bioassays. First bioactivity screen was lipid reducing activity and was performed in zebrafish larvae 5 days post-fertilization (DPF), using the zebrafish Nile red fat metabolism assay. Dimethyl sulfoxide (DMSO) was used as solvent control and showed a strong red fluorescence signal on zebrafish yolk sac, indicating lipid accumulation in that region. Resveratrol (Rev) was used as a positive control and was able to significantly reduce lipid accumulation on zebrafish yolk sac.

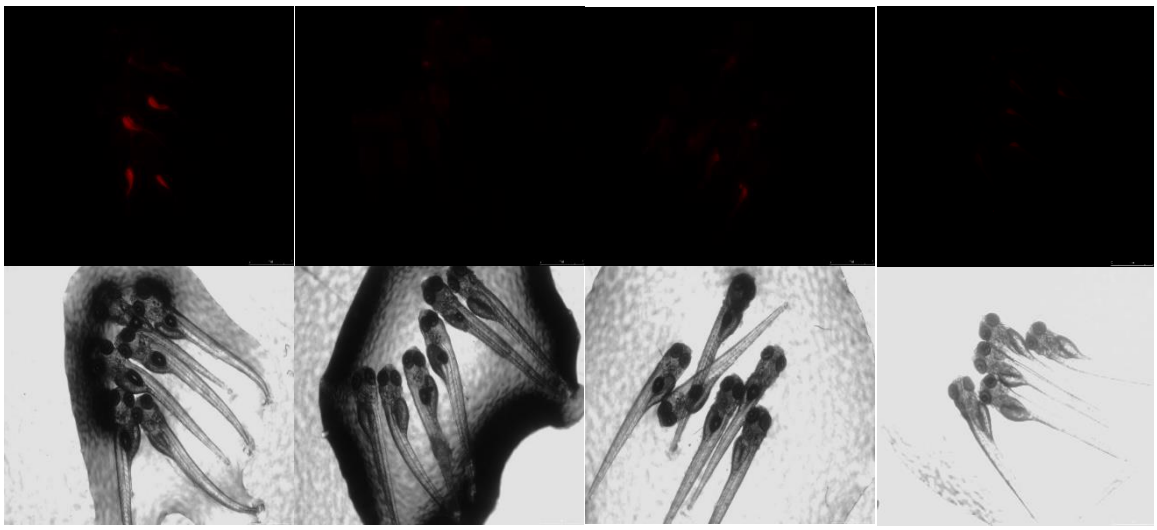

Figure 10 *Representative images of zebrafish Nile red fat metabolism assay of fraction C.ateralbus R2.6 and C.3.1. Top images show fluorescence with red contrast, and bottom images represent phase contrast of zebrafish larvae. Dimethyl sulfoxide (DMSO) was used as a solvent control, at a concentration of 0.1%, and resveratrol (Rev) was used as a positive control, at a concentration of 50 µM.*

Results from anti-obesity screening are showed in Figure 10. Results concerning *Conus ateralbus* fractions showed that only fraction *C.ateralbus* R2.6 led to a significant decrease in fluorescence intensity compared with the DMSO group. Fluorescence quantification and statistical analyses proved that fraction *C.ateralbus* R2.6 had significant lipid reducing activity comparing with DMSO at 48 h of exposure, as represented in Figure 11. *C.ateralbus* R2.6 reduced fluorescent staining by 39%, at a final concentration of 10 µg/mL. This fraction is marked by an asterisk (*) in Figure 7. Fractions *C.ateralbus* R1.7 and *C.ateralbus* R1.14 showed statistical differences from DMSO, and increased lipid accumulation in approximately 45% and 42%, respectively.

Additionally, *Conus venulatus* fractions were tested using zebrafish Nile red fat metabolism assay. Results showed that no fraction significantly decreased fluorescence intensity compared with DMSO (Figure 11).

Given the results obtained during this assay for *Conus ateralbus* and *Conus venulatus*, we decided to test a third specie, *Conus genuanus*, where the venom was already fractionated and stored at -80 ºC from previous studies. Results showed that only fraction C3.1 reduced fluorescence intensity compared with solvent control group (DMSO) (Figure 10). Fluorescence quantification followed by statistical analysis confirmed what could be observed in the images (Figure 11). Fraction C3.1 had a statistically significant difference from DMSO control, leading to a reduction on fluorescent staining of 52%, after 48 h of exposition to fractions at 10 µg/mL.

The screening for bioactive compounds that act on lipid metabolism showed that from 68 tested fractions, two fractions (3%) were able to significantly reduce lipid staining on zebrafish yolk sac, two fractions (3%) increased neutral lipid staining, and 64 had no effect on zebrafish larvae 5DPF lipid metabolism.

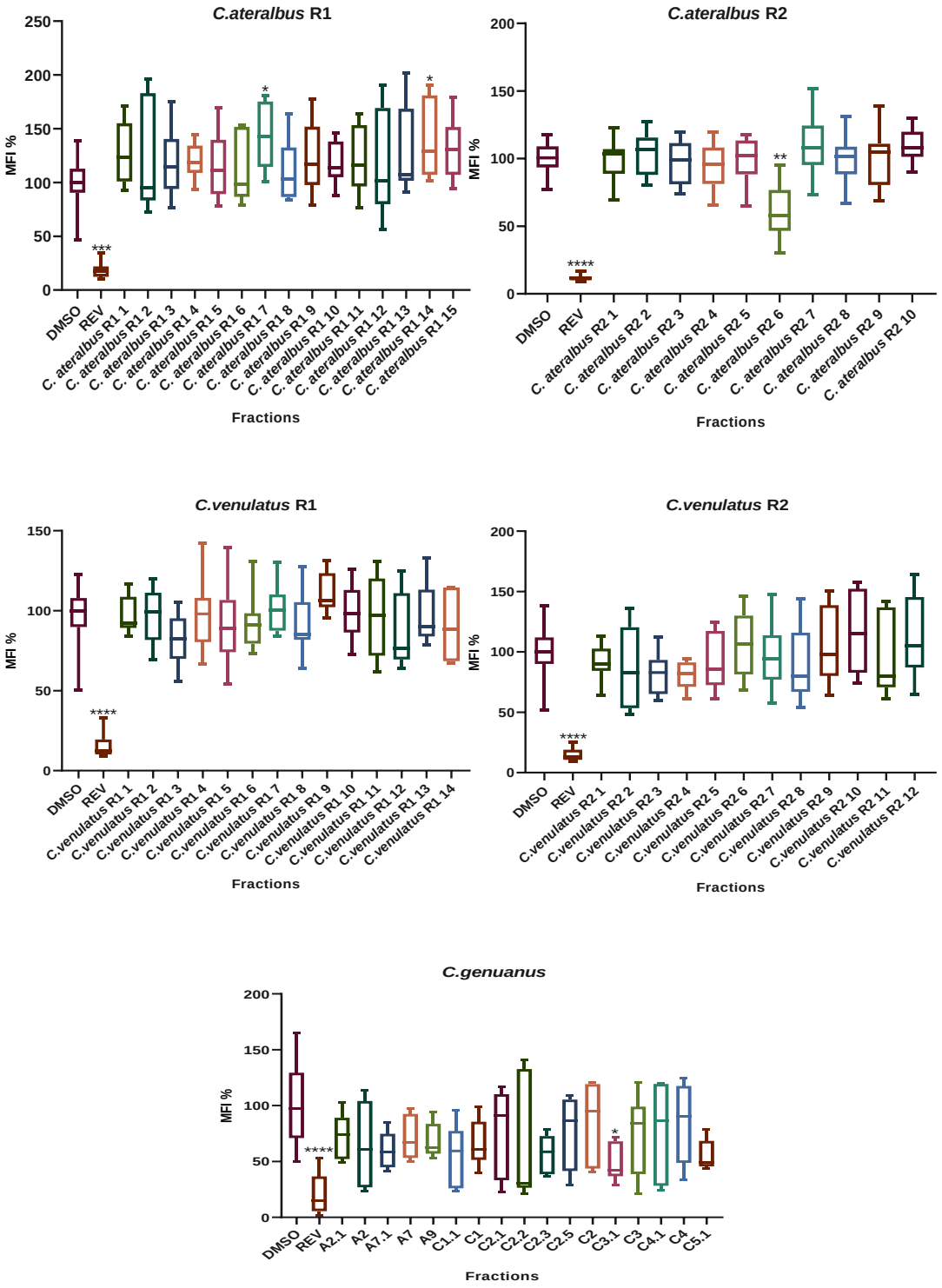

Figure 11 *Quantification of the lipid-reducing effects of different fractions from three Conus species at a final concentration of 10 µg/mL using the zebrafish Nile red fat metabolism assay. Solvent control had 0.1% DMSO and the positive control 50 µM REV. Values are expressed as mean fluorescence intensity (MFI) percentage relative to the DMSO group. Data have been derived from 5-7 individuals per treatment group and are shown as box-and-whisker plots (5-95 percentiles). Statistical differences from solvent control (DMSO) were analysed by Kruskal-Wallis with Dunn´s posthoc (C.ateralbus R1, C.venulatus R1, C.venulatus R2 and C.genuanus) and Brown-Forsythe and Welch ANOVA tests and Holm-Sidak's multiple comparisons test (C.ateralbus R2). Differences are indicated by asterisks, * p < 0.05; ** p < 0.01; *** p < 0.001; **** p < 0.0001.*

3.3.1.1. *C.ateralbus* R2.6 proteomic analyses

C.ateralbus R2.6 was the first fraction showing promising bioactivity, namely in the zebrafish Nile red fat metabolism assay. In order to identify some of the present peptides, *C.ateralbus* R2.6 was sent to University of Aveiro where Prof Pedro Domingues proceeded with a proteomics analysis using high resolution mass spectrometry. Figure 12 shows the chromatographic profile from fraction *C.ateralbus* R2.6 obtain using LC-ESI-HR-MS/MS method. As can be observed, more abundant peaks were detected after 48 min, as well as the presence of many peaks showing a complex mixture of the sample.

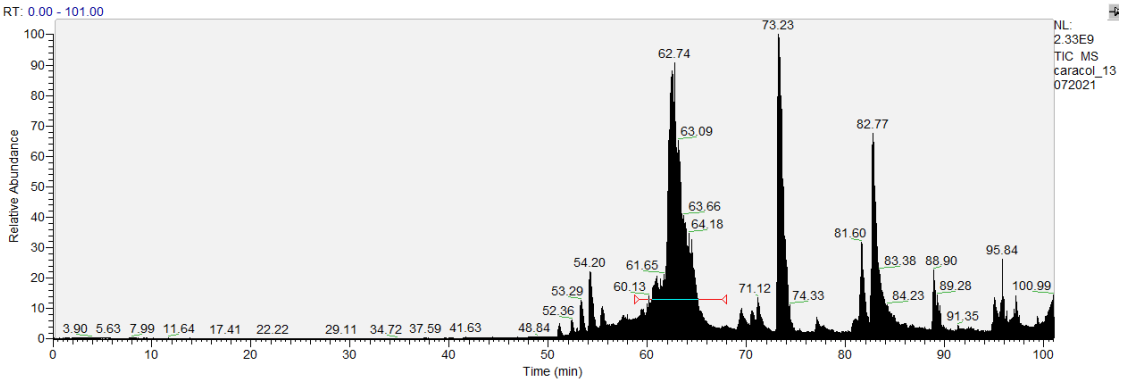

Figure 12 *Chromatographic profile of C.ateralbus R2.6 fraction. More abundante peaks in C.ateralbus R2.6 fraction eluted after 48 minutes of run.*

After analysing the recovered raw sequences and comparing them to the Uniprot (TrEMBL and Swiss-Prot) protein sequence database, ten sequences of known conotoxins matched to peptide sequences from the experimental LC-ESI-HR-MS/MS chromatogram (Table 7). Identified peptides using this approach had a wide variety of molecular weights, ranging from 419 m/z (Da) to 1579 m/z (Da). For five of the eleven sequences, the software could determine the relative abundance in the tested fraction. The peptide sequence with similarity to Conotoxin Cl10.1 was identified as the most abundant.

Peptides found in *C.ateralbus* R2.6 fraction have similarities with conotoxins already isolated from several *Conus* species, with peptide sequence coverage of 46% to 6% (Table 8). Sequences similarities suggest that this fraction has in its constitution peptides found in vermivorous, molluscivorous and piscivorous species. Among these conotoxins, two (18%) belong to O1 superfamily known for inhibit ion channels, three (27%) belong to T superfamily targeting ion channels, one (9%) inhibit nAChRs and belong to superfamily D. Additionally, O2 superfamily was also identified. Peptides BLAST with conotoxins sequences revealed that our sequences aligned mostly with signal peptide and/or with propeptide sequences. Only alignment with Cysteine-rich venom protein occur in the mature peptide region.

Table 7 *Peptides detected by LC-ESI-HR-MS/MS, relative abundance peptides masses and putative sequences by mass-matching using BLAST search on UniProtKB database.*

Conotoxin	Sequence	m/z (Da)	Relative abundance
Alpha-conotoxin-like Ml20.3	[-].MPKLEMMLLVLLILPLSYFSAAGGQVVQGDWRGDGLARYLQR.[G]	1579,82788	-
Omega-conotoxin SVIA	[T].ACQLITAEDSRGTQKHRTLRSTARRSKS.[E]	1579,32495	-
Conotoxin VnMLCL-031	[F].IILLLLASPAAPNPLQTRXQSNLIR.[A]	688,159	-
Conotoxin Vc6a	[F].LTANTFATADDPRNGLENLFLKAHHEMN.[P]	1570,75366	-
Conotoxin Ar5.1 b	[F].IILLLLASPAASNPLKTRIQSDLIRAAL.[E]	595,16095	2419242,25
Conotoxin Vc6.17	[K].LIILLLVAAVLMSTQALF.[Q]	483,04846	510537,625
Conotoxin Ca5.1	[F].IILLLLASPAASD.[P]	432,93192	-
Conotoxin vc5b (Fragment)	[-].VILLLLI.[A]	419,80408	17915710
Conotoxin Cl10.1	[T].MLVLLLLL.[P]	-	98395568
Cysteine-rich venom protein	[A].MQCILGHDSGRRGEPDL.[P]	471,73135	11530,8418

- Unknown

Table 8 *Conotoxins identification by BLAST search on UniProtKB database. Signal peptide, propeptide and mature peptide are shown in orange, green and blue, respectively. Peptides identified by LC-ESI-HR-MS/MS are underlined.*

Conotoxin (Accession)	Species (Diet)	Peptide sequence	Coverage [%]	Superfamily (target)	Ref
MI (P0CE32)	*C. miles* (v)	MPKLEMMLLVLLILPLSYFSAAGGQVVQGDWRGDGLARYLQRGDRDAQGCQV VTPGSKWGRCCLNRVCGPMCCPASHCYCIYHRGRGHGCSC	46	D (inhibitor of nicotinic acetylcholine receptors (nAChRs))	Loughnan *et al.*, 2009
SVIA (P28880)	*C. striatus* (p)	MKLTCVMIVAVLLLTACQLITAEDSRGTQKHRTLRSTAR RSKSESTTRCRSSGSPCGVTSICCGRCYRGKCT	39	O1 (Ca channel-targeted)	Ramilo *et al.*, 1992
VnMLCL (Q9BP53)	*C. ventricosus* (v)	MLCLPXFIILLLLASPAAP NPLQTRXQSNLI RAGPEDANIKTXKRVIISGLXXSILVPLIDAIIG	38	-	Conticello *et al.*, 2001
Vc6a (P69758)	*C. victoriae* (m)	MKLTCVVIVAVLFLTANTFATADDPRNGLENLFLKA HHEMNPEASKLNERCLSGGEVCDFLFPKCCNYCILLFCS	37	O1 (ion channel inhibitor)	Jakubowski *et al.*, 2004
Ar5.1b(Q9BP51)	*C. arenatus* (v)	MLCLPVFIILLLLASPAASNPLKTRIQSDLIRAALEDADMK NEKNILSSIMGSLGTIGNVVGNVCCSITKSCCASEE	36	T (ion channel inhibitor)	Conticello *et al.*, 2001
Vc6.17(G1AS83)	*C. victoriae* (m)	MQKLIILLLVAAVLMSTQALEQEKRRKEKIDLLSKRKTDA EKQHKRLCPDYTDPCSNAYECCSWNCHNGHCTG	33	O2 (inhibits voltage-gated ion channels)	Safavi-Hemami *et al.* 2011
Ca5.1 (P0C666)	*C. caracteristicus* (v)	MRCVPVFIILLLLASPAASDPLEKRIQSDLIRAALEDAD TKNDPRILEDIVSTALATCCKFQFLNFCCNEK	18	T (ion channel inhibitor)	Peng *et al.*, 2007
Vc5b (P69768)	*C. victoriae* (m)	VILLLLIASAPSVDAQPKTKDDVPLAPLH DNAKSALQHLNQRCCQTFYWCCGQGK	13	T (ion channel inhibitor)	Jakubowski *et al.*, 2004
Cl10.1(D6C4H8)	*Californiconus californicus* (p)	MTTLGMTMLVLLLLLPLATCLGDGERSPWDSLLRALRSDP QACEPTISGGEMICRDEVCASTGCNCGYNIAKAHCYCACP	10	-	Biggs *et al.*, 2010
(Q7YT83)	*C. textile* (m)	MLSTMQTVGAVLMLSIVLVAGRKRHHCDSKYYELTPAHTMCLTDKPNAVAVPLTQ ETEHEILEMHNKIRADVTDAANMLKMEWDERLATVAQKWAMQCILGHDSGRRG EPDLPGSVGQNVAWSSGDLTFLGAVQMWADEIVDFQYGVWTDGTGHYIQQVFAG ASRIGCGQSACGNNKYFVCNYYKGTMGDEPYQLGRPCSQCRSSCQHIRGS QGRWGSLCDCTNGPDACFNGGIFNINTCQCECSGIWGGADCQEKHCPNEDFDD MCRYPDALRRPQHWCQYDNFQSDCPILCGYCPNPN	6	-	-

v- vermivorous; p- piscivorous; m- molluscivorous; - unknown

3.3.2. Glucose Uptake in Zebrafish Larvae

A 2-(N-(7-Nitrobenz-2-oxa-1,3-diazol-4-yl) Amino)-2-Deoxyglucose (2-NBDG) assay was performed using zebrafish larvae 3DPF. Glucose uptake was evaluated by fluorescent microscopy. Dimethyl sulfoxide (DMSO) was used as solvent control and showed light fluorescence signal on zebrafish yolk sac and eyes. Emodin was use as a positive control as it is known to increase glucose uptake on zebrafish larvae. Fluorescence quantification was done separately on zebrafish yolk sac and eyes. Figure 13 demonstrates images from control groups used in this assay.

Figure 13 *Representative images of glucose uptake in zebrafish larvae. Top images show fluorescence with green contrast, and bottom images represent phase contrast of zebrafish larvae. Dimethyl sulfoxide (DMSO) was used as a solvent control, at a concentration of 0.1%, and EMODIN was used as a positive control, at a concentration of 10 µM.*

Results from 2-NBDG assay in zebrafish yolk sac can be observed in Figure 14. *Conus ateralbus* fractions demonstrated that no fraction increased fluorescence intensity compared with DMSO group in yolk sac. Instead, majority of fractions showed decreased fluorescence when compared with solvent control. Fluorescence quantification and statistical analyses confirmed this observation. *C.ateralbus* R2.3, *C.ateralbus* R2.4, *C.ateralbus* R2.7 and *C.ateralbus* R2.9 were the most statistically different fractions and led to a decrease in mean fluorescence intensity (MFI) of 47%, 34%, 44% and 39%, respectively, compared with DMSO group. Interestingly, fraction *C.ateralbus* R2.6 showed no difference from solvent control.

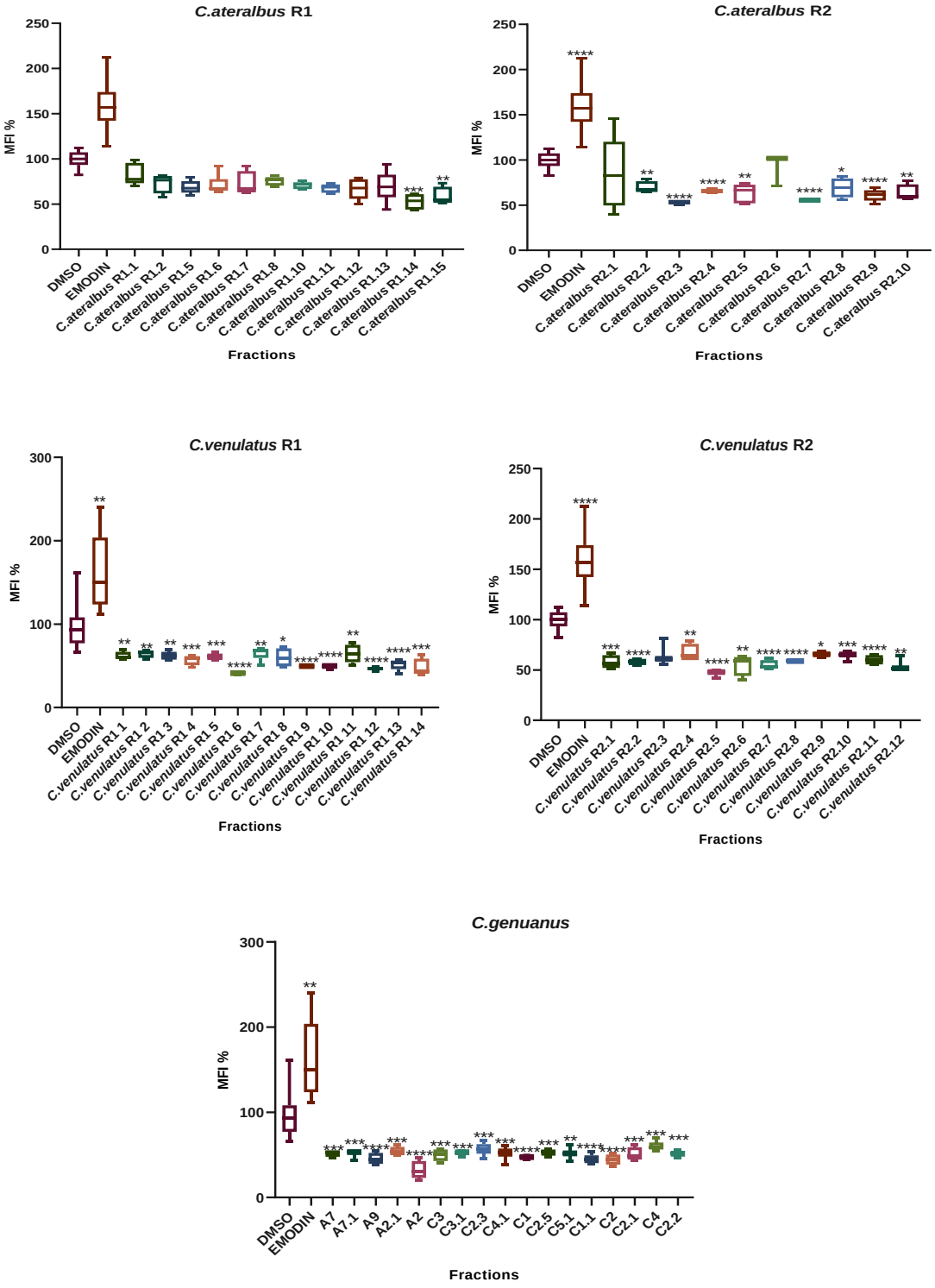

Figure 14 *Quantification of glucose uptake in yolk sac by embryos expose to fractions from three Conus species at a final concentration of 10 µg/mL. Solvent control had 0.1% DMSO and the positive control 10 µM EMODIN. Values are expressed as mean fluorescence intensity (MFI) percentage relative to the DMSO group. Data have been derived from 5-6 individuals per treatment group and are shown as box-and-whisker plots (5-95 percentiles). Statistical differences from solvent control (DMSO) were analysed by Kruskal-Wallis with Dunn´s posthoc (C.ateralbus R1) and by Brown-Forsythe and Welch ANOVA tests and Holm-Sidak's multiple comparisons test (C.ateralbus R2, C.vennulatus R1, C.venulatus R2, C.genuanus) and are indicated by asterisks, * p < 0.1; ** p < 0.01; *** p < 0.001; **** p < 0.0001.*

Conus venulatus fractions were also tested in this assay. Results of yolk sac observation indicated no increase in fluorescence intensity compared with DMSO group. And, as observed in *Conus ateralbus* results, a decrease in fluorescence intensity was noticed. Statistical analyses indicated that most active fractions (*C.venulatus* R1.6, *C.venulatus* R1.9, *C.venulatus* R1.10, *C.venulatus* R1.12, *C.venulatus* R1.13, *C.venulatus* R2.2, *C.venulatus* R2.5, *C.venulatus* R2.7, *C.venulatus* R2.8 and *C.venulatus* R2.11) led to a decrease of fluorescence between 49% and 59%.

Conus genuanus showed the same propensity as *Conus ateralbus* and *Conus venulatus*. When compared to the DMSO groups, all fractions exhibit little fluorescence intensity. After fluorescence quantification, statistical studies revealed that most active fractions (A9, A2, C1, C1.1 and C2) cause a 53% to 68% drop in mean fluorescence intensity on zebrafish yolk sacs compared with solvent control.

Quantification of glucose uptake in eyes of embryos expose to fractions can be observed in Figure 15. Fluorescence intensity in eyes of zebrafish larvae exposed to *Conus ateralbus* fractions was similar to fluorescence intensity observed in DMSO group. Statistical analyses confirm this observation. No fraction was able to enhanced fluorescence intensity and glucose uptake in zebrafish eyes. Similar results were noted in embryos exposed to *Conus venulatus* and *Conus genuanus* fractions. However, fraction C3 showed a statistical difference from solvent control, decreasing mean fluorescence intensity in 47%.

Overall, screening for bioactive compounds produced by these three *Conus* species found that 52 out of 65 fractions (80%) decreased significantly fluorescence intensity in yolk sac compared DMSO control. In contrast, no fraction increased glucose uptake in zebrafish yolk sac. Additionally, no fraction significantly increased glucose uptake in zebrafish eyes, but one fraction (2%) induced a decrease in glucose uptake.

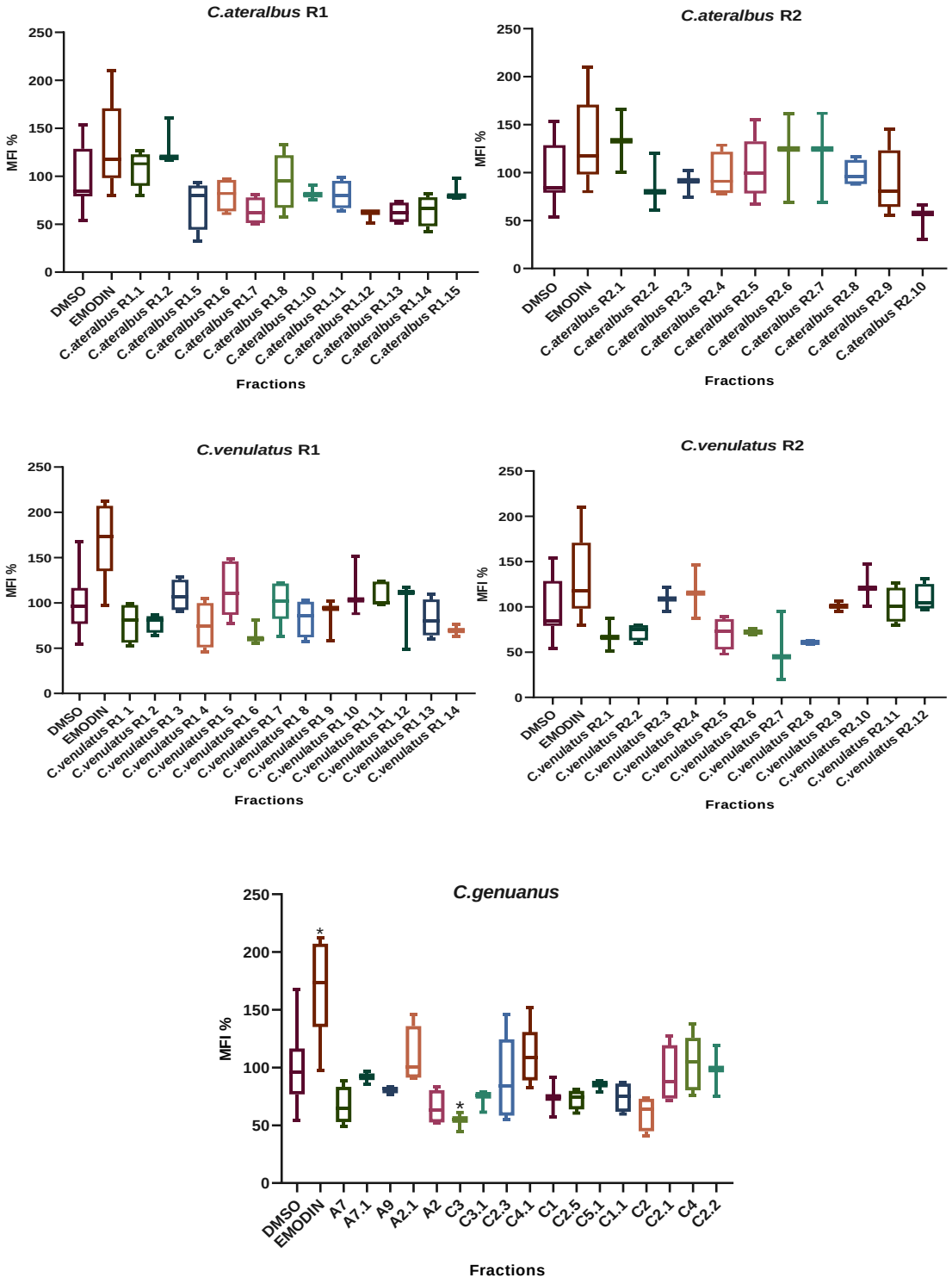

Figure 15 *Quantification of glucose uptake in eyes of embryos expose to fractions from three Conus species at a final concentration of 10 µg/mL. Solvent control had 0.1% DMSO and the positive control 10 µM EMODIN. Values are expressed as mean fluorescence intensity (MFI) percentage relative to the DMSO group. Data have been derived from 5-6 individuals per treatment group and are shown as box-and-whisker plots (5-95 percentiles). Statistical differences from solvent control (DMSO) were analysed by Ordinary one-way ANOVA (C.ateralbus R1, C.ateralbus R2, C.venulatus R2), by Kruskal-Wallis with Dunn´s posthoc (C.venulatus R1) and by Brown-Forsythe and Welch ANOVA tests and Holm-Sidak's multiple comparisons test (C.genuanus) and are indicated by asterisks, * p < 0.1; ** p < 0.01; *** p < 0.001; **** p < 0.0001.*

3.3.3. Anti-Steatosis Activity in HepG2 Cells

Cellular bioassays were also performed to test *Conus* fractions. The first cellular assay involved quantifying cellular lipids in HepG2 cells using a steatosis assay. As negative controls, dimethyl sulfoxide (DMSO) and methanol (MeOH) were utilized. To stimulate lipid droplet production, HepG2 cells were treated to 62 µM sodium oleate (SO). After 6 hours of co-exposure to SO and *Conus* fractions, the reduction in lipid accumulation was measured. Figure 16 depicts images from the assay's control groups, showing the fatty acid overloading in SO treated cells (increased fluorescence of neutral lipids).

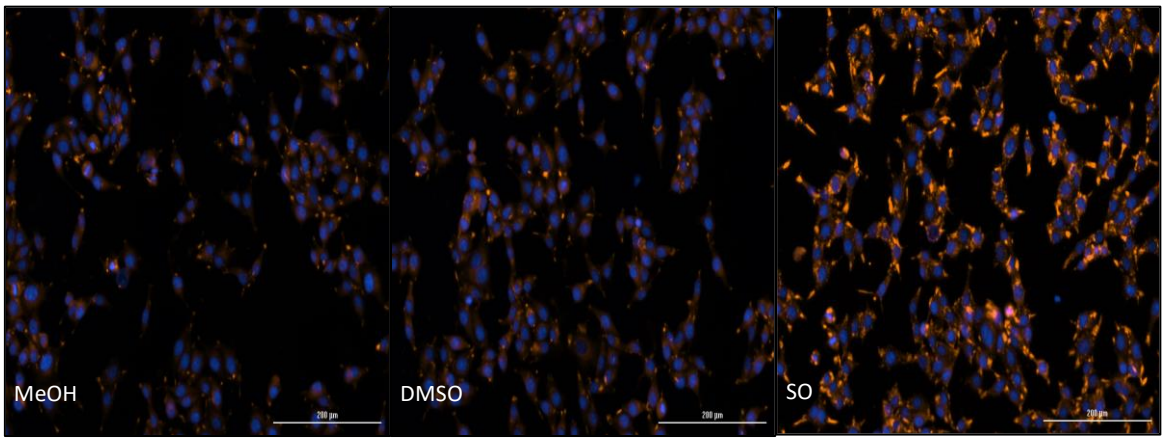

Figure 16 *Representative images of anti-steatosis activity in HepG2 cells. Methanol (MeOH) at a final concentration of 0.5%, and Dimethyl sulfoxide (DMSO) at 0.5% were used as negative controls. Sodium oleate (SO) was used to induce the formation of lipid droplets, which can be observed as intense lipid accumulation in cells, at a final concentration of 62 µM. Hoechst 33342 (HO) was used as staining for DNA (blue) and Nile red (NR) was used as a lipid staining (orange).*

Results from bioactivity screening using the anti-steatosis assay in HepG2 cells can be observed in Figure 17. Cells exposed to SO show high lipid staining, according to the results of the anti-steatosis activity screening using *Conus ateralbus* fractions. Only fractions *C.ateralbus* R1.1, *C.ateralbus* R1.14, and *C.ateralbus* R2.10 showed statistical differences from the solvent control (SO) group. Exposure to these fractions resulted in a 7%, 20%, and 17% increase in mean fluorescence intensity, respectively. No fraction reduced lipid accumulation in exposed HepG2 cells.

Additionally, *Conus venulatus* fractions were also tested in HepG2 cells. As observed in *Conus ateralbus* results, SO supplementation led to an increase in lipid accumulation and fractions did not influence the mean fluorescence intensity compared to SO control group.

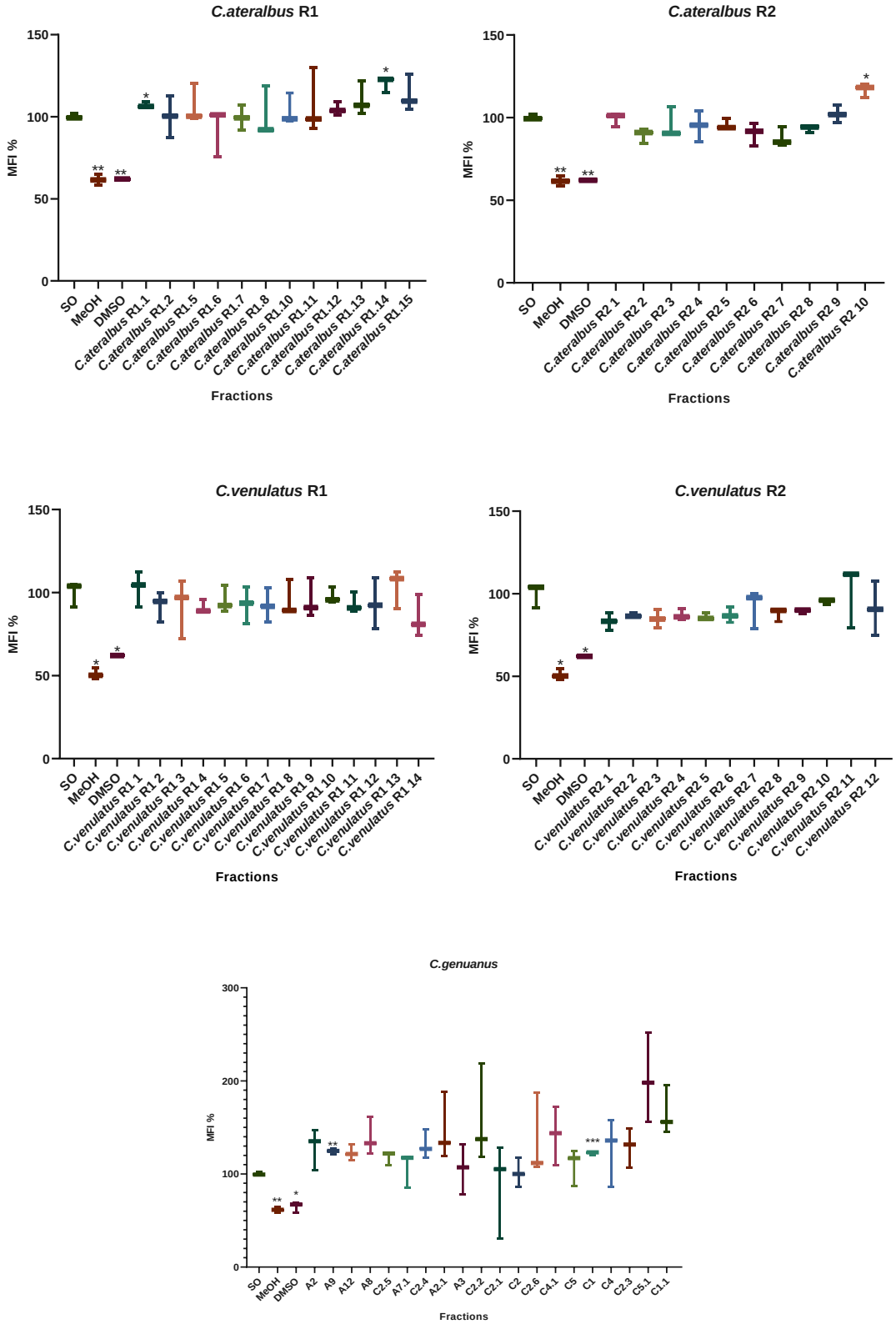

Figure 17 *Bioactivity screening using the anti-steatosis assay in HepG2 cells. Values are expressed as mean fluorescence intensity (MFI) percentage relative to solvent control (DMSO 0.5%, SO 62 µM). Two negative controls (MeOH 0.5%, DMSO 0.5%) were included. HepG2 cells were exposed for 6 h to 62 µM sodium oleate (SO 62 µM) and 10 µg mL^{-1} Conus fractions. The data are shown as box-and-whisker plots (5-95 percentiles). Statistical differences from solvent control were analysed by Brown-Forsythe and Welch ANOVA tests and Holm-Sidak's multiple comparisons test and are indicated by asterisks, * p < 0.1, ** p < 0.01, *** p < 0.001, **** p < 0.0001.*

Conus genuanus produced similar outcomes to *Conus ateralbus* and *Conus venulatus*. Except for A9 and C1, cells exposed to SO and co-exposed to fractions had similar mean fluorescence intensities. These fractions showed a 25% and 22% increase in fluorescence intensity, respectively.

Following, the sulforhodamine B (SRB) assay was used to determine cellular vitality (Figure 18). Results showed that incubation with *Conus ateralbus* fractions did not reduce cellular viability, and some fractions increased cellular protein content compared with DMSO group. Fractions *C.ateralbus* R1.2, *C.ateralbus* R1.5, *C.ateralbus* R1.10, *C.ateralbus* R1.11, *C.ateralbus* R1.12, *C.ateralbus* R1.13 and *C.ateralbus* R2.7 enhanced cellular viability by about 22%. Additionally, fractions *C.venulatus* 2.5, *C.venulatus* 2.6, *C.venulatus* 2.7, and *C.venulatus* 2.8 exhibited a statistical difference from the DMSO control, increasing cellular viability by about 25%. On the other hand, *Conus genuanus* fractions also did not affect protein content and consequently cellular viability.

Thereupon, from 68 analysed fractions, five fractions (7%) significantly increased the lipid accumulation in HepG2, and 63 fractions had no effect on cellular lipid content. Results concerning cellular viability also demonstrated that no fraction decreased cellular protein content, and eleven fractions (16%) were able to increase cellular viability when sulforhodamine B (SRB) assay was performed.

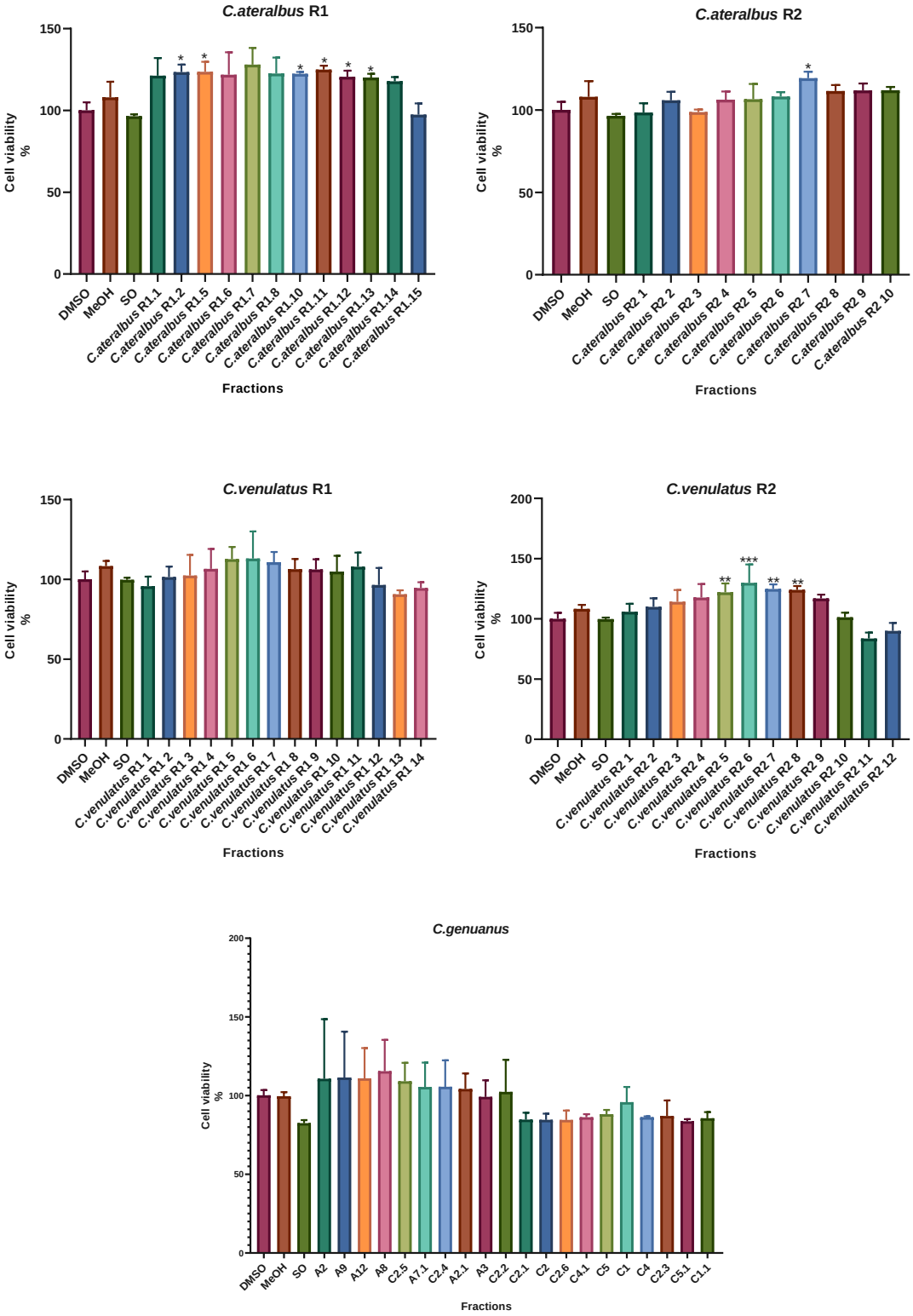

Figure 18 *Cell viability after 6h of exposure to Conus fractions at a concentration of 10 µg mL^{-1}. Cells on solvent control were exposed to DMSO 0.5% and SO 62 µM. Two negative controls (MeOH 0.5%, DMSO 0.5%) were included. The data are shown as column bar graph. Statistical differences from DMSO control were analysed by Brown-Forsythe and Welch ANOVA tests and Holm-Sidak's multiple comparisons test (C.ateralbus R1, C.ateralbus R2) and by Ordinary one-way ANOVA test (C.venulatus R1, C.venulatus R2, C.genuanus) and are indicated by asterisks, * p < 0.1; ** p < 0.01; *** p < 0.001; **** p < 0.0001.*

3.3.4. Inflammatory assays

3.3.4.1. Pro-inflammatory assay

RAW 264.7 macrophages were subjected to pro-inflammatory tests. The solvent control was 0.5% dimethyl sulfoxide (DMSO). Lipopolysaccharide (LPS) was used to cause inflammation in RAW 264.7 cells. Nitric oxide (NO) concentration was assessed after 24 hours of exposure to *Conus* fractions without the addition of LPS in these wells. The results demonstrated that LPS exposure caused exposed macrophages to produce more NO, which is a normal response to this pro-inflammatory chemical.

Results from pro-inflammatory assay can be observed in Figure 19. No significant differences in NO production were found between the DMSO group and cells exposed to *Conus ateralbus* fractions at a 10 µg/mL final concentration. The same assay was performed using *Conus venulatus* and *Conus genuanus* fractions, and a similar outcome was obtained, NO levels similar to solvent control.

The cytotoxicity of fractions was assessed using the MTT (3-(4,5-Dimethylthiazol-2-yl)-2 assay (Figure 20). According to the data, no fraction reduced cellular viability significantly, even if viability reductions were observed in some groups.

After testing the pro-inflammatory ability of 59 fractions, results demonstrated that studied *Conus* species should not produce peptides able to interfere with pro-inflammatory pathways of macrophages. In addition, cellular viability after fractions exposure revealed that these are not cytotoxic for RAW 264.7.

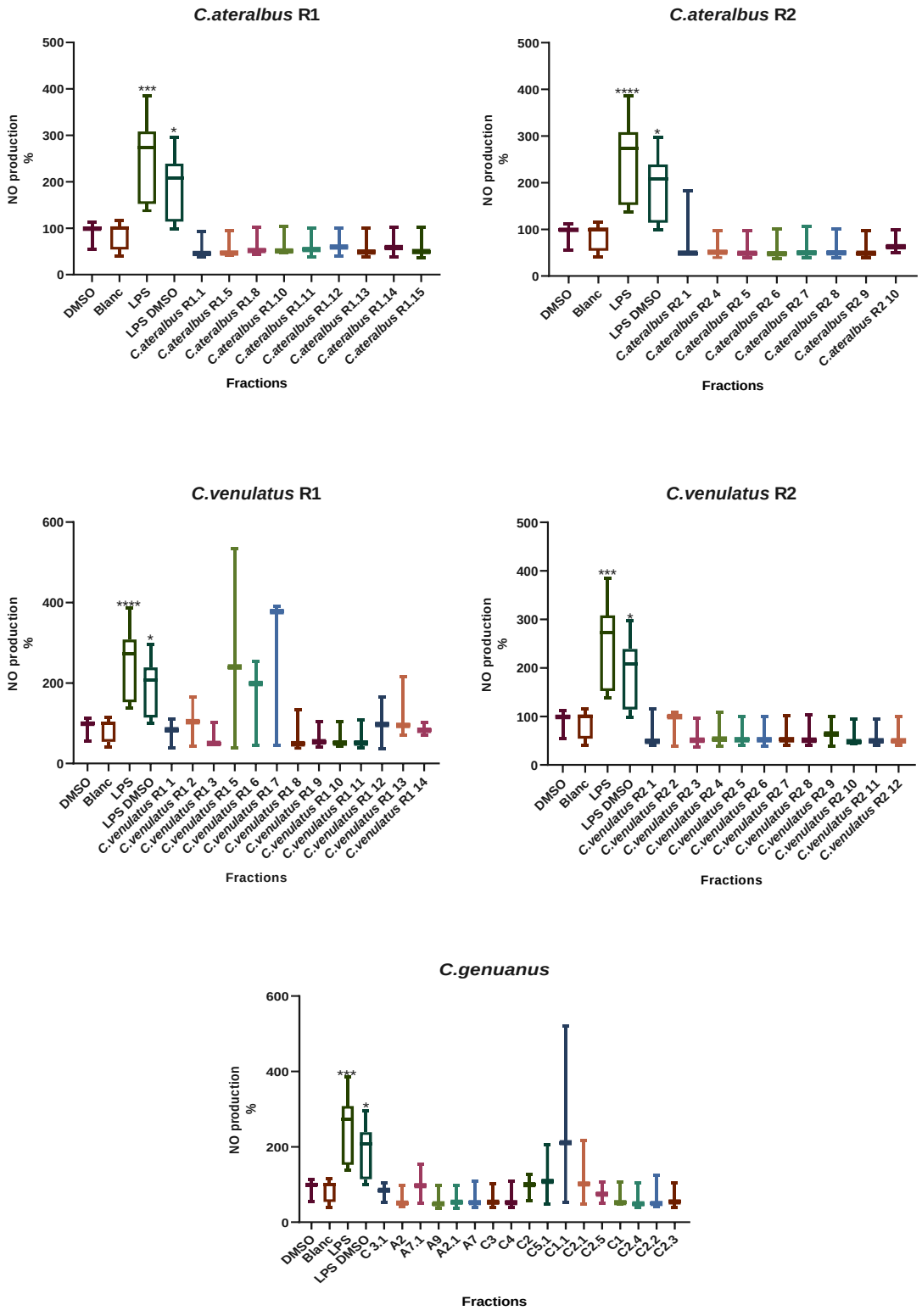

Figure 19 *Bioactivity screening using pro-inflammatory assay in RAW 264.7 macrophages. Cells on positive control were exposed to DMSO 0.5% and LPS 1µg/mL. A solvent control (DMSO 0.5%) and two quality controls (LPS and Blanc) were included. Values are expressed as percentage of NO production relative to solvent group (DMSO). Raw 264.7 were exposed for 24 h to Conus fractions at a final concentration of 10 µg mL^{-1}. The data are shown as box-and-whisker plots (5-95 percentiles). Statistical differences from solvent control were analysed by Kruskal-Wallis with Dunn´s posthoc and are indicated by asterisks, * p < 0.1, ** p < 0.01, *** p < 0.001, **** p < 0.0001.*

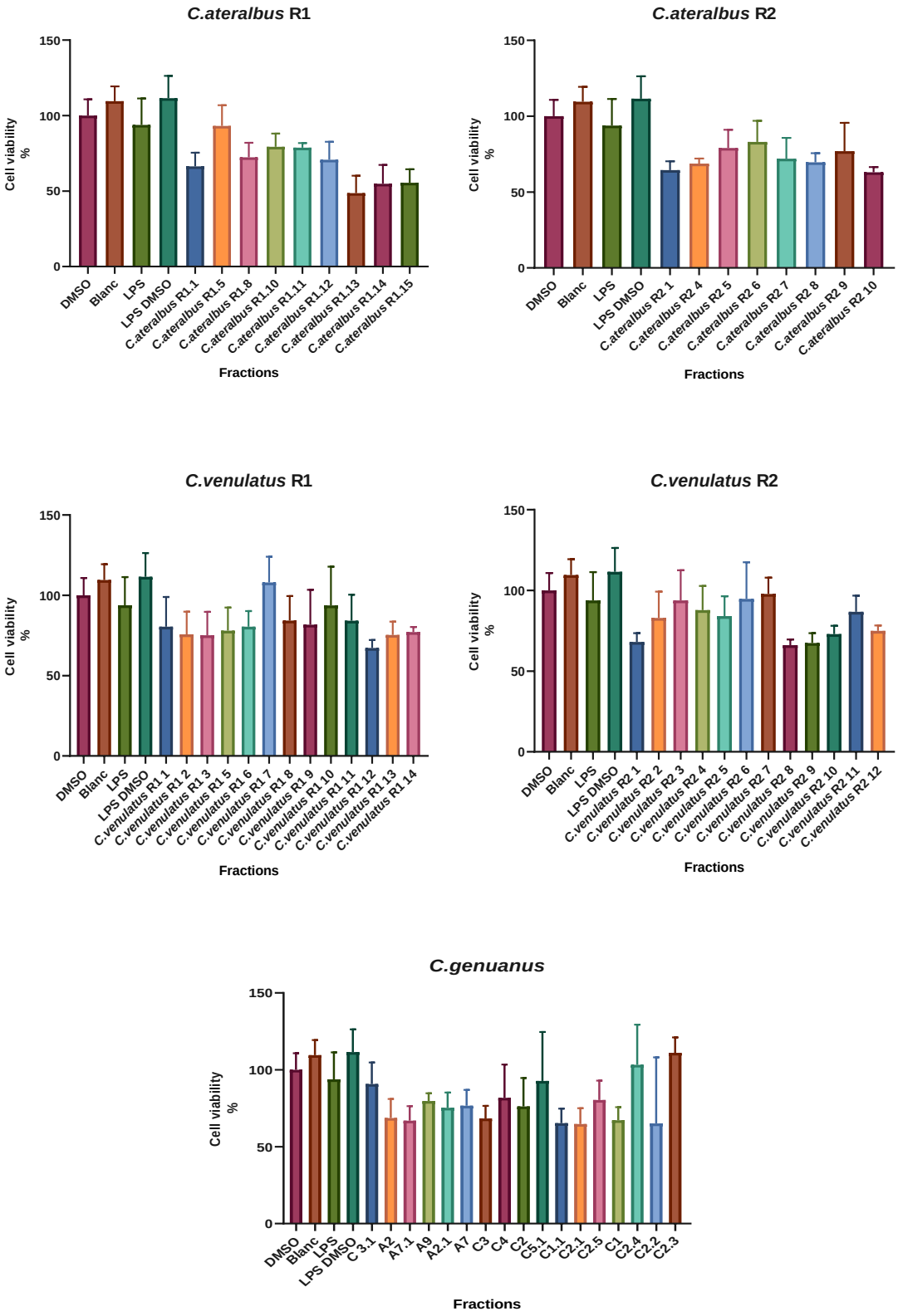

Figure 20 *Cell viability after 24h of exposure to Conus fractions at a concentration of 10 µg mL⁻¹. Cells on positive control were exposed to DMSO 0.5% and LPS 1µg/mL. A solvent control (DMSO 0.5%) and two quality controls (LPS and Blanc) were included. The data are shown as column bar graph. Statistical differences from solvent control (DMSO) were analysed by Kruskal-Wallis with Dunn´s posthoc and are indicated by asterisks, * p < 0.1, ** p < 0.01, *** p < 0.001, **** p < 0.0001.*

3.3.4.2. Anti-inflammatory assay

Anti-inflammatory assays were performed in RAW 264.7 macrophages. Cells on solvent control were exposed to DMSO 0.5% and LPS 1µg/mL. A negative control (DMSO 0.5%) and two quality controls (LPS and Blanc) were included in the assay. After 24 h of exposure to LPS and *Conus* fractions, Nitric oxide (NO) content was measured.

Results from anti-inflammatory activity screening can be observed in Figure 21. Exposure to *Conus ateralbus* fractions demonstrates that most fractions reduced NO level compared to the LPS + DMSO control group. The most active fractions in this experiment were *C.ateralbus* R1.14 and *C.ateralbus* R1.15, which resulted in a 66% and 77% drop in NO concentration, respectively. Macrophages were exposed to *Conus venulatus* fractions and results suggest that when compared to the solvent control, NO production was lower in some fractions. The most statistically significant fractions were *C.venulatus* R2.2 and *C.venulatus* R2.5, which caused 74% and 76% reduction in NO content. *Conus genuanus* produced similar results to *Conus ateralbus* and *Conus venulatus*. NO production was shown to be lower in exposed cells when compared to the LPS + DMSO control. C2.5, C1, and A7 were the most statistically significant fractions, causing a 74%, 76%, and 67 % decline in NO content.

MTT test was used to assess the cytotoxicity of fractions (Figure 22). According to the findings, fraction *C.ateralbus* R1.13 reduced cellular viability by 25%, compared with DMSO control group. Fraction C2.2 too led to a decrease of 62% of cellular viability. Additionally, *C.venulatus* R1.4 resulted in a 14% increase in cellular viability. All the other fractions did not have statistical differences from control group.

The anti-inflammatory potential of 65 fractions was tested, and the results revealed that 43 fractions (66%) led to a decrease in NO content after co-exposure to LPS and fractions, suggesting that the examined *Conus* species may produce peptides that interfere with macrophage anti-inflammatory pathways. Furthermore, cellular viability following fraction exposure demonstrated that two fractions (3%) resulted in lower cellular viability in RAW 264.7 cells in this experiment, and one fraction (2%) increased cellular viability.

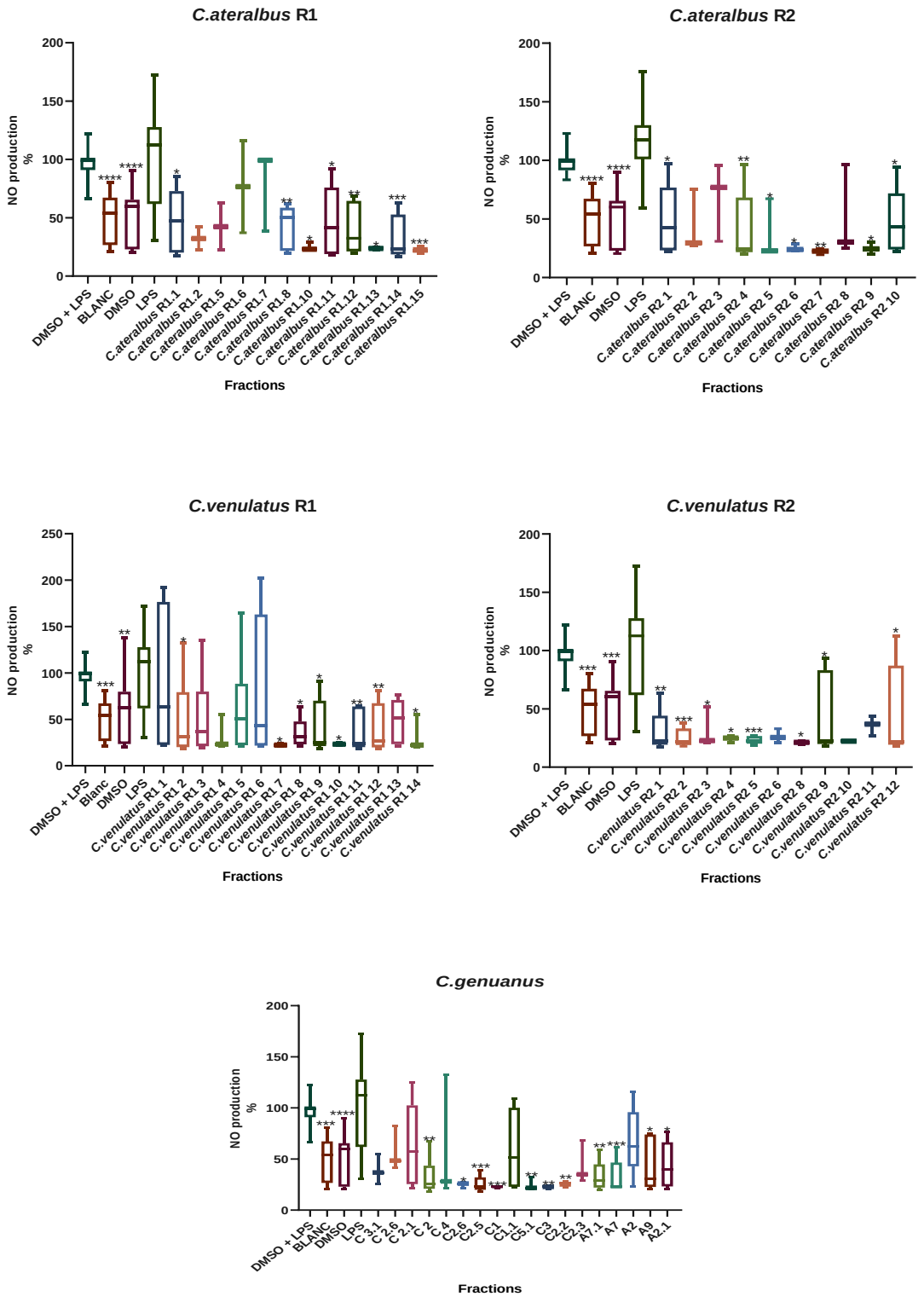

Figure 21 *Bioactivity screening using anti-inflammatory assay in RAW 264.7 macrophages. Cells on solvent control were exposed to DMSO 0.5% and LPS 1µg/mL. A negative control (DMSO 0.5%) and two quality controls (LPS and Blanc) were included. Values are expressed as percentage of NO production relative to solvent group (DMSO and LPS) from cell exposed to Conus fractions. Raw 264.7 were exposed for 24 h to Conus fractions at a final concentration of 10 µg mL^{-1}. The data are shown as box-and-whisker plots (5-95 percentiles). Statistical differences from solvent control were analysed by Kruskal-Wallis with Dunn´s posthoc and are indicated by asterisks, * p < 0.1, ** p < 0.01, *** p < 0.001, **** p < 0.0001.*

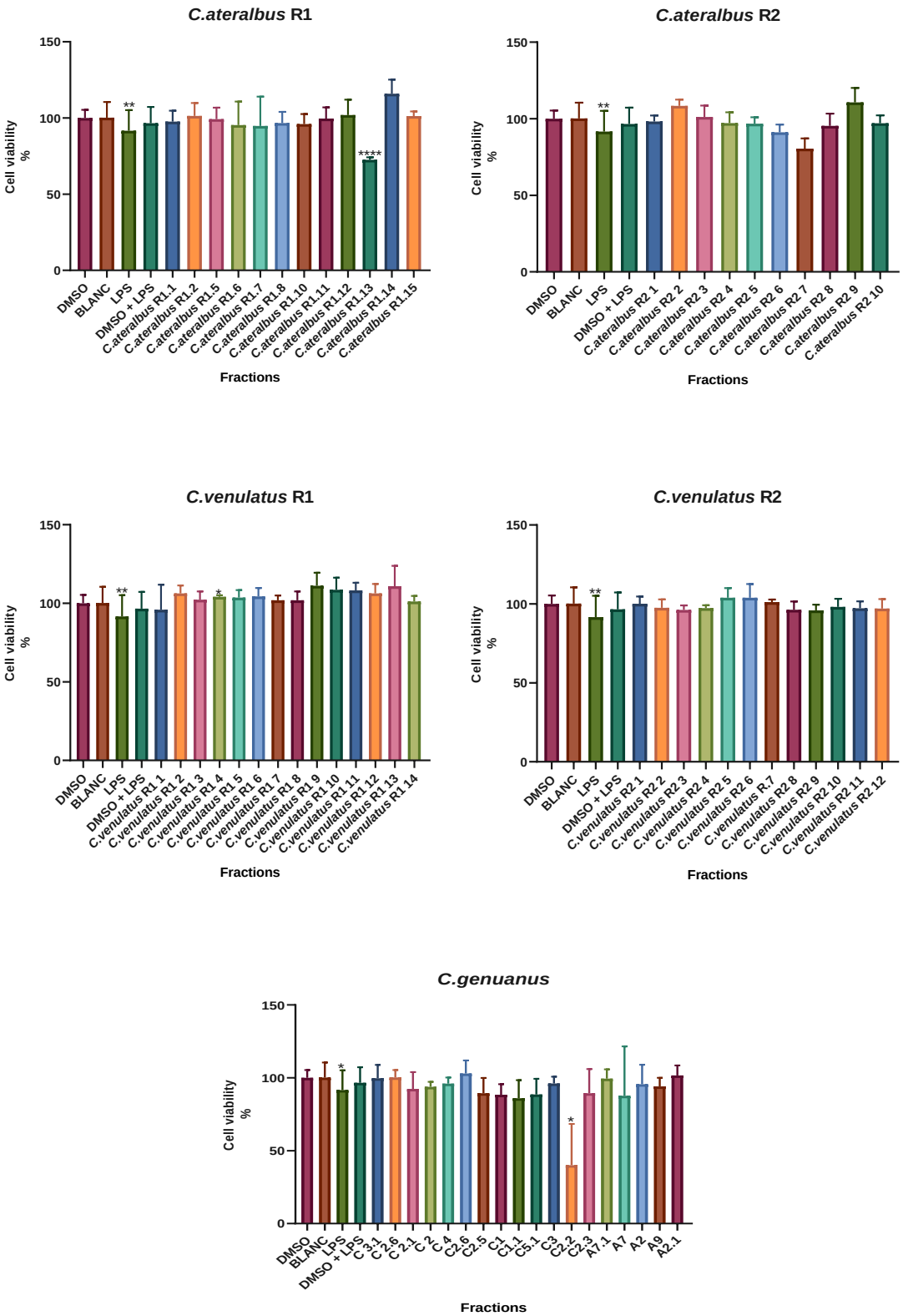

Figure 22 *Cell viability after 24h of exposure to Conus fractions at a concentration of 10 µg mL^{-1}. Cells on solvent control were exposed to DMSO 0.5% and LPS 1µg/mL. A solvent negative control (DMSO 0.5%) and two quality controls (LPS and Blanc) were included. The data are shown as column bar graph. Statistical differences from solvent negative control (DMSO) were analysed by Brown-Forsythe and Welch ANOVA tests and Holm-Sidak's multiple comparisons test and are indicated by asterisks, * p < 0.1, ** p < 0.01, *** p < 0.001, **** p < 0.0001.*

4. Discussion

Cone snails are venomous invertebrates with a growing potential for identifying pharmacologically interesting chemicals, particularly those with a piscivorous and molluscivorous feeding behaviour. Fish-hunting and snail-hunting species have a tight association with humans and vertebrates because they prey on more complex animals, and compound research has mostly centred on these species (Pi *et al.*, 2006). However, less studied vermivorous species have shown increasing potential for the discovery of equally important compounds. Three worm-hunting species (*Conus ateralbus*, *Conus venulatus* and *Conus genuanus*) belonging to Kalloconus subgenus were studied throughout this work. *Conus ateralbus* is an endemic species most found at the island of Sal in Cabo Verde, and it is currently endangered (Tenorio, 2012a). This species had previously been the subject of research, and a conotoxin, δ -conotoxin-like AtVIA (δ-AtVIA; GenBank accession number is MH025915), was found (Neves *et al.*, 2019). Calcium imaging of DRG neurons using this conotoxin showed its potential to increase cytosolic Ca^{2+} in DRG cells by inhibiting vertebrate voltage-gated Na^{+} channel inactivation, which consequently stops the repolarization of cells membranes (Aman *et al.*, 2015; Neves *et al.*, 2019). *Conus genuanus* is found along the West African coast, from Senegal to the islands of Cabo Verde and São Tomé and Príncipe, and is non-endemic to the Cabo Verde islands. According to the IUCN Red List of Threatened Species 2012, this species is now categorized as Least Concern (Tenorio, 2012b). Previous studies involving *Conus genuanus* identified a small molecule, a guanine derivative (genuanine), that provokes paralytic activity in mice, although its molecular target is still unknown (Neves *et al.*, 2015; Lin *et al.*, 2021). *Conus venulatus* can mostly be found in Boavista, Santiago, and Maio's islands and is an endemic specie from Cabo Verde archipelago. According to Tenorio and his IUCN Red List of Threatened Species from 2012, *Conus venulatus* is classified as Least Concern (Tenorio, 2012c). To the best of our knowledge, no research has been done on *Conus venulatus* venom in order to characterize it and identify bioactive fractions and conotoxins, unlike the other species under investigation.

4.1. Venoms chromatographic characterization

Although *Conus ateralbus* is already a studied species, research began with optimization of RP-HPLC conditions to acquire a decent chromatographic characterisation of its venom and a separation into fractions for screening bioactivities. The same process was done for *Conus venulatus*. The chromatographic profiles observed for these species suggest that *Conus ateralbus* has more natural products in its venom makeup than *Conus venulatus*, (Figure 7 and Figure 8). However, observed peaks are far from completely purified and venoms could be more complex than what can be elucidated from the profiles obtained. The polarity of the conopeptides identified in *Conus ateralbus* venom was as expected and identical to the chromatographic profile first described by Neves *et al.* (2019). *Conus venulatus* venom exhibited a similar chromatographic profile to *Conus ateralbus* venom, although apparently this venom contains fewer conopeptides, and retention time of more apolar compounds was later than what could be observed in *Conus ateralbus* profile.

Conus species' venom contains between 50 to 200 peptides, according to several studies (Jakubowski *et al.*, 2006; Davis *et al.*, 2009; Mir *et al.*, 2016). Although Davis *et al.* (2009) claims that some species can fabricate a more complex combination of conopeptides, such as *Conus textile*, which has been found to produce over 1000 distinct conopeptides in its venom. This study suggests that *Conus venulatus* and *Conus ateralbus* exhibit a mixture of roughly 81 and 109 peptides in their venoms (Figure 9). These data reinforce what was discovered in the chromatographic profiles, which indicated that *Conus venulatus* had less components in its chromatographic profile than *Conus ateralbus*. Both species had a multimodal peptides distribution without a clear pattern, like what was observed by Davis *et al.* (2009) for *Conus imperialis* (vermivorous) peptides. *Conus ateralbus* also had a more extraordinary occurrence of short peptides, especially those with a molecular mass between 600 and 2000 Da, similar to the distribution of *Conus textile* (molluscivorous) compounds, that showed a predominant mass range between 1300 and 2000 Da. *Conus venulatus*, on the other hand, has a distribution of compounds with a greater molecular mass (3000 Da or more) that is more similar to that of *Conus imperialis*, that exhibit high frequency of compounds with molecular masses between 3400 and 3800 Da. *Conus genuanus* chromatographic profile was already characterized by Neves *et al.* (2015). The venom duct was divided into distal and proximal sections, with polar molecules being more plentiful in the distal portion and apolar compounds being more abundant in the proximal segment (Neves *et al.* 2015). *Conus genuanus* venom molecular mass range was also characterized in Neves *et al.*, (2015). Small components, with molecular masses between 200 and 700

Da, were more common in the venom recovered from the distal section of the venom duct, while compounds with higher molecular mass (2000 Da or more) were detected in the proximal part of the venom duct (Neves *et al.*, 2015).

Non-peptidic small compounds have been found in *Conus genuanus* and *Conus imperialis*. Genuanine and Conazolium A were both extracted from the venom of the distal venom duct and demonstrated remarkable bioactivity, paralyzing mouse limbs and mimicking natural polychaete pheromones, respectively (Neves *et al.*, 2015; Torres *et al.*, 2021). These findings highlighted a novel possibility for non-peptide compounds to play a significant role in *Conus* biology and hunting techniques (Neves *et al.*, 2015; Torres *et al.*, 2021). According to Dutertre *et al.* (2014), the distal portion of the venom duct is responsible for predation, whereas the proximal section contains chemicals responsible for animals' defence. In the defence-evoked, paralytic peptides and other compounds active in vertebrate receptors were detected, while non-paralytic peptides were found in the predation-evoked. On the other hand, paralytic molecules identified in the distal area of the venom duct were discovered to play a predation role in *Conus genuanus* hunting strategy (Neves *et al.*, 2015). The results discussed here, suggest that *Conus ateralbus* has a high concentration of smaller compounds that, like in *Conus imperialis* and *Conus genuanus* (worm-hunting species), could be non-peptides molecules with an important role in worm predation and with activity in vertebrate receptors (Torres *et al.*, 2021). In order to better understand the location and importance of these substances in *Conus ateralbus* interactions with predators and preys, studies incorporating the examination of distinct venom duct sections could be useful.

4.2. Screening for fractions with anti-obesity activity

Drug side effects, including cardiovascular side effects, drug misuse, and psychological issues, limit the utilization of anti-obesity medications (Arya *et al.*, 2020). Natural products have been studied to develop anti-obesity substances with fewer adverse effects than pharmaceutical medications. Sponges, marine microbe extracts, and algae are already reported to produce metabolites with anti-obesity activities (Arya *et al.*, 2020). Intriguingly, bioactive fractions, such as *C.ateralbus* R2.6 and C3.1, belonging to *Conus ateralbus* and *Conus genunaus,* respectively, were discovered to reduce fluorescence staining in the zebrafish yolk sac, indicating a reduction in lipid deposition in that location (Figure 11). Other *Conus ateralbus* venom fractions, such as *C.ateralbus* R1.7 and *C.ateralbus* R1.14, have also been shown to interfere with lipid metabolism, causing fat buildup in the yolk sac. However*, Conus venulatus* fractions showed no bioactivity using Nile red fat metabolism assay. These findings demonstrated for the first time that the components in these fractions, probably conotoxins, can

interfere with the lipid metabolism in zebrafish larvae. These results corroborate what was reported by Sousa *et al.* (2018) and Neves *et al.* (2019), that showed that peptides synthetised by vermivorous cone snails can interact with vertebrates receptors. In the first, it was demonstrated that *Conus moncuri* has in its venom composition a conotoxin (ω-conotoxins) that interacts with $Ca_v2.2$ voltage-gated calcium channels when tested using a human SH-SY5Y neuroblastoma cell line (Sousa *et al.*, 2018). ω-conotoxins are usually found in piscivorous species, which use them as part of their predation strategies, and they might have a defensive role in vermivorous species. In Neves *et al.* (2019) report was first discovered a conotoxin in *Conus ateralbus*, a δ-conotoxin-like, capable of triggering excitatory activity in DGR mouse neurons by acting in Na channels. This conotoxin can also be found in piscivorous species. Conotoxins and conopeptides have been studied primarily for their neuropharmacological potential, particularly in the treatment of Alzheimer's disease, Parkinson's disease, and chronic pain. (Gao *et al.*, 2017; Hoggard *et al.*, 2017). And, as far as we know, this is the first study involving conopeptides and their potential as a treatment for metabolic illnesses such as obesity.

The first fraction showing promising bioactivity was *C.ateralbus* R2.6, and it was only after this positive heat, we decided to include *Conus genuanus* in our research. This fraction was sent to the chemistry department of University of Aveiro to proceed with fraction proteomic profiling. Alignment of all discovered mass fragments from LC-ESI-HR-MS/MS with sequences from the Uniprot protein sequence database resulted in the identification of ten sequences that were comparable to previously identified conotoxins (Table 7). Results from proteomic profile of *C.ateralbus* R2.6 (fraction) showed a mixture of sequences from fish-hunter, worm-hunter, and snail-hunter cone snails (Table 8). These findings suggest that *Conus ateralbus* venom can be employed for more than only feeding purposes, and that it can also be used to protect from predators in a variety of situations. The sequences revealed a higher coverage percentage among the identified conotoxins with an Alpha-conotoxin-like MI20.3 (superfamily D), a conotoxin isolated from *Conus miles* (vermivorous specie), that is known to inhibit nicotine acetylcholine receptors. This sample also contained sequences comparable to conotoxins from the O1 and O2 superfamilies, suggesting the presence of conotoxins capable of inhibiting ion channels by binding to and blocking voltage-gated calcium channels. Sequences similar to T-superfamily conotoxins were also discovered. Conotoxins from this superfamily can inhibit norepinephrine receptors or block tetrodotoxin sensitive (TTX-S) Na channels and target neuronal nicotinic acetylcholine receptors (Wang *et al.*, 2014; Rajesh, 2015). Additionally, the algorithm was able to calculate the relative abundance of five of these sequences in the tested fraction. The relative abundance of a sequence similar to a

cysteine-rich venom peptide recovered from *Conus textile* (vermivorous) was determined and this was the only sequence that aligned with the mature component of conopeptide. The presence of a cysteine common to both our sequence and this previously identified peptide was discovered in this sequence. Even though cysteines are present in the mature section of the peptide, the remaining sequences all align with the signal and/or propeptide regions, which are poor-cysteine regions. The signal peptide (endoplasmatic reticulum signal), N-terminal pro-region (propeptide), and C-terminal region of conopeptides are cleaved during maturation, and the mature peptide region can be subjected to post-translational changes (Kaas *et al.*, 2008). According to ConoServer database (http://www.conoserver.org), to maintain proteins shape, cysteine residues are oxidised to form disulfide bridges. However, it is known that cone snails also produce cysteine-poor peptides, that show no or few disulfide bridges. Conopeptide diversity is due to the considerable variation found in the mature domain, whereas the signal peptide is known to be a conserved sequence, originating the identified conotoxins superfamilies (Kaas *et al.*, 2008; Kaas *et al.*, 2010). Therefore, these results could indicate that conopeptides found in this fraction are still non-identified.

Although we found sequences similar to conotoxins already categorized in superfamilies such as O, T, and D and have a high relative abundance, observed bioactivity could be due to other molecules present in the fraction other than the ones identified in the proteomic profiling. This way, to determine the compounds responsible for reduction of lipid accumulation in zebrafish embryos, more studies need to be performed, namely further purification of *C.ateralbus* R2.6, isolation and testing of separated compounds or the synthesis of the ten peptides and re-testing in the anti-obesity assay.

4.3. Screening for fractions with anti-diabetic activity

Natural compounds, particularly those derived from plants, have been shown to have anti-diabetic characteristics and are being studied to develop anti-diabetic pharmaceuticals (Xu *et al.*, 2018). Anti-diabetic properties have also been reported in marine species such as sponges and sea cucumbers, which inhibit glycogen synthase 3 beta (GSK-3B), protect beta pancreatic cells, manage glycemic status, and reduce diabetic cardiovascular problems (Khanfar *et al.*, 2009; El Barky *et al.*, 2016; Arya *et al.*, 2020). Concerning *Conus* species and their potential as sources of anti-diabetic agents, an insulin-like conotoxin (Con-Ins G1) was discovered in *Conus geographus* (Safavi-Hemami *et al.*, 2015). This conotoxin can induce hypoglycemic shock in animals, facilitating their capture. In addition, transcriptome analyses have revealed that all molluscivorous cone snail venom contains insulins. The majority of vermivorous cone

snails and a minor percentage of piscivorous snails share this trait. These insulin-like conotoxins are used as a technique of predation by snail-hunting and piscivorous *Conus*. However, the purpose of these compounds in worm-hunting cone snails is unknown (Robinson & Safavi-Hemami, 2016; Safavi-Hemami *et al.*, 2016). Different results were observed when quantifying fluorescence staining in zebrafish yolk sac (Figure 14) and eyes (Figure 15) using the 2-NBDG assay on zebrafish embryos exposed to cone snails' fractions. The majority of fractions decreased fluorescence staining in the yolk sac, showing that exposure to fractions reduced glucose uptake and may hinder its uptake into cells. The results of fluorescence quantification in eyes, on the other hand, showed that fluorescence staining was similar to the solvent control, implying that fractions were not capable of significantly shifting glucose homeostasis. Polakof *et al.* (2012) and Dalmolin *et al.* (2018) reported that glucose transporters, specifically the GLUT family, are expressed differently in different tissues. Fish have already been found to have GLUT1-4. The blood-brain barrier and erythrocytes are the major sites of GLUT1 expression. GLUT2 is more commonly found in the gastrointestinal tract, whereas GLUT3 is found in neurons. Adipose tissue and skeletal muscles both express GLUT4. The results of this assay could indicate that distinct conotoxins found in the venom of certain *Conus* species have varying affinities for glucose transporters, as evidenced by interactions with transporters found in the zebrafish yolk sac in the opposite of transporters expressed in the eyes.

Based on these findings, it is reasonable to conclude that the vermivorous species studied here do not produce insulin-like conotoxins or other conopeptides capable of increasing glucose transport into zebrafish cells. But, on the other hand, it may produce conopeptides capable of interacting with glucose receptors. These findings may corroborate what Safavi-Hemami *et al.* (2016) discovered, which found that venom insulins expressed differently in different cone snail species. Snail-hunter and fish-hunter venom glands showed higher expression, while worm-hunter venom glands showed lower or no expression. According to Safavi-Hemami *et al.* (2016), insulins produce by cone snails are similar to prey signalling insulins. Snail-hunting species synthetise insulin-like conotoxins comparable with gastropods insulins, and fish-hunting species have venom insulins similar to fish insulins. The low levels of expression in vermivorous cone snails could be due to the low importance of these conotoxins in these species hunting strategies.

4.4. Screening for fractions with anti-steatosis activity

Marine proteins produced by *Chlorella vulgaris* and *Arthrospira platensi*, as well as spirulina have shown promise as dietary supplements that inhibit oxidative and

inflammatory processes and improve NALFD symptoms (Zhao *et al.*, 2021). Small peptides found in Kefir, digestion-resistant peptides derived from potato protein hydrolysate, the bioactive peptide DIKTNKPVIF, and the MTL small oral peptide have all been shown to be dietary proteins that can help reduce hepatic fat accumulation (Teng *et al.*, 2020; Zhao *et al.*, 2021). The ability of venom from these three *Conus* species to influence cellular metabolism and cause alterations in lipid accumulation in HepG2 cells was therefore investigated (Figure 17). Although conotoxins have been proven to be bioactive in other biological assays, the results showed that almost all tested fractions had no effect on the steatosis *in vitro*. In contrast, it was observed that some fractions resulted in more significant lipid accumulation in cells. Concerning cellular viability, fractions showed no cytotoxicity against HepG2 cells (Figure 18). These results are different from those obtained in the Nile red fat metabolism assay, where two fractions decrease lipid accumulation in zebrafish embryos (Figure 11). Carotenoids and terpenes are among the known compounds that interfere with lipid metabolism in this human hepatoma cell line (Zeng *et al.*, 2016; Costa *et al.*, 2019). To our knowledge, no studies have been carried out with conotoxins to evaluate their potential against hepatic steatosis, although there are studies that evaluated conopeptides cytotoxicity in this cell line (Sun *et al.*, 2011). According to Sun *et al.* (2011), cell viability was tested with MTT assay using conotoxin lt14a from *Conus litteratus*. Cells were exposed to conotoxins at a final concentration of 0.5 and 0.1 mg/ml, and both concentrations induce low cytotoxicity, presenting a cell viability of 90%. Another report combining HepG2 cells and *Conus* venom suggests that *Conus geographus* extracts have strong antiproliferative activity against the HepG2 cells line. MTT assay results revealed IC_{50} values for cytotoxicity of 19 ± 2.1 µg/mL (Alburae & Mohammed, 2020). Because *Conus litteratus* is a worm hunter and *Conus geographus* is a fish hunter cone snail, the cytotoxic variations described in these reports could be linked to the cellular pathways impacted by conotoxins, the concentrations of conopeptides evaluated, or the fact that isolated conotoxins or venom extracts were used in these reports. In this way, though HepG2 are proved to be a decent hepatic steatosis model, these cells show low metabolic capacity and reduced expression of enzymes and transporters (McMillian *et al.*, 2001), the findings reported in this work might suggest that lack of bioactivity could be related with the type of receptors involved in the lipid storage in hepatic cells and zebrafish yolk sac, and low cytotoxicity could be linked to the test concentrations employed or to conotoxins found in the venoms of the investigated vermivorous species.

4.5. Screening for fractions with inflammatory activity

Carotenoids, flavonoids, and phenolic substances are known to inhibit the production of inflammatory mediators, resulting in an anti-inflammatory action (Al-okbi, 2014; Howes, 2017). Anti-inflammatory properties have also been reported in a few marine nutraceuticals. Among the chemicals with proven antioxidant and anti-inflammatory activity are lipids from marine microalgae, polysaccharides from seaweeds, and proteins from *Phaeodactylum tricornutum* and *Arthrospira platensis* (Chojnacka & Michalak, 2016). The ability of these three *Conus* species' venoms to impact macrophage metabolism was investigated. Exposure of RAW 264.7 cells to *Conus* fractions revealed that the peptides found in each fraction had no ability to cause an inflammatory response, implying that these are not pro-inflammatory chemicals (Figure 19). In an anti-inflammatory experiment in which cells were exposed to LPS, a known inflammatory agent, there was a clear decrease in NO content following exposure to fractions, indicating that peptides present in these fractions may interfere with anti-inflammatory pathways (Figure 21). Cell viability following fraction exposure in the pro-inflammatory experiment demonstrated that these are not cytotoxic (Figure 20), while anti-inflammatory assay revealed cytotoxicity of two fractions after cells were exposed to LPS and conopeptides (Figure 22). Nicotinic acetylcholine receptors (nAChRs), sodium channels, potassium channels, and calcium channels are identical receptors that exist both in neuronal cells and in immune cells, like macrophages (Padilla *et al.*, 2017). Although conotoxins have already been largely studied on the nervous system, only a few studies have been conducted to establish their pharmacological potential in these non-excitable cells. α-conotoxins have been demonstrated to interact with diverse subtypes of n-AChRs, resulting in different metabolic responses in cells linked to oncogenesis and tumor-associated inflammation. The importance of acetylcholine regulation during the inflammatory process and the selectivity, affinity, and inhibitory effect of these conotoxins on human macrophage AChRs were revealed in these investigations (Terpinskaya *et al.*, 2015; Padilla *et al.*, 2017). Additionally, from the same family of the already FDA approved Ziconotide (ω-MVIIA), a novel ω-conotoxins was isolated from *Conus catus* and exhibit selectivity to inhibit N-type voltage-gated calcium channels, reversing chronic inflammatory pain in mouse paws (Sadeghi *et al.*, 2013). As a result, the findings reported in this work showed for the first time that conopeptides produced by *Conus ateralbus*, *Conus venulatus*, and *Conus genuanus* could interact with receptors expressed in RAW264.7 macrophages and elicit strong anti-inflammatory activities.

4.6. Zebrafish as model organism on screening for conotoxins bioactivity

The use of zebrafish as a model organism for screening bioactive chemicals is growing. Several investigations evaluating toxicity, anti-cancer activity, and screening for novel medicines have previously been performed. Furthermore, these species are frequently used in researching metabolic and genetic illnesses (Lieschke & Currie, 2007; Morash *et al.*, 2011; Zang *et al.*, 2018). The bioactive potential of conotoxins applied to zebrafish has revealed that they can reduce the locomotor activity of larvae when applied to water or injected directly into individuals and affect the escape behaviour of individuals. Insulin secreted by *Conus geograhus* (Con-Ins G1) and a peptide (ρ-TIA) produced by *Conus tulipa*, among other conotoxins, have already been studied using this model organism (Bosse *et al.*, 2021). Despite this potential, no research has been done before on the influence of conotoxins on the improvement of metabolic conditions in zebrafish larvae. As a result of the findings presented here, it is clear that zebrafish can be used to screen for conotoxins bioactivities against a variety of pathologies, expanding the number of model organisms suitable for conotoxins research and the diseases that can be investigated.

5. Conclusions

Cone snails are one of the most diverse groups of extant marine invertebrates, accounting for a significant portion of the ocean's biodiversity. These gastropods developed powerful venoms to seek their prey and defend themselves against predators. The majority of previous research has concentrated on identifying and characterizing conopeptides with neurological action, resulting in the discovery of conotoxins that interact with human receptors and develop a number of interesting pharmaceutical compounds. On the other hand, cone snails from the Cabo Verde archipelago remain an underexploited source of peptides due to their endemism and variety. This study aimed to investigate and characterize the venom of Cabo Verde's endemic and non-endemic *Conus* species, mainly bioactive potential against metabolic diseases like obesity, diabetes, non-alcoholic fatty liver disease, and inflammation.

According to venom characterization data, *Conus ateralbus* may synthesize more compounds for its venom than *Conus venulatus*. *Conus ateralbus* also has a higher prevalence of smaller peptides. Bioactivity assays revealed two fractions (*C.ateralbus* R2.6 and C3.1) with significant lipid reducing activity in zebrafish embryos. In addition, proteomic analyses were performed in *C.ateralbus* R2.6, and ten conotoxins were identified, which revealed sequences similarities with already described conotoxins. However due to the complexity of the fraction, peptides responsible for observed bioactivity will need to be uncovered in the future. An anti-inflammatory ability of fractions was also revealed during this project, where majority of fractions affected NO content after cells exposure to LPS. To the best of our knowledge, this was the first time conotoxins were investigated against obesity, steatosis and inflammation.

As a result, this research highlights the importance of exploring cone snail venoms for diseases other than neurological diseases. Furthermore, the zebrafish model organism demonstrates its compatibility with screening for conotoxins bioactivities against various pathologies as well as the use of immune system cells, expanding the range of model systems suitable for conotoxins research as well as the diseases that can be assessed.

6. Future perspectives

In terms of future research, it would be interesting to separate the venom duct content of *Conus ateralbus* to better understand the location of small molecules discovered in the venom and compare it to other species known to have small molecules, such as *Conus genuanus* and *Conus imperialis*.

In order to discover the responsible compounds, further purification and isolation of compounds contained in *C.ateralbus* R2.6 fraction would be necessary. This would require another sampling campaign and collection of the species. Alternatively, synthesis of identified conotoxins/conopeptides could be performed. Those ten conopeptides could then be exposed directly in the zebrafish fat metabolism assay to verify if some of these are responsible, at least in part, for the observed bioactivity. After bioactive compounds were identified, researchers could focus on the molecular mechanisms of action of these compounds and other bioactivities in zebrafish embryos, such as fatty acid and cholesterol uptake.

Proteomic investigations of other bioactive fractions could also be carried out in order to identify the responsible peptides for the bioactivities and better understand how conopeptides interfere with the anti-inflammatory response.

References

Abdulkhaleq, L. A., Assi, M. A., Abdullah, R., Zamri-Saad, M., Taufiq-Yap, Y. H., & Hezmee, M. (2018). The crucial roles of inflammatory mediators in inflammation: A review. *Veterinary world*, *11*(5), 627–635. https://doi.org/10.14202/vetworld.2018.627-635

Alburae, N. A., & Mohammed, A. E. (2020). Antiproliferative effect of the Red Sea cone snail, Conus geographus. *Tropical Journal of Pharmaceutical Research*, *19*(3), 577-581. https://doi.org/10.4314/tjpr.v19i3.17

Al-Okbi S. Y. (2014). Nutraceuticals of anti-inflammatory activity as complementary therapy for rheumatoid arthritis. *Toxicology and industrial health*, *30*(8), 738–749. https://doi.org/10.1177/0748233712462468

Al-Okbi S. Y. (2014). Nutraceuticals of anti-inflammatory activity as complementary therapy for rheumatoid arthritis. *Toxicology and industrial health*, *30*(8), 738–749. https://doi.org/10.1177/0748233712462468

Aman, J. W., Imperial, J. S., Ueberheide, B., Zhang, M. M., Aguilar, M., Taylor, D., Watkins, M., Yoshikami, D., Showers-Corneli, P., Safavi-Hemami, H., Biggs, J., Teichert, R. W., & Olivera, B. M. (2015). Insights into the origins of fish hunting in venomous cone snails from studies of Conus tessulatus. *Proceedings of the National Academy of Sciences of the United States of America*, *112*(16), 5087–5092. https://doi.org/10.1073/pnas.1424435112

American Diabetes Association (2018). Economic Costs of Diabetes in the U.S. in 2017. *Diabetes care*, *41*(5), 917–928. https://doi.org/10.2337/dci18-0007

Anjos, L. A. D. (2006). *Obesidade e saúde pública*. Editora Fiocruz. https://doi.org/10.7476/9788575413449

Arya, A., Nahar, L., Khan, H. U., & Sarker, S. D. (2020). Anti-obesity natural products. In *Annual Reports in Medicinal Chemistry* (1st ed., Vol. 55, Issue April). Elsevier Inc. https://doi.org/10.1016/bs.armc.2020.02.006

Banga, J. D. (1998). Invited Review. Vascular Surgery, 32(3), 245–247. https://doi.org/10.1177/153857449803200307

Barbier, P., & Schneider, F. (1987). Syntheses of tetrahydrolipstatin and absolute configuration of tetrahydrolipstatin and lipstatin. *Helvetica Chimica Acta*, *70*(1), 196-202. https://doi.org/10.1002/hlca.19870700124

Biggs, J. S., Watkins, M., Puillandre, N., Ownby, J. P., Lopez-Vera, E., Christensen, S., Moreno, K. J., Bernaldez, J., Licea-Navarro, A., Corneli, P. S., & Olivera, B. M. (2010). Evolution of Conus peptide toxins: analysis of Conus californicus Reeve, 1844. *Molecular phylogenetics and evolution*, *56*(1), 1–12. https://doi.org/10.1016/j.ympev.2010.03.029

Bosse, G. D., Urcino, C., Watkins, M., Flórez Salcedo, P., Kozel, S., Chase, K., Cabang, A., Espino, S. S., Safavi-Hemami, H., Raghuraman, S., Olivera, B. M., Peterson, R. T., & Gajewiak, J. (2021). Discovery of a Potent Conorfamide from *Conus episcopatus* Using a Novel Zebrafish Larvae Assay. *Journal of natural products*, *84*(4), 1232–1243. https://doi.org/10.1021/acs.jnatprod.0c01297

Buzzetti, E., Pinzani, M., & Tsochatzis, E. A. (2016). The multiple-hit pathogenesis of non-alcoholic fatty liver disease (NAFLD). *Metabolism: clinical and experimental*, *65*(8), 1038–1048. https://doi.org/10.1016/j.metabol.2015.12.012

Cherng, S. C., Cheng, S. N., Tarn, A., & Chou, T. C. (2007). Anti-inflammatory activity of c-phycocyanin in lipopolysaccharide-stimulated RAW 264.7 macrophages. *Life sciences*, *81*(19-20), 1431–1435. https://doi.org/10.1016/j.lfs.2007.09.009

Chojnacka, K., & Michalak, I. (2016). Marine nutraceuticals. *Marine OMICS: Principles and Applications*, *August*, 329–345. https://doi.org/10.1201/9781315372303

Chooi, Y. C., Ding, C., & Magkos, F. (2019). The epidemiology of obesity. *Metabolism: clinical and experimental*, *92*, 6–10. https://doi.org/10.1016/j.metabol.2018.09.005

Church, C., Horowitz, M., & Rodeheffer, M. (2012). WAT is a functional adipocyte?. *Adipocyte*, *1*(1), 38–45. https://doi.org/10.4161/adip.19132

Conticello, S. G., Gilad, Y., Avidan, N., Ben-Asher, E., Levy, Z., & Fainzilber, M. (2001). Mechanisms for evolving hypervariability: the case of conopeptides. *Molecular biology and evolution*, *18*(2), 120–131. https://doi.org/10.1093/oxfordjournals.molbev.a003786

Costa, M., Rosa, F., Ribeiro, T., Hernandez-Bautista, R., Bonaldo, M., Gonçalves Silva, N., Eiríksson, F., Thorsteinsdóttir, M., Ussar, S., & Urbatzka, R. (2019). Identification of Cyanobacterial Strains with Potential for the Treatment of Obesity-Related Co-Morbidities by Bioactivity, Toxicity Evaluation and Metabolite Profiling. *Marine drugs*, *17*(5), 280. https://doi.org/10.3390/md17050280

Cui, W., Chen, S. L., & Hu, K. Q. (2010). Quantification and mechanisms of oleic acid-induced steatosis in HepG2 cells. *American journal of translational research*, *2*(1), 95–104.

Cunha, R. L., Castilho, R., Rüber, L., & Zardoya, R. (2005). Patterns of cladogenesis in the venomous marine gastropod genus Conus from the Cape Verde islands. *Systematic biology*, *54*(4), 634–650. https://doi.org/10.1080/106351591007471

Cunha, R. L., Tenorio, M. J., Afonso, C., Castilho, R., & Zardoya, R. (2008). Replaying the tape: recurring biogeographical patterns in Cape Verde Conus after 12 million years. *Molecular ecology*, *17*(3), 885–901. https://doi.org/10.1111/j.1365-294X.2007.03618.x

da Cunha Oliveira, R. L. (2008). *Tempo and more or evolution of the genus conus (gastropoda: Neogastropoda) in the cape verde islands* (Doctoral dissertation, Universidad Autónoma de Madrid).

Dalmolin, C., Almeida, D. V., Figueiredo, M. A., & Marins, L. F. (2018). Expression profile of glucose transport-related genes under chronic and acute exposure to growth hormone in zebrafish. *Comparative biochemistry and physiology. Part A, Molecular & integrative physiology*, *221*, 1–6. https://doi.org/10.1016/j.cbpa.2018.02.015

Davis, J., Jones, A., & Lewis, R. J. (2009). Remarkable inter- and intra-species complexity of conotoxins revealed by LC/MS. *Peptides*, *30*(7), 1222–1227. https://doi.org/10.1016/j.peptides.2009.03.019

Deshpande, A. D., Harris-Hayes, M., & Schootman, M. (2008). Epidemiology of diabetes and diabetes-related complications. *Physical therapy*, *88*(11), 1254–1264.

https://doi.org/10.2522/ptj.20080020

Díaz M., Juan Manuel, & Gracia C., Adriana M., & Cantera K., Jaime R. (2005). Checklist of the Cone Shells (Mollusca: Gastropoda: Neogastropoda: Conidae) of Colombia. Biota Colombiana, 6(1),73-85. ISSN: 0124-5376.

Donato, M. T., Tolosa, L., & Gómez-Lechón, M. J. (2015). Culture and Functional Characterization of Human Hepatoma HepG2 Cells. *Methods in molecular biology (Clifton, N.J.)*, *1250*, 77–93. https://doi.org/10.1007/978-1-4939-2074-7_5

El Barky, A. R., Hussein, S. A., Alm-Eldeen, A. A., Hafez, Y. A., & Mohamed, T. M. (2016). Anti-diabetic activity of Holothuria thomasi saponin. *Biomedicine & pharmacotherapy = Biomedecine & pharmacotherapie*, *84*, 1472–1487. https://doi.org/10.1016/j.biopha.2016.10.002

Flores-Garza, R., Garcia-Moctezuma, Y. M., Flores-Rodríguez, P., Michel-Morfín, J. E., & Torreblanca-Ramírez, C. (2014). The Conidae Family (Snails Producers of Poisons) Associated with the Rocky Intertidal Zone of Acapulco, Mexico. *Natural Resources*, *05*(08), 343–350. https://doi.org/10.4236/nr.2014.58032

Gao, B., Peng, C., Yang, J., Yi, Y., Zhang, J., & Shi, Q. (2017). Cone Snails: A Big Store of Conotoxins for Novel Drug Discovery. *Toxins*, *9*(12), 397. https://doi.org/10.3390/toxins9120397

George, P., & Abisheck, A. (2020). In Silico Facets of Biochemical Research: Accounts from Protein Folding and Protein-Ligand Interaction Studies.

Gerets, H. H., Tilmant, K., Gerin, B., Chanteux, H., Depelchin, B. O., Dhalluin, S., & Atienzar, F. A. (2012). Characterization of primary human hepatocytes, HepG2 cells, and HepaRG cells at the mRNA level and CYP activity in response to inducers and their predictivity for the detection of human hepatotoxins. *Cell biology and toxicology*, *28*(2), 69–87. https://doi.org/10.1007/s10565-011-9208-4

Gorson, J., Ramrattan, G., Verdes, A., Wright, E. M., Kantor, Y., Rajaram Srinivasan, R., Musunuri, R., Packer, D., Albano, G., Qiu, W. G., & Holford, M. (2015). Molecular Diversity and Gene Evolution of the Venom Arsenal of Terebridae Predatory Marine Snails. *Genome biology and evolution*, *7*(6), 1761–1778. https://doi.org/10.1093/gbe/evv104

Halai, R., & Craik, D. J. (2009). Conotoxins: natural product drug leads. *Natural product reports*, *26*(4), 526–536. https://doi.org/10.1039/b819311h

Hoggard, M. F., Rodriguez, A. M., Cano, H., Clark, E., Tae, H. S., Adams, D. J., Godenschwege, T. A., & Marí, F. (2017). In vivo and in vitro testing of native α-conotoxins from the injected venom of Conus purpurascens. *Neuropharmacology*, *127*, 253–259. https://doi.org/10.1016/j.neuropharm.2017.09.020

Howes, M. J. R. (2018). Phytochemicals as anti-inflammatory nutraceuticals and phytopharmaceuticals. In *Immunity and Inflammation in Health and Disease* (pp. 363-388). Academic Press. https://doi.org/10.1016/B978-0-12-805417-8.00028-7

Huang, M. T., Ghai, G., & Ho, C. T. (2004). Inflammatory Process and Molecular Targets for Antiinflammatory Nutraceuticals. *Comprehensive reviews in food science and food*

safety, *3*(4), 127–139. https://doi.org/10.1111/j.1541-4337.2004.tb00063.x

Jakubowski, J. A., Keays, D. A., Kelley, W. P., Sandall, D. W., Bingham, J. P., Livett, B. G., Gayler, K. R., & Sweedler, J. V. (2004). Determining sequences and post-translational modifications of novel conotoxins in Conus victoriae using cDNA sequencing and mass spectrometry. *Journal of mass spectrometry : JMS*, *39*(5), 548–557. https://doi.org/10.1002/jms.624

Jakubowski, J. A., Kelley, W. P., & Sweedler, J. V. (2006). Screening for post-translational modifications in conotoxins using liquid chromatography/mass spectrometry: an important component of conotoxin discovery. *Toxicon : official journal of the International Society on Toxinology*, *47*(6), 688–699. https://doi.org/10.1016/j.toxicon.2006.01.021

James, D., Prator, C. A., Martin, G. G., & Schulz, J. R. (2014). Morphology of sensory papillae on the feeding proboscis of cone snails (Mollusca, Gastropoda). *Invertebrate biology*, *133*(3), 221-231. https://doi.org/10.1111/ivb.12058

Kaas, Q., Westermann, J. C., & Craik, D. J. (2010). Conopeptide characterization and classifications: an analysis using ConoServer. *Toxicon : official journal of the International Society on Toxinology*, *55*(8), 1491–1509. https://doi.org/10.1016/j.toxicon.2010.03.002

Kaas, Q., Westermann, J. C., Halai, R., Wang, C. K., & Craik, D. J. (2008). ConoServer, a database for conopeptide sequences and structures. *Bioinformatics*, *24*(3), 445-446. https://doi.org/10.1093/bioinformatics/btm596

Kauferstein, S., Porth, C., Kendel, Y., Wunder, C., Nicke, A., Kordis, D., Favreau, P., Koua, D., Stöcklin, R., & Mebs, D. (2011). Venomic study on cone snails (Conus spp.) from South Africa. *Toxicon : official journal of the International Society on Toxinology*, *57*(1), 28–34. https://doi.org/10.1016/j.toxicon.2010.09.009

Kelly, T., Yang, W., Chen, C. S., Reynolds, K., & He, J. (2008). Global burden of obesity in 2005 and projections to 2030. *International journal of obesity (2005)*, *32*(9), 1431–1437. https://doi.org/10.1038/ijo.2008.102

Khanfar, M. A., Asal, B. A., Mudit, M., Kaddoumi, A., & El Sayed, K. A. (2009). The marine natural-derived inhibitors of glycogen synthase kinase-3beta phenylmethylene hydantoins: In vitro and in vivo activities and pharmacophore modeling. *Bioorganic & medicinal chemistry*, *17*(16), 6032–6039. https://doi.org/10.1016/j.bmc.2009.06.054

Kim, H. G., Shrestha, B., Lim, S. Y., Yoon, D. H., Chang, W. C., Shin, D. J., Han, S. K., Park, S. M., Park, J. H., Park, H. I., Sung, J. M., Jang, Y., Chung, N., Hwang, K. C., & Kim, T. W. (2006). Cordycepin inhibits lipopolysaccharide-induced inflammation by the suppression of NF-kappaB through Akt and p38 inhibition in RAW 264.7 macrophage cells. *European journal of pharmacology*, *545*(2-3), 192–199. https://doi.org/10.1016/j.ejphar.2006.06.047

Kong, L., Smith, W., & Hao, D. (2019). Overview of RAW264.7 for osteoclastogensis study: Phenotype and stimuli. *Journal of cellular and molecular medicine*, *23*(5), 3077–3087. https://doi.org/10.1111/jcmm.14277

Lee J. K. (2011). Anti-inflammatory effects of eriodictyol in lipopolysaccharide-stimulated raw 264.7 murine macrophages. *Archives of pharmacal research*, *34*(4), 671–679.

https://doi.org/10.1007/s12272-011-0418-3

Leonelli, S., & Ankeny, R. A. (2013). What makes a model organism?. *Endeavour*, *37*(4), 209–212. https://doi.org/10.1016/j.endeavour.2013.06.001

Lieschke, G. J., & Currie, P. D. (2007). Animal models of human disease: zebrafish swim into view. *Nature reviews. Genetics*, *8*(5), 353–367. https://doi.org/10.1038/nrg2091

Lin, Z., Torres, J. P., Watkins, M., Paguigan, N., Niu, C., Imperial, J. S., Tun, J., Safavi-Hemami, H., Finol-Urdaneta, R. K., Neves, J., Espino, S., Karthikeyan, M., Olivera, B. M., & Schmidt, E. W. (2021). Non-Peptidic Small Molecule Components from Cone Snail Venoms. *Frontiers in pharmacology*, *12*, 655981. https://doi.org/10.3389/fphar.2021.655981

Livett, B. G., Gayler, K. R., & Khalil, Z. (2004). Drugs from the sea: conopeptides as potential therapeutics. *Current medicinal chemistry*, *11*(13), 1715–1723. https://doi.org/10.2174/0929867043364928

Loughnan, M. L., Nicke, A., Lawrence, N., & Lewis, R. J. (2009). Novel alpha D-conopeptides and their precursors identified by cDNA cloning define the D-conotoxin superfamily. *Biochemistry*, *48*(17), 3717–3729. https://doi.org/10.1021/bi9000326

Marshall, J., Kelley, W. P., Rubakhin, S. S., Bingham, J. P., Sweedler, J. V., & Gilly, W. F. (2002). Anatomical correlates of venom production in Conus californicus. *The Biological bulletin*, *203*(1), 27–41. https://doi.org/10.2307/1543455

McMillian, M. K., Grant, E. R., Zhong, Z., Parker, J. B., Li, L., Zivin, R. A., Burczynski, M. E., & Johnson, M. D. (2001). Nile Red binding to HepG2 cells: an improved assay for in vitro studies of hepatosteatosis. *In vitro & molecular toxicology*, *14*(3), 177–190. https://doi.org/10.1089/109793301753407948

Merly, L., & Smith, S. L. (2017). Murine RAW 264.7 cell line as an immune target: are we missing something?. *Immunopharmacology and immunotoxicology*, *39*(2), 55-58. https://doi.org/10.1080/08923973.2017.1282511

Mir, R., Karim, S., Kamal, M. A., Wilson, C. M., & Mirza, Z. (2016). Conotoxins: Structure, Therapeutic Potential and Pharmacological Applications. *Current pharmaceutical design*, *22*(5), 582–589. https://doi.org/10.2174/1381612822666151124234715

Morash, M. G., Douglas, S. E., Robotham, A., Ridley, C. M., Gallant, J. W., & Soanes, K. H. (2011). The zebrafish embryo as a tool for screening and characterizing pleurocidin host-defense peptides as anti-cancer agents. *Disease models & mechanisms*, *4*(5), 622–633. https://doi.org/10.1242/dmm.007310

Musso, G., Gambino, R., Cassader, M., & Pagano, G. (2011). Meta-analysis: natural history of non-alcoholic fatty liver disease (NAFLD) and diagnostic accuracy of non-invasive tests for liver disease severity. *Annals of medicine*, *43*(8), 617–649. https://doi.org/10.3109/07853890.2010.518623

Neves, J. D. L. B. (2016). Analysis of Venom in Cape Verde Cone Snails.

Neves, J. L., Lin, Z., Imperial, J. S., Antunes, A., Vasconcelos, V., Olivera, B. M., & Schmidt, E. W. (2015). Small Molecules in the Cone Snail Arsenal. *Organic letters*, *17*(20), 4933–4935. https://doi.org/10.1021/acs.orglett.5b02389

Neves, J., Campos, A., Osório, H., Antunes, A., & Vasconcelos, V. (2013). Conopeptides from Cape Verde Conus crotchii. *Marine drugs*, *11*(6), 2203–2215. https://doi.org/10.3390/md11062203

Neves, J., Imperial, J. S., Morgenstern, D., Ueberheide, B., Gajewiak, J., Antunes, A., Robinson, S. D., Espino, S., Watkins, M., Vasconcelos, V., & Olivera, B. M. (2019). Characterization of the First Conotoxin from *Conus ateralbus*, a Vermivorous Cone Snail from the Cabo Verde Archipelago. *Marine drugs*, *17*(8), 432. https://doi.org/10.3390/md17080432

Nguyen, M., Yang, E., Neelkantan, N., Mikhaylova, A., Arnold, R., Poudel, M. K., Stewart, A. M., & Kalueff, A. V. (2013). Developing 'integrative' zebrafish models of behavioral and metabolic disorders. *Behavioural brain research*, *256*, 172–187. https://doi.org/10.1016/j.bbr.2013.08.012

Olivera, B. M. (2002). Conus venom peptides: Reflections from the biology of clades and species. *Annual Review of Ecology and Systematics*, *33*, 25–47. https://doi.org/10.1146/annurev.ecolsys.33.010802.150424

Olivera, B. M., Imperial, J. S., & Concepcion, G. P. (2013). Snail peptides. *Handbook of Biologically Active Peptides, 2nd ed.; Kastin, AJ, Ed*, 437-450. https://doi.org/10.1016/B978-0-12-385095-9.00061-0

Olivera, B. M., Showers Corneli, P., Watkins, M., & Fedosov, A. (2014). Biodiversity of cone snails and other venomous marine gastropods: evolutionary success through neuropharmacology. *Annual review of animal biosciences*, *2*, 487–513. https://doi.org/10.1146/annurev-animal-022513-114124

Padilla, A., Keating, P., Hartmann, J. X., & Marí, F. (2017). Effects of α-conotoxin ImI on TNF-α, IL-8 and TGF-β expression by human macrophage-like cells derived from THP-1 pre-monocytic leukemic cells. *Scientific reports*, *7*(1), 12742. https://doi.org/10.1038/s41598-017-11586-2

Peng, C., Wu, X., Han, Y., Yuan, D., Chi, C., & Wang, C. (2007). Identification of six novel T-1 conotoxins from Conus pulicarius by molecular cloning. *Peptides*, *28*(11), 2116–2124. https://doi.org/10.1016/j.peptides.2007.08.026

Pi, C., Liu, J., Peng, C., Liu, Y., Jiang, X., Zhao, Y., Tang, S., Wang, L., Dong, M., Chen, S., & Xu, A. (2006). Diversity and evolution of conotoxins based on gene expression profiling of Conus litteratus. *Genomics*, *88*(6), 809–819. https://doi.org/10.1016/j.ygeno.2006.06.014

Piwowarski, J. P., Kiss, A. K., Granica, S., & Moeslinger, T. (2015). Urolithins, gut microbiota-derived metabolites of ellagitannins, inhibit LPS-induced inflammation in RAW 264.7 murine macrophages. *Molecular nutrition & food research*, *59*(11), 2168–2177. https://doi.org/10.1002/mnfr.201500264

Polakof, S., Panserat, S., Soengas, J. L., & Moon, T. W. (2012). Glucose metabolism in fish: a review. *Journal of comparative physiology. B, Biochemical, systemic, and environmental physiology*, *182*(8), 1015–1045. https://doi.org/10.1007/s00360-012-0658-7

Prashanth, J. R., Dutertre, S., Jin, A. H., Lavergne, V., Hamilton, B., Cardoso, F. C., Griffin, J., Venter, D. J., Alewood, P. F., & Lewis, R. J. (2016). The role of defensive ecological

interactions in the evolution of conotoxins. *Molecular ecology*, *25*(2), 598–615. https://doi.org/10.1111/mec.13504

Puillandre N., Fedosov A.E., Kantor Y.I. (2017) Systematics and Evolution of the Conoidea. In: Gopalakrishnakone P., Malhotra A. (eds) *Evolution of Venomous Animals and Their Toxins*. Toxinology. Springer, Dordrecht. https://doi.org/10.1007/978-94-007-6458-3_19

Puillandre, N., Samadi, S., Boisselier, M. C., Sysoev, A. V., Kantor, Y. I., Cruaud, C., Couloux, A., & Bouchet, P. (2008). Starting to unravel the toxoglossan knot: molecular phylogeny of the "turrids" (Neogastropoda: Conoidea). *Molecular phylogenetics and evolution*, *47*(3), 1122–1134. https://doi.org/10.1016/j.ympev.2007.11.007

Rainsford K. D. (2007). Anti-inflammatory drugs in the 21st century. *Sub-cellular biochemistry*, *42*, 3–27. https://doi.org/10.1007/1-4020-5688-5_1

Rajesh R. P. (2015). Novel M-Superfamily and T-Superfamily conotoxins and contryphans from the vermivorous snail Conus figulinus. *Journal of peptide science : an official publication of the European Peptide Society*, *21*(1), 29–39. https://doi.org/10.1002/psc.2715

Ramilo, C. A., Zafaralla, G. C., Nadasdi, L., Hammerland, L. G., Yoshikami, D., Gray, W. R., Kristipati, R., Ramachandran, J., Miljanich, G., & Olivera, B. M. (1992). Novel alpha- and omega-conotoxins from Conus striatus venom. *Biochemistry*, *31*(41), 9919–9926. https://doi.org/10.1021/bi00156a009

Reddy, D. B., & Reddanna, P. (2009). Chebulagic acid (CA) attenuates LPS-induced inflammation by suppressing NF-kappaB and MAPK activation in RAW 264.7 macrophages. *Biochemical and biophysical research communications*, *381*(1), 112–117. https://doi.org/10.1016/j.bbrc.2009.02.022

Robinson, S. D., & Safavi-Hemami, H. (2016). Insulin as a weapon. *Toxicon : official journal of the International Society on Toxinology*, *123*, 56–61. https://doi.org/10.1016/j.toxicon.2016.10.010

Rodgers, R. J., Tschöp, M. H., & Wilding, J. P. (2012). Anti-obesity drugs: past, present and future. *Disease models & mechanisms*, *5*(5), 621–626. https://doi.org/10.1242/dmm.009621

Sadeghi, M., Murali, S. S., Lewis, R. J., Alewood, P. F., Mohammadi, S., & Christie, M. J. (2013). Novel ω-conotoxins from C. catus reverse signs of mouse inflammatory pain after systemic administration. *Molecular pain*, *9*, 51. https://doi.org/10.1186/1744-8069-9-51

Safavi-Hemami, H., Gajewiak, J., Karanth, S., Robinson, S. D., Ueberheide, B., Douglass, A. D., Schlegel, A., Imperial, J. S., Watkins, M., Bandyopadhyay, P. K., Yandell, M., Li, Q., Purcell, A. W., Norton, R. S., Ellgaard, L., & Olivera, B. M. (2015). Specialized insulin is used for chemical warfare by fish-hunting cone snails. *Proceedings of the National Academy of Sciences of the United States of America*, *112*(6), 1743–1748. https://doi.org/10.1073/pnas.1423857112

Safavi-Hemami, H., Lu, A., Li, Q., Fedosov, A. E., Biggs, J., Showers Corneli, P., Seger, J., Yandell, M., & Olivera, B. M. (2016). Venom Insulins of Cone Snails Diversify Rapidly and Track Prey Taxa. *Molecular biology and evolution*, *33*(11), 2924–2934. https://doi.org/10.1093/molbev/msw174

Safavi-Hemami, H., Siero, W. A., Kuang, Z., Williamson, N. A., Karas, J. A., Page, L. R., MacMillan, D., Callaghan, B., Kompella, S. N., Adams, D. J., Norton, R. S., & Purcell, A. W. (2011). Embryonic toxin expression in the cone snail Conus victoriae: primed to kill or divergent function?. *The Journal of biological chemistry*, *286*(25), 22546–22557. https://doi.org/10.1074/jbc.M110.217703

Seth, A., Stemple, D. L., & Barroso, I. (2013). The emerging use of zebrafish to model metabolic disease. *Disease models & mechanisms*, *6*(5), 1080–1088. https://doi.org/10.1242/dmm.011346

Shih, P. H., Shiue, S. J., Chen, C. N., Cheng, S. W., Lin, H. Y., Wu, L. W., & Wu, M. S. (2021). Fucoidan and Fucoxanthin Attenuate Hepatic Steatosis and Inflammation of NAFLD through Modulation of Leptin/Adiponectin Axis. *Marine drugs*, *19*(3), 148. https://doi.org/10.3390/md19030148

Sousa, S. R., McArthur, J. R., Brust, A., Bhola, R. F., Rosengren, K. J., Ragnarsson, L., Dutertre, S., Alewood, P. F., Christie, M. J., Adams, D. J., Vetter, I., & Lewis, R. J. (2018). Novel analgesic ω-conotoxins from the vermivorous cone snail Conus moncuri provide new insights into the evolution of conopeptides. *Scientific reports*, *8*(1), 13397. https://doi.org/10.1038/s41598-018-31245-4

Srivastava, G., & Apovian, C. (2018). Future Pharmacotherapy for Obesity: New Anti-obesity Drugs on the Horizon. *Current obesity reports*, *7*(2), 147–161. https://doi.org/10.1007/s13679-018-0300-4

Sterrett, J. J., Bragg, S., & Weart, C. W. (2016). Type 2 Diabetes Medication Review. *The American journal of the medical sciences*, *351*(4), 342–355. https://doi.org/10.1016/j.amjms.2016.01.019

Sun, D., Ren, Z., Zeng, X., You, Y., Pan, W., Zhou, M., Wang, L., & Xu, A. (2011). Structure-function relationship of conotoxin lt14a, a potential analgesic with low cytotoxicity. *Peptides*, *32*(2), 300–305. https://doi.org/10.1016/j.peptides.2010.11.012

Taciak, B., Białasek, M., Braniewska, A., Sas, Z., Sawicka, P., Kiraga, Ł., Rygiel, T., & Król, M. (2018). Evaluation of phenotypic and functional stability of RAW 264.7 cell line through serial passages. *PloS one*, *13*(6), e0198943. https://doi.org/10.1371/journal.pone.0198943

Tamayo, T., Rosenbauer, J., Wild, S. H., Spijkerman, A. M., Baan, C., Forouhi, N. G., Herder, C., & Rathmann, W. (2014). Diabetes in Europe: an update. *Diabetes research and clinical practice*, *103*(2), 206–217. https://doi.org/10.1016/j.diabres.2013.11.007

Teng, B., Huang, C., Cheng, C. L., Udduttula, A., Yu, X. F., Liu, C., Li, J., Yao, Z. Y., Long, J., Miao, L. F., Zou, C., Chu, J., Zhang, J. V., & Ren, P. G. (2020). Newly identified peptide hormone inhibits intestinal fat absorption and improves NAFLD through its receptor GPRC6A. *Journal of hepatology*, *73*(2), 383–393. https://doi.org/10.1016/j.jhep.2020.02.026

Tenorio, M.J. 2012a. *Conus ateralbus*. *The IUCN Red List of Threatened Species* 2012:e.T192744A2154590. https://dx.doi.org/10.2305/IUCN.UK.2012-1.RLTS.T192744A2154590.en

Tenorio, M.J. 2012b. *Conus genuanus*. *The IUCN Red List of Threatened*

Species 2012:e.T192608A2126619. https://dx.doi.org/10.2305/IUCN.UK.2012-1.RLTS.T192608A2126619.en

Tenorio, M.J. 2012c. *Conus venulatus*. *The IUCN Red List of Threatened Species* 2012: e.T192455A2098106. https://dx.doi.org/10.2305/IUCN.UK.2012-1.RLTS.T192455A2098106.en

Terlau, H., & Olivera, B. M. (2004). Conus venoms: a rich source of novel ion channel-targeted peptides. *Physiological reviews*, *84*(1), 41–68. https://doi.org/10.1152/physrev.00020.2003

Terpinskaya, T. I., Osipov, A. V., Kuznetsova, T. E., Ryzhkovskaya, E. L., Ulaschik, V. S., Ivanov, I. A., Tsetlin, V. I., & Utkin, Y. N. (2015). α-conotoxins revealed different roles of nicotinic cholinergic receptor subtypes in oncogenesis of Ehrlich tumor and in the associated inflammation. *Doklady. Biochemistry and biophysics*, *463*, 216–219. https://doi.org/10.1134/S1607672915040055

Torres, J. P., Lin, Z., Watkins, M., Salcedo, P. F., Baskin, R. P., Elhabian, S., Safavi-Hemami, H., Taylor, D., Tun, J., Concepcion, G. P., Saguil, N., Yanagihara, A. A., Fang, Y., McArthur, J. R., Tae, H. S., Finol-Urdaneta, R. K., Özpolat, B. D., Olivera, B. M., & Schmidt, E. W. (2021). Small-molecule mimicry hunting strategy in the imperial cone snail, *Conus imperialis*. *Science advances*, *7*(11), eabf2704. https://doi.org/10.1126/sciadv.abf2704

Urbatzka, R., Freitas, S., Palmeira, A., Almeida, T., Moreira, J., Azevedo, C., Afonso, C., Correia-da-Silva, M., Sousa, E., Pinto, M., & Vasconcelos, V. (2018). Lipid reducing activity and toxicity profiles of a library of polyphenol derivatives. *European journal of medicinal chemistry*, *151*, 272–284. https://doi.org/10.1016/j.ejmech.2018.03.036

Vane, J. R., & Botting, R. M. (1998). Anti-inflammatory drugs and their mechanism of action. *Inflammation research : official journal of the European Histamine Research Society ... [et al.]*, *47 Suppl 2*, S78–S87. https://doi.org/10.1007/s000110050284

Vianna Braga, M. C., Konno, K., Portaro, F. C., de Freitas, J. C., Yamane, T., Olivera, B. M., & Pimenta, D. C. (2005). Mass spectrometric and high performance liquid chromatography profiling of the venom of the Brazilian vermivorous mollusk Conus regius: feeding behavior and identification of one novel conotoxin. *Toxicon : official journal of the International Society on Toxinology*, *45*(1), 113–122. https://doi.org/10.1016/j.toxicon.2004.09.018

Wang, S., Du, T., Liu, Z., Wang, S., Wu, Y., Ding, J., Jiang, L., & Dai, Q. (2014). Characterization of a T-superfamily conotoxin TxVC from Conus textile that selectively targets neuronal nAChR subtypes. *Biochemical and biophysical research communications*, *454*(1), 151–156. https://doi.org/10.1016/j.bbrc.2014.10.055

Weibel, E. K., Hadvary, P., Hochuli, E., Kupfer, E., & Lengsfeld, H. (1987). Lipstatin, an inhibitor of pancreatic lipase, produced by Streptomyces toxytricini. I. Producing organism, fermentation, isolation and biological activity. *The Journal of antibiotics*, *40*(8), 1081–1085. https://doi.org/10.7164/antibiotics.40.1081

Xu, L., Li, Y., Dai, Y., & Peng, J. (2018). Natural products for the treatment of type 2 diabetes mellitus: Pharmacology and mechanisms. *Pharmacological research*, *130*, 451–465. https://doi.org/10.1016/j.phrs.2018.01.015

Yoon, S. B., Lee, Y. J., Park, S. K., Kim, H. C., Bae, H., Kim, H. M., Ko, S. G., Choi, H. Y., Oh, M. S., & Park, W. (2009). Anti-inflammatory effects of Scutellaria baicalensis water extract on LPS-activated RAW 264.7 macrophages. *Journal of ethnopharmacology*, *125*(2), 286–290. https://doi.org/10.1016/j.jep.2009.06.027

Zang, L., Maddison, L. A., & Chen, W. (2018). Zebrafish as a Model for Obesity and Diabetes. *Frontiers in cell and developmental biology*, *6*, 91. https://doi.org/10.3389/fcell.2018.00091

Zeng, L., Tang, W., Yin, J., Feng, L., Li, Y., Yao, X., & Zhou, B. (2016). Alisol A 24-Acetate Prevents Hepatic Steatosis and Metabolic Disorders in HepG2 Cells. *Cellular physiology and biochemistry : international journal of experimental cellular physiology, biochemistry, and pharmacology*, *40*(3-4), 453–464. https://doi.org/10.1159/000452560

Zhao, M., Chen, S., Ji, X., Shen, X., You, J., Liang, X., Yin, H., & Zhao, L. (2021). Current innovations in nutraceuticals and functional foods for intervention of non-alcoholic fatty liver disease. *Pharmacological research*, *166*, 105517. https://doi.org/10.1016/j.phrs.2021.105517

Zon, L. I., & Peterson, R. T. (2005). In vivo drug discovery in the zebrafish. *Nature reviews. Drug discovery*, *4*(1), 35–44. https://doi.org/10.1038/nrd1606

Appendixes

- **Appendixes I- Chromatographic profile of *Conus ateralbus* using gradient 1**

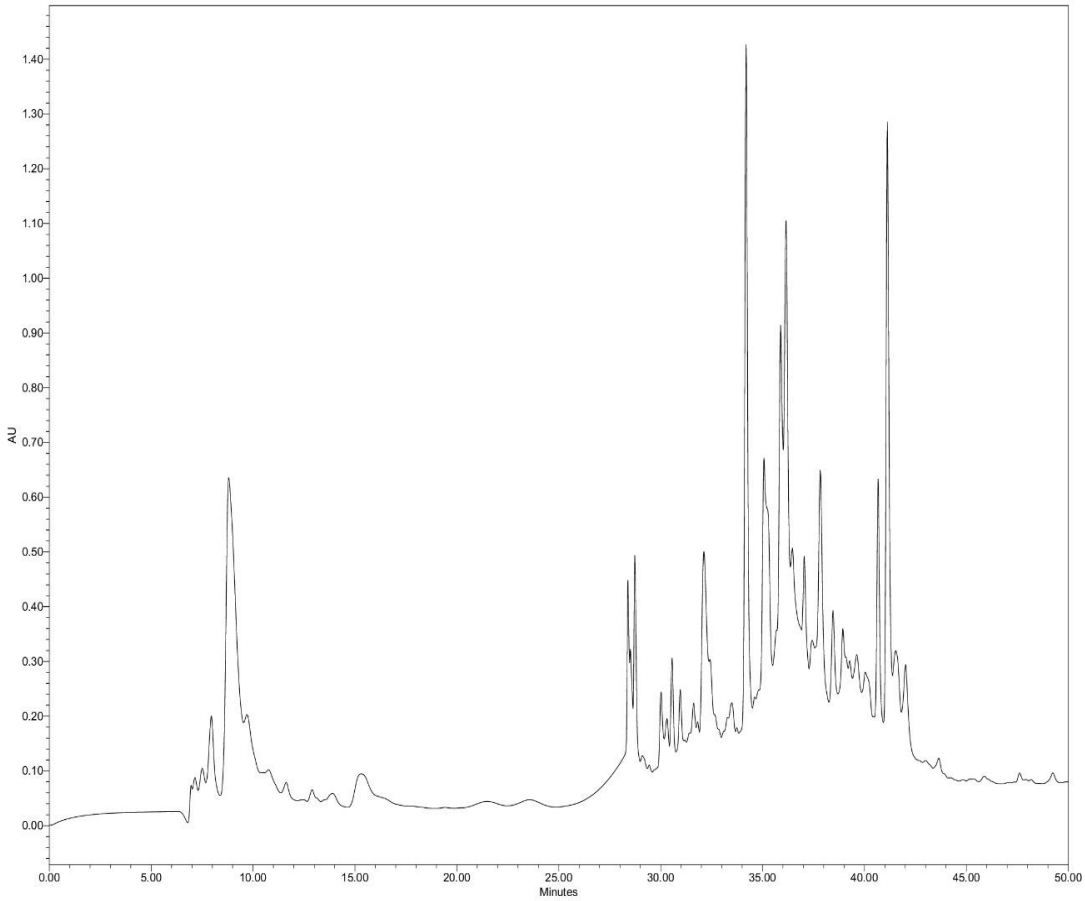

Figure A *Chromatographic profile of Conus ateralbus using gradient 1. More polar compounds eluted around 7 min of running with good resolution. Nonpolar compounds eluted with almost 36% of solvent B. Compounds eluted in this phase show poor separation, suggesting a mixture of detected compounds.*

- **Appendixes II - Chromatographic profile of *Conus ateralbus* using a flow rate of 3 mL/min**

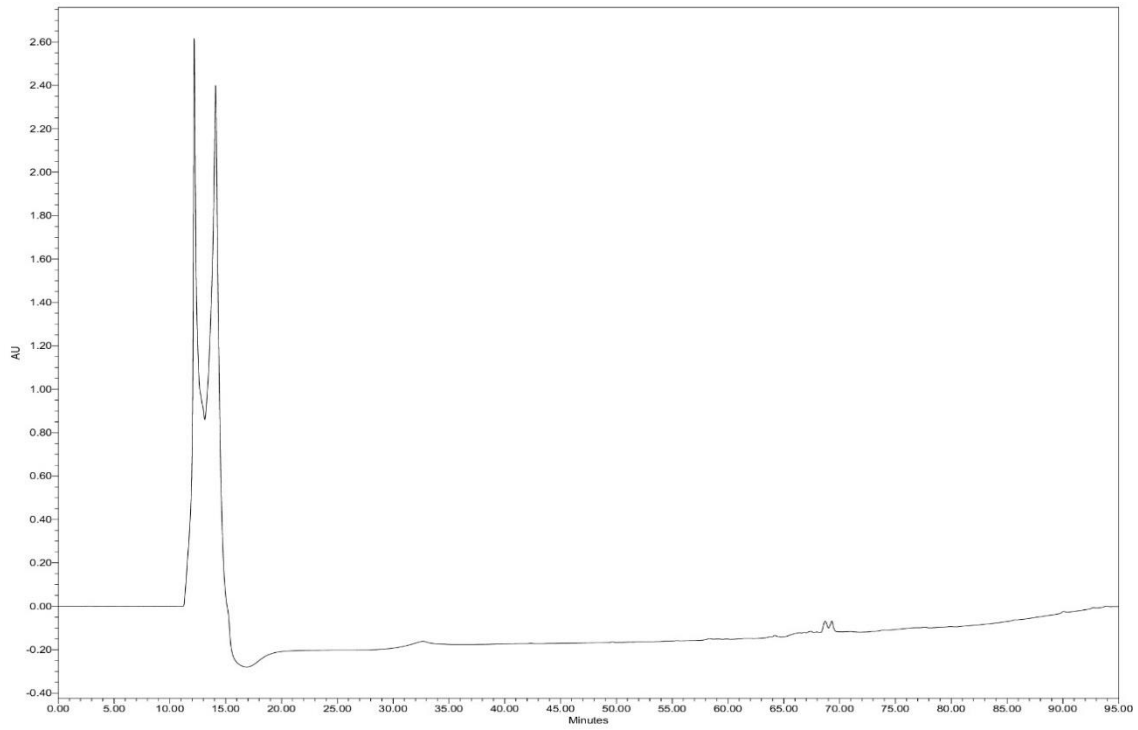

Figure A *Chromatographic profile of Conus ateralbus using a flow rate of 3 mL/min. It was observed a higher intensity in the recorded peaks, but it was also obvious a premature elution of compounds, indicating that compounds did not have enough time to bind to the column and were dragged at the beginning of race.*

- ## Appendixes III – Fractions masses

Table A *Fractions weight after dried. Fractions were dissolved in DMSO 40% to a concentration of 4 mg/mL.*

Sample	Fractions weight (mg)		Sample	Fractions weight (mg)		Sample	Fractions weight (mg)
C. ate R1 #1	4.46		**C. ven R1 #1**	1.79		**281 A #12**	0.18
C. ate R1 #2	0.12		**C. ven R1 #2**	0.45		**281 A #2**	0.59
C. ate R1 #3	0.02		**C. ven R1 #3**	2.59		**281 A #2.1**	0.45
C. ate R1 #4	0.02		**C. ven R1 #4**	0.16		**281 A #7**	0.36
C. ate R1 #5	0.11		**C. ven R1 #5**	2.22		**281 A #7.1**	0.88
C. ate R1 #6	0.09		**C. ven R1 #6**	0.58		**281 A #8**	0.04
C. ate R1 #7	0.08		**C. ven R1 #7**	0.16		**281 A #9**	1.47
C. ate R1 #8	0.45		**C. ven R1 #8**	0.41		**281 A #3**	0.07
C. ate R1 #9	0.04		**C. ven R1 #9**	0.36		**281 C #4**	0.2
C. ate R1 #10	0.2		**C. ven R1 #10**	0.19		**281 C #5**	0.08
C. ate R1 #11	1.67		**C. ven R1 #11**	0.4		**281 C #1**	0.57
C. ate R1 #12	0.41		**C. ven R1 #12**	2.17		**282 C #5.1**	0.25
C. ate R1 #13	0.19		**C. ven R1 #13**	1.34		**282 C #2.6**	0.07
C. ate R1 #14	0.44		**C. ven R1 #14**	0.28		**282 C #3**	0.25
C. ate R1 #15	0.36		**C. ven R2 #1**	2.03		**282 C #2**	0.34
C. ate R2 #1	4.28		**C. ven R2 #2**	1.02		**283 C #2.1**	0.39
C. ate R2 #2	0.08		**C. ven R2 #3**	0.15		**284 C #2.2**	0.22
C. ate R2 #3	0.08		**C. ven R2 #4**	0.19		**285 C #2.3**	0.13
C. ate R2 #4	0.35		**C. ven R2 #5**	2.56		**286 C #2.4**	0.18
C. ate R2 #5	0.2		**C. ven R2 #6**	0.15		**287 C #2.5**	0.55
C. ate R2 #6	0.23		**C. ven R2 #7**	0.16		**288 C #3.1**	0.11
C. ate R2 #7	0.18		**C. ven R2 #8**	0.33		**289 C #1.1**	0.89
C. ate R2 #8	0.18		**C. ven R2 #9**	0.35		**290 C #4.1**	0.05
C. ate R2 #9	0.18		**C. ven R2 #10**	0.25			
C. ate R2 #10	0.29		**C. ven R2 #11**	0.17			
			C. ven R2 #12	1.25			

- **Appendixes IV - Work dissemination**

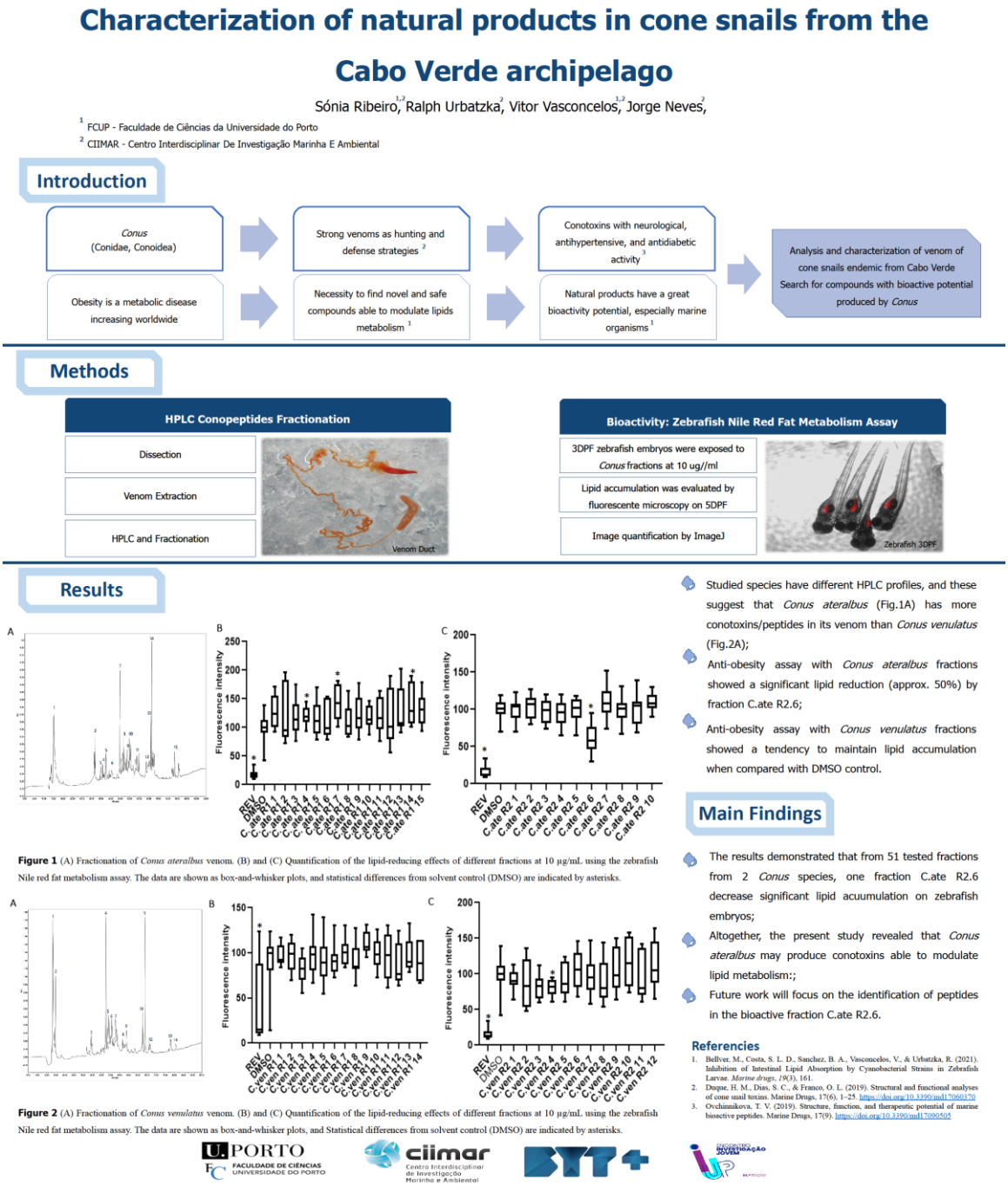

Figure A *Poster communication for IJUP 14.º Encontro de Jovens Investigadores da Universidade do Porto 2021.*

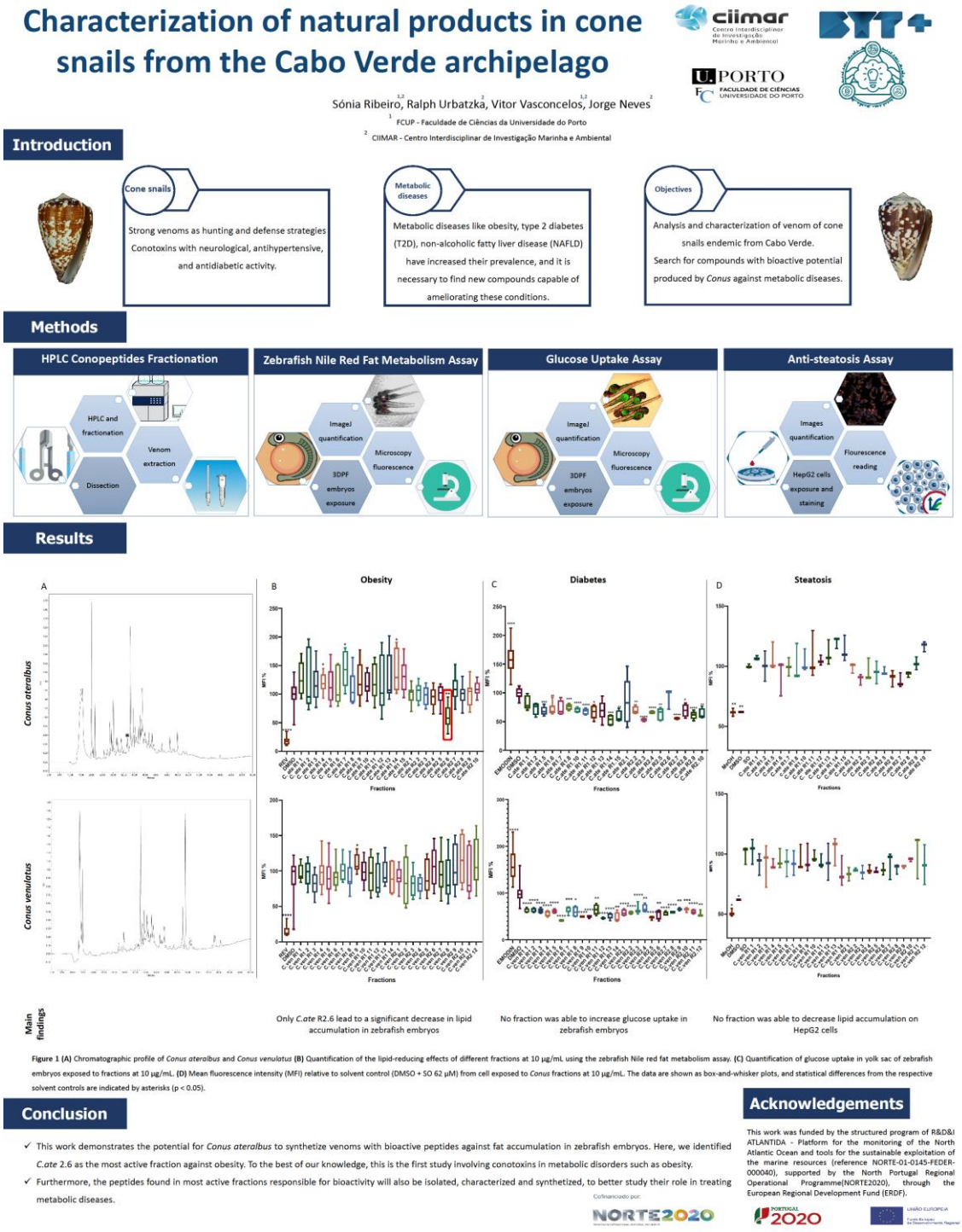

Figure B *Poster communication for BLUE THINK CONFERENCE 2021.*